UNIVERSITY OF OKLAHOMA

GRADUATE COLLEGE

COPPER CHEMISTRY OF PYRIDYLALKYLBENZAMIDE LIGANDS: MODELING THE Cu_Z CENTER OF N_2OR AND COORDINATION POLYMER CHEMISTRY

A DISSERTATION

SUBMITTED TO THE GRADUATE FACULTY

In partial fulfillment of the requirement for the

Degree of

DOCTOR OF PHILOSOPHY

By

ZHAODONG WANG

Norman, Oklahoma

2011

COPPER CHEMISTRY OF PYRIDYLALKYLBENZAMIDE LIGANDS: MODELING THE Cu_Z CENTER OF N_2OR AND COORDINATION POLYMER CHEMISTRY

A DISSERTATION APPROVED FOR THE

DEPARTMENT OF CHEMISTRY AND BIOCHEMISTRY

BY

Robert P. Houser

Michael T. Ashby

Kenneth M. Nicholas

Chuanbin Mao

Mark A. Nanny

ACKNOWLEDGEMENTS

With the complete of this dissertation, I would like to thank all of the individuals who give me support and encouragement for my research work and personal life.

Firstly, thanks to my advisor, Dr. Robert P. Houser, he has been giving me advice on choosing the project, solving problems in research, writing and editing of the papers and this dissertation. Without his valuable work and dedication to this project, the dissertation cannot be done on time.

My thanks to my graduate advisory committee members, Dr. Houser, Dr. Ashby, Dr. Nicholas, Dr. Mao and Dr. Nanny. Who offer me suggestions and ideas on my research work. Without their support for me to pursue the PhD study in general exam, this dissertation will never be done.

Thanks to Dr. Powell for wonderful work on solving all the X-ray structures in this thesis. Thanks for the help by Laura Cornell from the stockroom. Thanks to Carol Jones, Sandra Fisher, Bobby Collins, Nancy Palmer from chemistry office.

Thanks to my previous group members, Dr. Rajendra Skakya, Dr. Lei Yang . Dr. Urmila Pal Chaudhuri. They all gave me a lot of helpful and valuable suggestions on my project and learned many lab skills from both Lei Yang and Rajendra Shakya.

Thanks to my current group members, Mike McClain, Anna Jozwiuk, Audrey Myers, and Adam Campbell. It is my pleasure to work with all of you and discuss the research work.

Thanks to graduate students and friends who had been in inorganic division. Dr. Nan Xu, Adam Warhausen, Dr. Bheki Xulu, Dr. Penghe Qiu for sharing your knowledge and discuss inorganic chemistry research and literature.

Thanks to Dr. Tim Hubin from Southwestern Oklahoma State University for providing some pyrazine-containing ligand used in Chapter 4.

Finally, thanks to my parents and brother of support and understanding for my graduate study. Without their support, I will not be able to come to USA and pursue the graduate studies.

CONTENTS

LIST OF FIGURES

LIST OF TABLES

ABBREVIATIONS

CSD	Cambridge Structural Database
CuNir	Copper-containing nitrite reductase
CV	Cyclic voltammetry
DFT	Density functional theory
DMF	Dimethylformamide
EPR	Electron paramagnetic resonance
ESI-MS	Electrospray ionization mass spectrometry
ET	Electron transfer
Et_3N	Triethylamine
Et_2O	Diethyl ether
FTIR	Fourier transform infrared spectroscopy
His	Histidine
LMCT	Ligand to metal charge transfer transitions
LUMO	Lowest occupied molecular orbital
MCD	Magnetic circular dichroism
NMR	Nuclear magnetic resonance spectroscopy
N_2O	Nitrous oxide
NO	Nitric oxide
NOR	Nitric oxide reductase
N_2OR	Nitrous oxide reductase
OTf	Trifluoromethanesulfonate
rR	Resonance Raman
TBASH	Tetrabutylammonium hydrogen sulfide

THF	Tetrahydrofuran
TMEDA	N, N, N',N'-tetramethylethylendiamine
TMPA	Tris (2-pyridylmethyl)amine
UV-Vis	Ultraviolet visible spectroscopy
XAS	X-ray absorption spectroscopy

ABSTRACT

In order to pursue the goal of modeling Cu_Z of nitrous oxide reductase (N_2OR), we have explored the copper chemistry of two new pyridylalkylamide ligands containing phenol groups appended to the amide, 2-hydroxyl-*N*-(2-pyridylmethyl) benzamide (HL^{PhOH}) and 2-hydroxyl-*N*-(2-pyridylethyl) benzamide ($HL^{PhOH'}$). Two copper(I) and three copper(II) complexes with HL^{PhOH} and $HL^{PhOH'}$ were synthesized and characterized by X-ray crystallography. Both $[Cu(HL^{PhOH})_2(CH_3CN)]BF_4$ **(1)** and $[Cu(HL^{PhOH'})_2]BF_4$ **(2)** are mononuclear copper(I) complexes. $[Cu(HL^{PhOH})_2Cl_2]$ **(3)** is a monocopper(II) complex with octahedral geometry. $[Cu_4(L^{PhO})_4]$ **(4)** is a tetracopper(II) complex with a cubane-like Cu_4O_4 core structure. $[Cu_2(L^{PhO'})_2(CH_3OH)_2]$ **(5)** is a binuclear copper(II) complex with a distorted square pyramidal geometry. A naked $[Cu_{16}S_{10}]^{4-}$ cluster was obtained by the reaction of $[Cu_4(L^{PhO})_4]$ with $(nBu_4N)SH$, which can partially model the structure of the Cu_Z center.

Three copper(II) complexes with substituted pyridyl(bis-phenol)amide ligands− 6,6'-(2-methyl-2(pyridine-2-yl)propane-1,3diyl)bis(azanediyl)bis(methylene)bis-(2,4-dibromophenol) ($H_2L^{Br2\text{-}amine}$), 6,6'-(2-methyl-2(pyridine-2-yl)propane-1,3diyl)bis(azanediyl)bis(methylene)bis-(2-methoxyphenol) ($H_2L^{MeO\text{-}amine}$), and 2,2'-(2-methyl-2(pyridine-2-yl)propane-1,3diyl)bis(azanediyl)bis(methylene)bis-(4-nitrophenol) ($H_2L^{NO2\text{-}amine}$) − were synthesized and characterized by spectroscopic studies. $[Cu(L^{Br2\text{-}amine})]$ **(6)** and $[Cu(L^{NO2\text{-}amine})]$ **(7)** are mononuclear copper(II) complexes with square pyramidal geometry. $[Cu(L^{MeO\text{-}amine})Na(CH_3OH)_2]$ **(8)** is a heterometallic binuclear complex.

The CV features of complexes $[Cu(L^{tBu\text{-}amine})(CH_3OH)]$, $[Cu_3(L^{amine})_2(CH_3CN)_2](ClO_4)_2$, **6** and **7** are interpreted by Hammett analysis.

Pyrazine-containing ligands N-(pyridine-2-yl)methyl)pyrazine-2-carboxamide (HL^{Pz}) and N-(pyridine-2-yl)ethyl)pyrazine-2-carboxamide ($HL^{Pz'}$) led us to the synthesis and characterization of a series of 1D coordination polymers. $[Cu(HL^{Pz})Cl]_n$ **(9)** is a 1D coordination polymer with Cu_2Cl_2 core bridged by two HL^{Pz} ligands. $[Cu(L^{Pz})(Py)_2]^+$ **(10)** is a mononuclear copper complex with a square pyramidal geometry. $[Cu_2(L^{Pz})_2(4,4'\text{-bipy})(OTf)_2]$ **(11)** is a binuclear copper complex bridged by a twisted 4,4′-bipy ligand. Both $[Cu(L^{Pz})(N_3)]_n$ **(12)** and $[Cu(L^{Pz'})(N_3)]_n$ **(13)** are 1D coordination polymers bridged by end-on and end-to-end bridging azides, respectively.

Thioether-containing ligands 2-(methylsulfanyl)-*N*-[2-(pyridine-2-yl)methyl]acetamide ($2\text{-}HL^{N2S}$) and 2-(methylsulfanyl)-*N*-[2-(pyridine-2-yl)ethyl]acetamide ($2\text{-}HL^{N2S'}$) were used in the synthesis of the copper complexes $[Cu(2\text{-}L^{N2S})(CH_3OH)]_n(OTf)$ **(14)** and $[Cu(2\text{-}L^{N2S'})(OTf)]_n$ **(15),** which are 1D coordination polymers connected by the carbonyl oxygen from the corresponding ligand. $Cu(2\text{-}HL^{N2S'})(CH_3OH)Cl]$ **(16)** is a mononuclear copper complex with a distorted square pyramidal geometry.

CHAPTER 1

INTRODUCTION AND BACKGROUND: COPPER-CONTAINING NITROUS OXIDE REDUCTASE AND PROGRESS OF Cu_Z MODELING CHEMISTRY

1.1. Introduction

Copper is one of the most important trace elements along with iron in biological systems. Copper-containing proteins or enzymes play very significant roles and involve different biological functions from electron transfer to oxygen (O_2) processing. For example, blue copper proteins are among the most widely investigated copper proteins. The intense blue color arises from an intense electronic absorption assigned as a cysteine sulfur-to-Copper(II) charge transfer observed at around 600 nm in its UV-Vis spectrum. The copper center is converted back and forth between the +1 and +2 oxidation states to complete the electron transfer function.

In order to obtain fundamental chemical insights into copper active site structures and mechanisms, synthetic modeling chemistry has grown significantly in the last thirty years. The research combines the design of the ligands with control of the reaction conditions to obtain small molecular complexes that resemble the targeted active site of the proteins.[1] The first step of synthetic model chemistry of copper proteins is to design and synthesize the supporting ligands to duplicate the donor groups in the amino acids of the proteins. This is then followed by the synthesis and spectroscopic studies of metal complexes, which can be compared to structural and spectroscopic features of the active sites of the proteins.

Our research goal is to explore the synthetic model chemistry of the catalytic Cu_Z center in the N_2OR (nitrous oxide reductase). This project involves the synthesis and characterization of N- and O-donor containing supporting ligands,

followed by the synthesis and spectroscopic studies of Cu-S model complexes. Some research background about nitrous oxide reductase and the Cu_Z center will be presented in Chapter 1. Copper chemistry studies of pyridylalkylamide ligand systems with phenol groups appended to the amide, 2-hydroxy-N-(2-pyridylmethyl)benzamide(HL^{PhOH}) and 2-hydroxy-N-(2-pyridylethyl)benzamide($HL^{PhOH'}$), are presented in Chapter 2. Chapter 3 focuses on the copper(II) chemistry with substituted pyridylbis(phenol) ligands. The copper coordination chemistry of pyrazine- and thioether-containing ligand system is presented in Chapter 4 and Chapter 5, respectively.

1.2 . Nitrogen Cycle

Nitrogen (N) is very important for the development of field crops and plants. In the past several decades, the excessive fertilizer application caused the massive alteration of the nitrogen cycle which affects the global climate, food and energy security, and atmospheric environment. The nitrogen cycle as shown in Figure 1-1 is one of the most important nutrient cycles in the atmosphere;[2] it can be illustrated as the transformation of nitrogen and nitrogen-containing compounds in nature. Understanding the whole N cycle helps people to use manure and fertilizers correctly in order to safeguard the environment. The largest nitrogen reservoir on Earth is the nitrogen gas in the air. Although it is ubiquitous in the atmosphere, nitrogen gas is not accessible to most living organisms. Only some bacteria, named nitrogen fixers, can break the strong N_2 triple bond and tap the atmospheric reservoir.

Nitrogen is also an important component of proteins and nucleic acids found in DNA and RNA. The nitrogen cycle is composed of different processes: nitrogen fixation, nitrification, and denitrification.

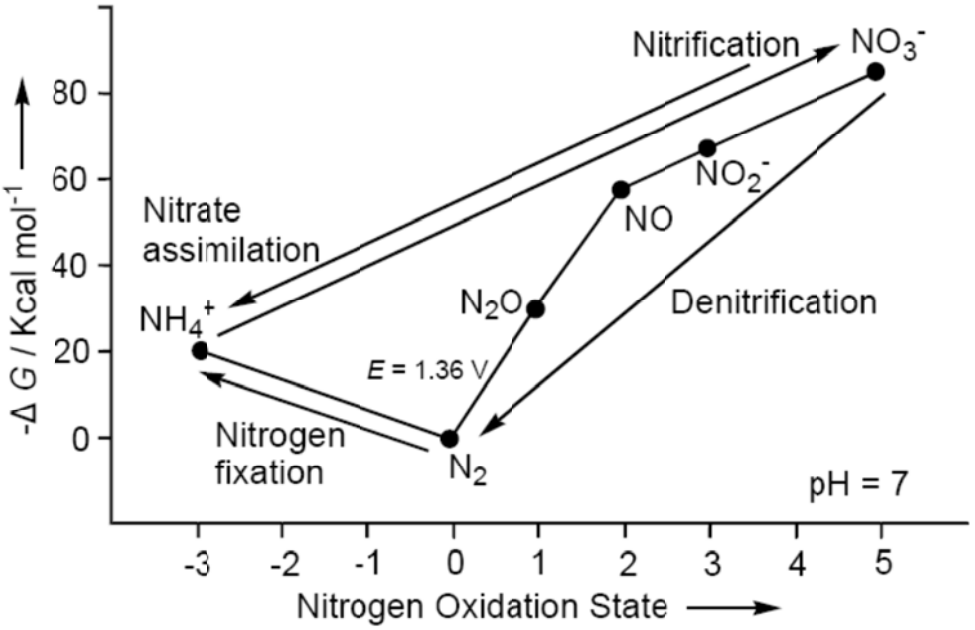

Figure 1-1. Bacterial nitrogen cycle. Figure is adapted from reference [2].

In industry, nitrogen can be converted to ammonia by the Haber process, which is used to produce fertilizers and explosives by the reaction N_2 with H_2 in the presence of catalysts at high temperature (at least 400 ^oC) and high pressure (around 200 atm). Nitrogen fixation is the conversion of atmospheric nitrogen into ammonia, which can be used by plants and animals. It is very important for life, since the fixed N is required to synthesize the basic building blocks of life, such as amino acids for proteins. This process can be achieved by both biological and abiotic methods. There are several different methods to convert N_2 into N-containing compounds.

Biological fixation is the most common method by which nitrogen can be fixed and assimilated into organic nitrogen by some symbiotic bacteria or free-living bacteria. This process can happen only in the presence of the enzyme nitrogenase, and is coupled with the hydrolysis of 16 equivalents of ATP. Only some plants of the legume family can contribute to nitrogen fixation through their symbiotic relationships with N-fixing bacteria. The crystal structure of the enzyme nitrogenase reveals that it consists of two component metalloproteins, the molybdenum iron (MoFe) protein and iron (Fe) protein.[3] In the MoFe protein, the P cluster with the construction of [8Fe-7S] participates in the interprotein electron transfer, the FeMo cofactor is the active site of N_2 binding and reduction.[4]

Followed by the nitrogen fixation process, NH_4^+ is converted to NO_3^- by soil-living bacteria and other nitrifying bacteria. The first step in the nitrification process is the oxidation of ammonium to nitrite (NO_2^-), which is carried out by bacteria in the genus *Nitrosomonsa*. Then nitrite is oxidized to nitrate by bacteria in the genus *Nitrobacter*. It is very important to oxidize nitrite to nitrate due to the toxicity of nitrite to plant life.

Denitrification is the terminal process of the whole nitrogen cycle, which involves the reduction of nitrate to nitrogen gas in anaerobic environments via nitrite, nitric oxide and nitrous oxide. Each step is catalyzed by specific enzyme. The enzymes involved in each step are nitrate reductase, nitrite reductase, nitric oxide reductase and nitrous oxide reductase, respectively.

The first step is the reduction of nitrate to nitrite catalyzed by dissimilatory membrane-bound nitrate reductase with both heme and nonheme irons and a Mo

cofactor.[5] The second step is the one electron reduction of nitrite to NO catalyzed by nitrite reductase (NIR). Two distinct types have been reported: multi-heme NIR and multi-copper NIR (CuNIR). Heme-containing NIR is a homodimer in which each monomer contains one heme *c* and one heme d_1. CuNIR is a 110 kDa trimer, each monomer contains both type I and type II copper center.[6] Reduction of NO to N_2O is catalyzed by nitric oxide reductase (NOR), which contains hemes *b* and *c*.[7] Terminal step of the process is catalyzed by nitrous oxide reductase (N_2OR). The details of N_2OR will be focused on in the following part of this chapter.

1.3. Nitrous Oxide Reductase (N_2OR) and Cu_Z Center

1.3.1. Crystal Structure of N_2OR

Nitrous oxide (N_2O) is a colorless and nontoxic gas; it is commonly referred to as laughing gas. N_2O is the third most important greenhouse gas behind only CO_2 and CH_4. The emission of N_2O is from both nature and human activities. 70% of N_2O emission is natural, mostly from bacterial breakdown of nitrogen in soil and in the ocean. 30% of N_2O emission is related to human activities, mostly from agricultural practices and activities like the use of organic fertilizers and fossil fuel combustion. Recently, scientists reported that the depletion of the stratospheric ozone layer is also related to nitrous oxide.[8] N_2O emission is the primary source of stratospheric NO_x. Both NO and NO_2 can destroy ozone catalytically. This research shows that N_2O emission is the single most important ozone-depleting emission and is expected to remain the largest throughout the 21st century.[8] So, the rising atmospheric

concentration of nitrous oxide contributes to both global warming and stratospheric ozone destruction.

N_2O also plays a very important role in the terminal step of the denitrification process. In this step, N_2O is reduced to N_2 catalyzed by nitrous oxide reductase (N_2OR) found in denitrifying bacteria in anaerobic respiration.[9] N_2OR is a copper-containing homodimer located in the bacterial periplasm. The crystal structure of N_2OR has been reported from three different bacterial species: *Pseudomonas nautica* (Pn),[10] *Paracoccus denitrificans* (Pd) and *Achromobacter cycloclastes.*[11] It is a dimer, and each monomer consists of two distinct domains that are formed by continuous segments in the amino acid sequence as shown in Figure 1-2.[10] There are two different multi-copper centers: (1) a binuclear Cu_A center, and (2) a tetra nuclear Cu_Z center. The distance between the Cu_A and Cu_Z centers is about 40 Å in one subunit, which is too far for electron transfer between them. The head-to-tail alignment of the N_2OR monomers brings the Cu_A center in one subunit to within about 10 Å of the Cu_Z center in the other subunit. This distance is totally reasonable for the electron transfer as shown in Figure 1-3.[12]

The Cu_A center is the electron transfer site, which is very similar to the Cu_A site found in cytochrome *c* oxidase, and its properties have been extensively characterized. Cu_A is an electron acceptor from a biological reducing agent, and then the electron is transferred to the catalytic Cu_Z center. It is defined as a binuclear $Cu_2(S_{Cys})_2$ cluster and each copper ion is further coordinated by two terminal histidine N and two axial S_{Met} or carbonyl O donors, forming a distorted tetrahedral geometry as shown in Figure 1-4. In its oxidized state, the Cu_A center is a

delocalized mixed-valence species characterized by its unique 7-line copper hyperfine splitting pattern in multifrequency electron paramagnetic resonance (EPR) spectra.

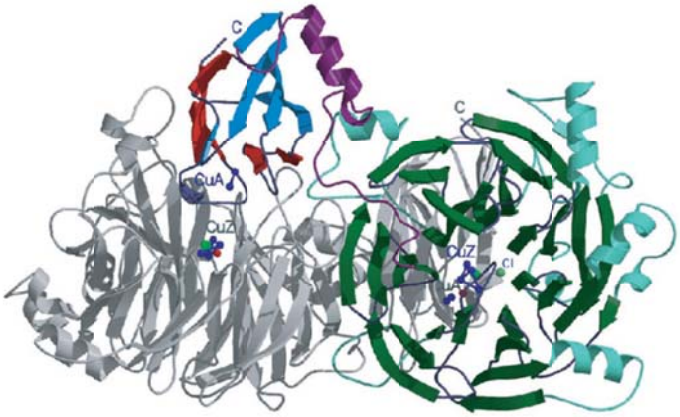

Figure 1-2. Protein crystal structure of N_2OR from *P. nautica*. Figure is adapted from reference[9a].

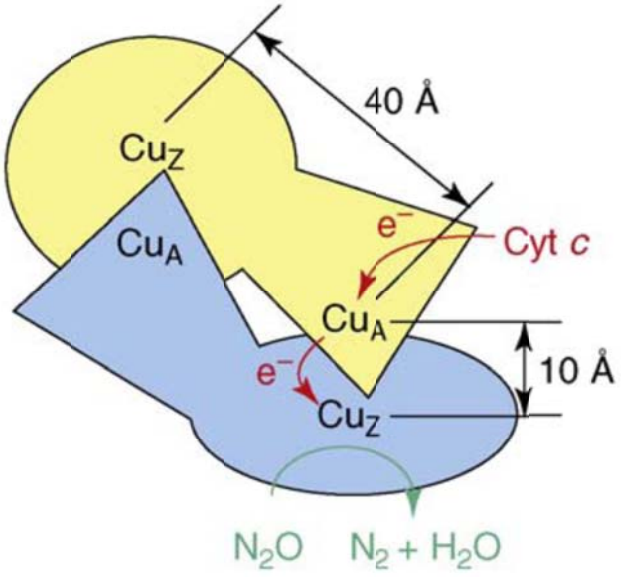

Figure 1-3. Schematic illustration of the dimeric form of N_2OR, illustrating the path of electrons from the donor cytochrome *c* via Cu_A to Cu_Z. Figure is adapted from reference [12].

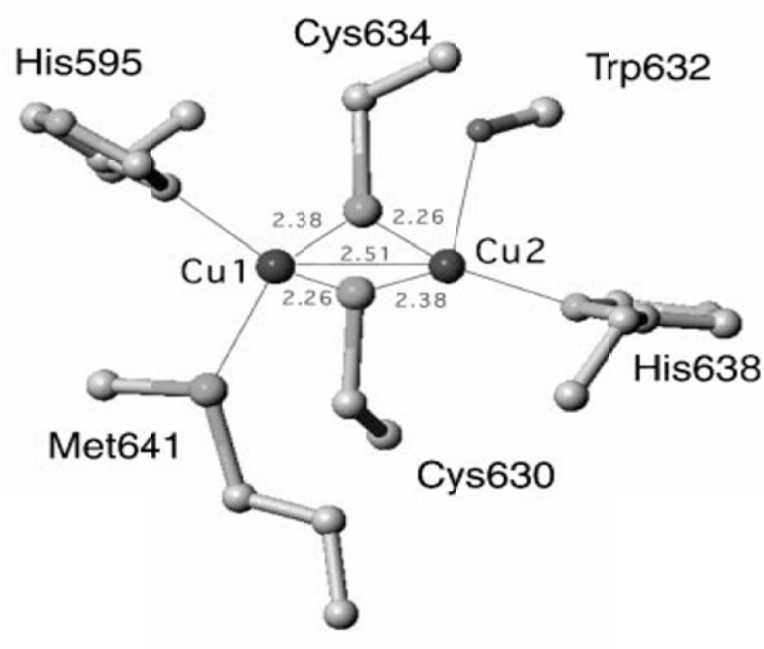

Figure 1-4. The crystal structure of the Cu_A site. Figure is adapted from reference[2].

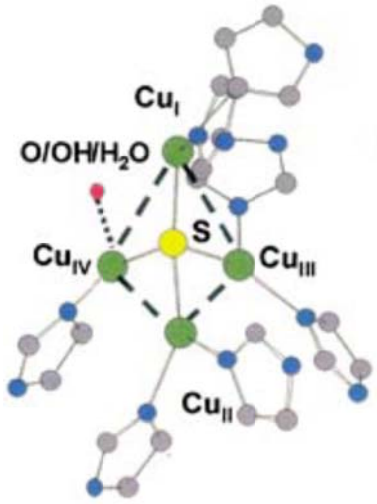

Figure 1-5. The Cu_4S cluster structure of Cu_Z site with approximate C_s symmetry.

Figure is adapted from reference[2].

The crystal structure of N_2O reductase from *P. denitrificans* shows that the Cu_Z center is a novel sulfide-bridged tetra nuclear copper cluster as shown in Figure 1-5. In the Cu_4S core structure, four copper ions are bridged by an inorganic sulfide ion. Cu_I, Cu_{II} and Cu_{III} are coordinated by two histidine N donor groups. Cu_{IV} is coordinated by one histidine N and one water-derived O donor group. The Cu_I-S-Cu_{II} angle is about 160º, while the other Cu-S-Cu angles are close to orthogonal. All of the Cu-S bond distances are very close to 2.3 Å. But the Cu-Cu distances are kind of different: Cu_I-Cu_{III}/Cu_I-Cu_{IV} ≈ 3.4 Å, Cu_{II}-Cu_{III}/Cu_{II}-Cu_{IV} ≈ 2.6 Å, Cu_{III}-Cu_{IV} ≈ 2.9 Å. The Cu_I/Cu_{IV} edge is proposed to be the side of binding and reduction of substrate N_2O, which is supported by spectroscopic and computational studies.

1.3.2. Spectroscopic Characterization of the Cu_Z Center

The unprecedented and novel Cu_4S cluster in the Cu_Z center has attracted much interest from bioinorganic chemists. Many spectroscopic studies have been reported since the structure was confirmed. In the UV-Vis absorption spectrum, there is an intense band at around 640 nm assigned as the origin of the blue color of reduced Cu_Z. Professor Edward Solomon's group did a lot of work to elucidate the electronic structure of the Cu_Z center, and proposed the enzymatic mechanism of the N_2O binding and reduction. Magnetic circular dichroism (MCD) can be used to determine the spin state of the resting Cu_Z center as shown in Figure 1-6.[2] The total spin state value of the Cu_Z center is 1/2. So, there are two possibilities for four copper to give a $S_{total} = 1/2$, either one Cu^{II} and three Cu^{I}, or one Cu^{I} and three Cu^{II}.

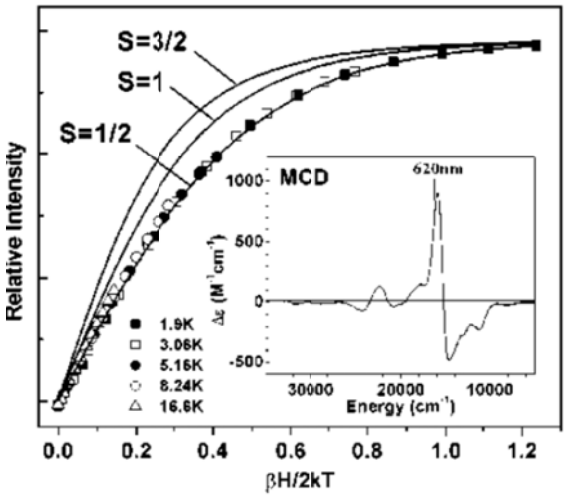

Figure 1-6. Saturation MCD (points) of Cu_Z along with simulated saturation curves (solid lines). Inset: 5 K 7 T MCD spectrum of Cu_Z. Figure is adapted from reference[2].

Cu K-edge XAS can be used to distinguish the two possibilities as shown in Figure 1-7. For a Cu^I complex, there is an intense absorption feature at about 8984 eV. But a Cu^{II} complex has no characteristic feature below 8985 eV. The Cu K-edge XAS spectrum clearly indicates that the $1Cu^{II} + 3Cu^I$ model is much better than $3Cu^{II} + 1Cu^I$, which means that there is only one oxidized Cu^{II} in the Cu_Z center with a single spin.[13]

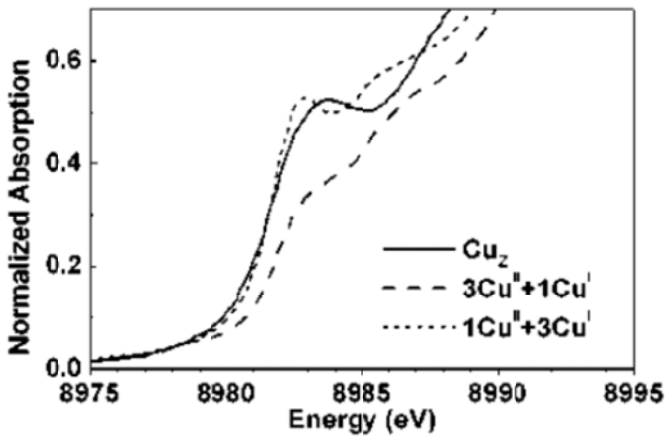

Figure 1-7. Cu K-edge XAS spectrum of Cu_Z and simulated spectra assuming $3Cu^{II}$ + $1Cu^{I}$ and $1Cu^{II}$ +$3Cu^{I}$. Figure is adapted from reference [13].

EPR spectroscopy was used to determine the unpaired electron spin distribution (Cu^{II}) over the Cu_Z center as shown in Figure 1- 8.[2] The Q-band EPR spectrum of the resting Cu_Z has an axial pattern with $g_{\parallel} = 2.16 > g_{\perp} \approx 2.04$, which indicates that the single spin resides in a Cu d_{x2-y2} orbital. The $g_{\parallel}$ is smaller than the normal tetragonal Cu^{II} complexes, which have values around 2.2-2.3. This could be due to the high $xy \rightarrow x^2\text{-}y^2$ ligand field transition energy.[14]

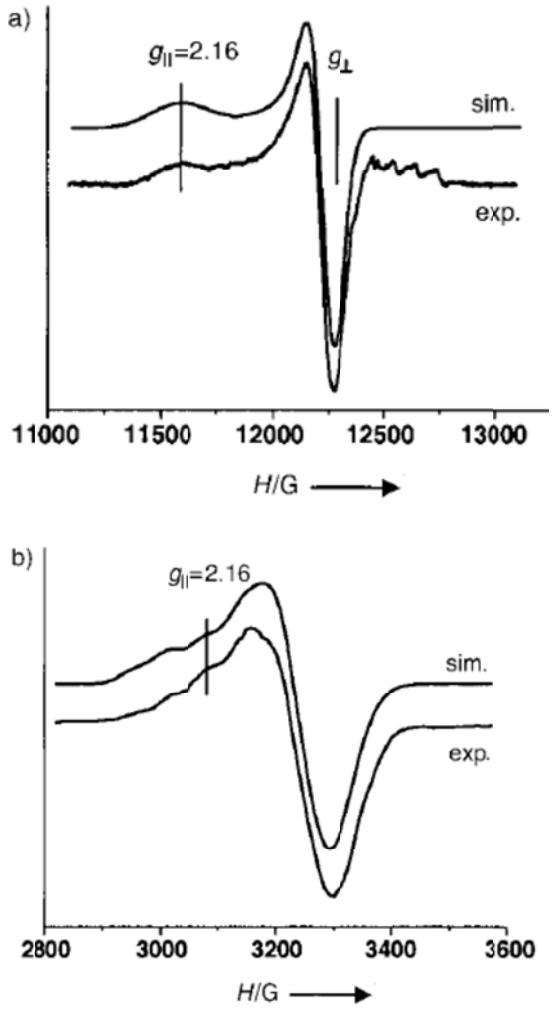

Figure 1-8. Experimental and simulated EPR spectra of resting Cu_Z from *P*n N_2OR at a) Q-band and b) X-band. Figure is adapted from reference[2].

Although the oxidized Cu_Z displays a $3Cu^I/1Cu^{II}$ mixed-valence state, the active redox center is the fully reduced $4Cu^I$ state. This statement was proved by the EPR signal change with the incubation time in excess methyl viologen and dithionite solution (reductant) as shown in Figure 1-9. Before incubation, there was no activity for the oxidized Cu_Z, and the EPR shows a signal at $g_{\parallel} = 2.16$. With increasing incubation time, the specific activity began to increase along with the

decrease of the EPR signal. The correlated changes revealed that the fully reduced $4Cu^{I}$ state is the redox active center for the reduction of N_2O to N_2 in the N_2OR enzyme.

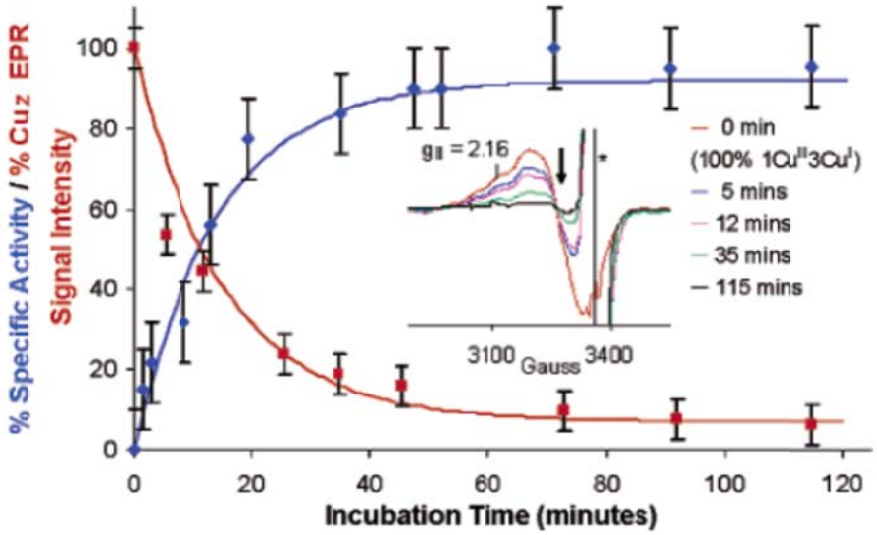

Figure 1-9. Incubation time correlation between enzyme activity growth rate and EPR signal decay rate (Insertion: EPR signal decreasing with incubation time). Figure is adapted from reference [14].

1.3.3. Mechanism of N_2O Reduction by the Cu_Z Center

The investigation of the catalytic mechanism of N_2O reduction is important to the understanding of the Cu_Z center. The fully reduced $4Cu^{I}$ center donates two electrons to N_2O and completes the reduction to N_2 and H_2O. This is followed by the two electron transfer from the Cu_A site in the second C-terminal domain to Cu^{II} and Cu^{IV}, and completion of the whole catalytic cycle as shown in Figure 1-10.

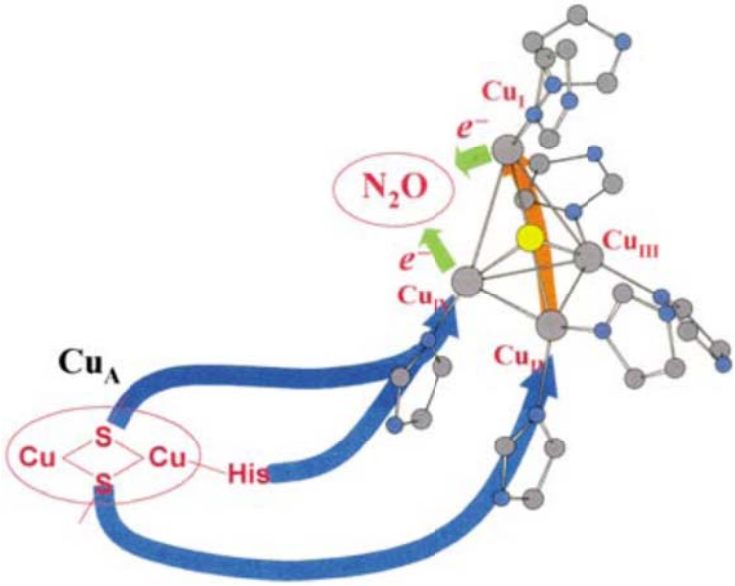

Figure 1- 10. Reduction of N_2O at the Cu_Z site. Figure is adapted from reference[2].

DFT calculations can be used to investigate the interaction between the N_2O substrate and the Cu ions in the Cu_Z center.[14] The most favorable binding modes for N_2O at Cu_I/Cu_{IV} edge are a bent μ-1, 3 bridging mode. The terminal N atom coordinates with Cu_I, and the O atom coordinates with Cu_{IV} as shown in Figure 1-11. The N-N-O bond angel is 139°, which is different from the linear free N_2O molecule. The bent geometry of N_2O resulted in a 2 eV splitting of the degenerate LUMO of N_2O into two nondegenerate π* orbitals. The strong back-bonding from the Cu^I *d* orbital to the stabilized LUMO π* orbital of N_2O increases the electron density of N_2O and elongates the N-N and N-O bonds as shown in Figure 1-12.

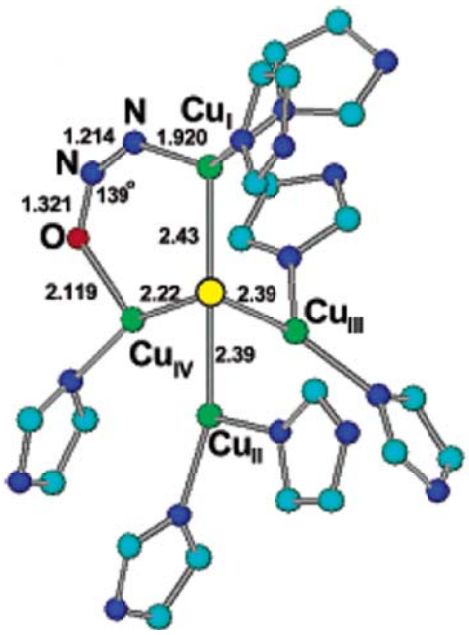

Figure 1-11. DFT-optimized geometries of the N_2O complexes with the all-reduced $4Cu^I$ Cu_Z. Figure is adapted from reference [14].

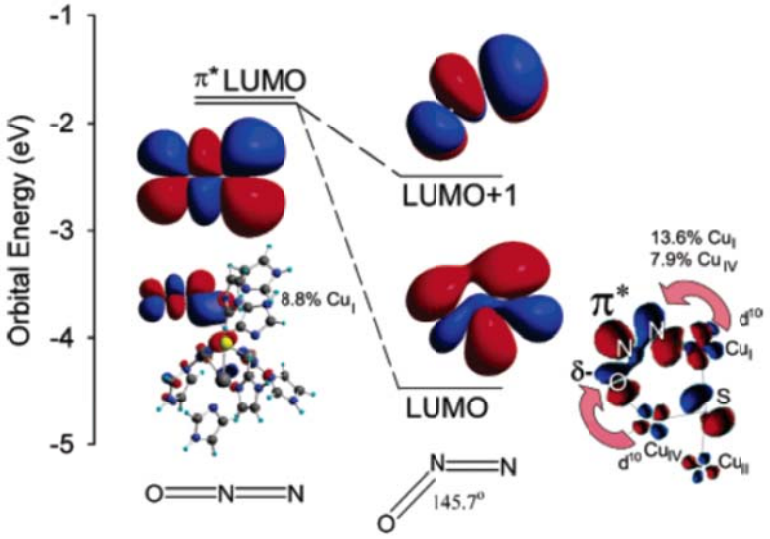

Figure 1-12. Splitting of LUMOs in bent N_2O substrate and back bonding interaction from the Cu_Z to bent N_2O. Figure is adapted from reference [14].

1.4. Model Chemistry of the Cu_Z Center

Because the behavior of the metal ions located in proteins can be related to the fundamental chemistry of the particular metal, the studies of the synthetic small molecule analogs attract the interest of inorganic chemists. Although the properties of the synthetic models can not totally duplicate the natural environment in proteins, it can focus on or give clues to certain unanswered questions. Structural and spectroscopic studies of the synthetic model analogs help chemists to understand the properties and the reactivity mechanisms in the active centers of metalloproteinase. It sometimes provides information that cannot be obtained from the protein studies alone.

The unprecedented Cu_4S structure and the provocative mechanism for the reactivity of the Cu_Z active center in nitrous oxide reductase (N_2OR) have attracted much interest from bioinorganic chemists. From the view of the bioinorganic chemists, the structural and spectroscopic studies of Cu-S model complexes will be the key goal for this project.

Two main strategies have been used to synthesize Cu-S complexes with designed N-donor supporting ligands. Both methods involve reaction between Cu (I) precursors and elemental sulfur or Cu (II) precursors and sulfide reagents. Here, I will give a brief summary about both strategies.

1.4.1. Reaction of Cu (I) Precursors with Elemental Sulfur

An important end-on μ-η^1:η^1-bound $Cu_2(S_2)$ complex, $\{(TMPA)Cu]_2(S_2)\}(ClO_4)_2$ (TMPA = tris(2-pyridylmethyl)amine), was reported by Karlin's group.[15] It was obtained from the redox reaction between the $[(TMPA)Cu(CH_3CN)]ClO_4$ precursor and elemental sulfur. In this complex, each copper is five-coordinate with four N donors from the TMPA ligand and one S donor from the disulfide anion, forming distorted trigonal bipyramidal geometry as shown in Figure 1-13. The S-S bond distance of 2.004(4) Å is shorter than the side-on complex $[Cu(HB(3,5\text{-}Pr^i{}_2pz)_3)]_2(S_2)$ which has a S-S bond distance of 2.073(4) Å.

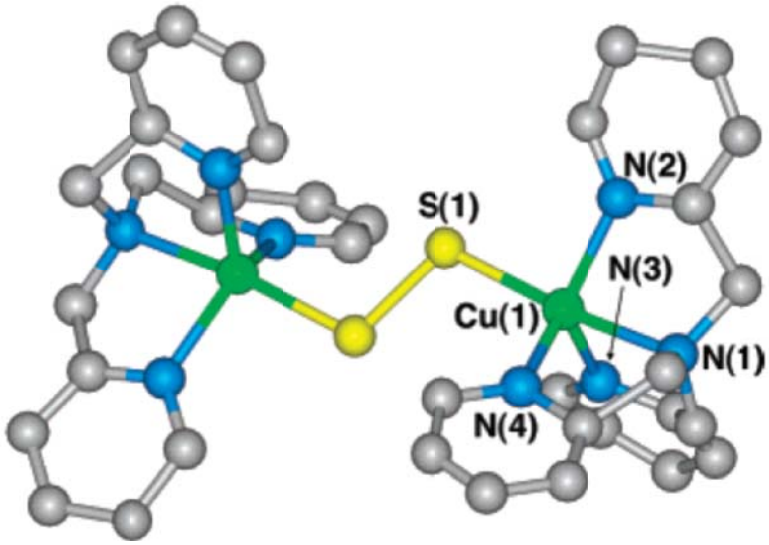

Figure 1-13. The crystal structure of the disulfide complex $[(TMPA)Cu]_2(S_2)]^{2+}$. Figure is adapted from reference [15].

The first reported Cu-S complex, $[Cu(HB(3,5\text{-}Pr^i{}_2pz)_3)]_2(S_2)$, with N-donor ligation from tris(pyrazolyl)hydroborate ligand $HB(3,5\text{-}Pr^i{}_2pz)_3$, was synthesized by

the thermal decomposition of a Cu(II)-thiolate complex concomitant with C-S bond cleavage, or between Cu(I) complex [Cu(HB(3,5-Pr^i_2pz)$_3$)(CH_3CN)] and elemental sulfur.[16] It is a side-on bound μ-η^2:η^2-disulfide (S_2^{2-}) bridged binuclear copper complex as shown in Figure 1-14. Each copper is five-coordinate with three N donors from the ligand and two S donors from the S_2^{2-} anion, forming a distorted square pyramidal geometry.

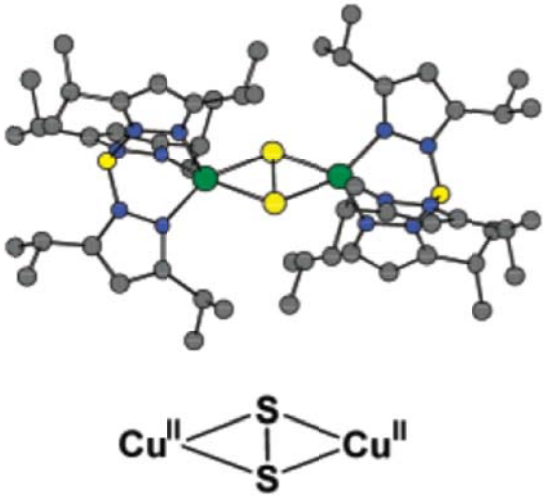

Figure 1-14. Crystal structure of the side-on $Cu_2(S_2)$ complex: [Cu(HB(3,5-Pr^i_2pz)$_3$)]$_2$(S_2). Figure is adapted from reference [16].

A similar μ-η^2:η^2-side-on disulfide bridged copper-sulfur complex, [{Cu^{II}(MePY2)^{Me2N}}$_2$(S_2)]$^{2+}$ ((MePY2)^{Me2N} = N, N-bis{2-[2-(N', N''-4-dimethylamino) pyridyl]ethyl}methylamine), was synthesized and characterized by Karlin's group.[17] In this complex, the copper ion is pent coordinated with three N donors from the supporting ligand and two S donors from the disulfide anion, forming a slightly distorted square-pyramidal geometry.

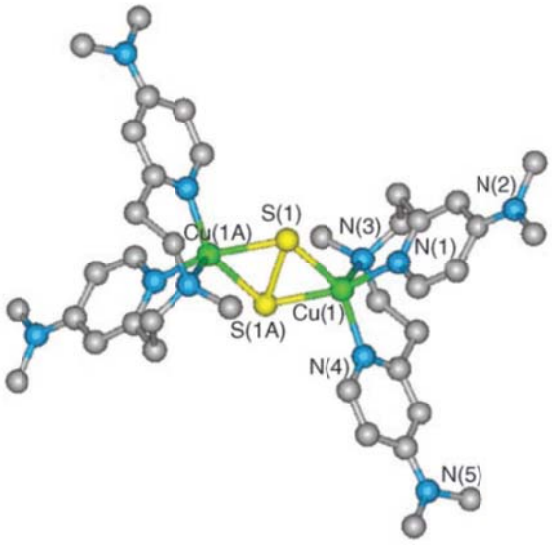

Figure 1- 15. X-ray structure of the cationic $[\{Cu^{II}(MePY2)^{Me2N}\}_2(S_2)]^{2+}$. Figure is adapted from reference [17].

This paper also reported the reactivity studies of the complex towards exogenous substrates as shown in Figure 1-16. The reaction with PPh_3 resulted in the formation of quantitative yields of triphenylphosphine sulfide, which means that sulfur transfer can happen in the reaction. As a contrast, there is no reaction of the complex with benzyl bromide. So, the disulfide anion can function as an electrophilic reagent.

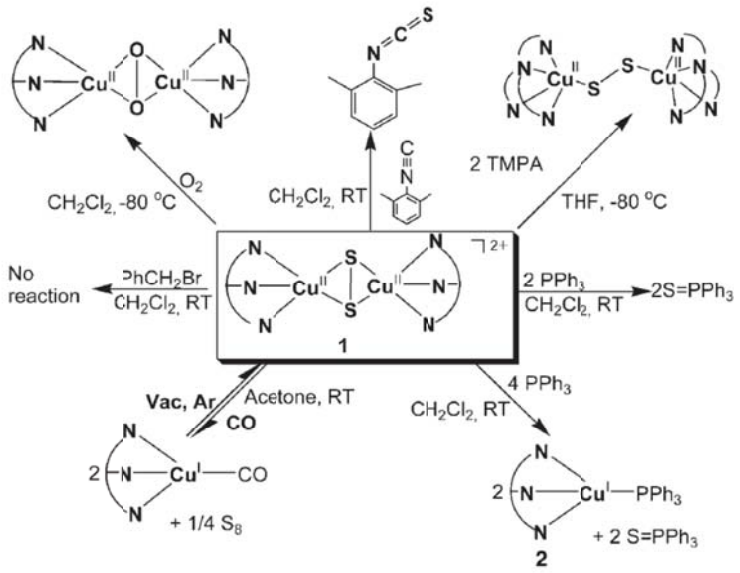

Figure 1-16. Reactivity of the $\{Cu_2S_2\}$ core in complex $[\{Cu^{II}(MePY2)^{Me2N}\}_2(S_2)]^{2+}$ towards exogenous substrates. Scheme is adapted from reference [17].

More comprehensive studies of a series of $[Cu_2(\mu\text{-}\eta^2\text{:}\eta^2\text{-}S_2)]^{2+}$ complexes with various *β*-diketiminate derived ligands or anilido-imine ligands were completed by Tolman's group.[18] Spectroscopic studies (resonance Raman, UV-Vis and NMR) and X-ray analysis revealed that the supporting ligands can enhance the Cu-S bonding interaction and lead to greater back-bonding from the copper d_{xy} orbitals to the S_2^{2-} σ* orbital. So, the S-S bond will be weakened due to the electron-donating effect of *β*-diketiminate derived ligands or anilido-imine ligands.

The ambition to obtain an accurate model for the Cu_4S center inspired chemists to do more investigation on this work. Tolman and coworkers reported a trinuclear $[Cu_3S_2]^{3+}$ complex with less sterically hindered and neutral bidentate N-donor supporting ligands.[19] The cluster was obtained by the reaction of a TMEDA-Cu(I)

complex (TMEDA= N,N,N′,N′-tetramethylethylenediamine) or a TMCHD-Cu(I) complex (TMCHD= N,N,N′,N′-tetraethyl-trans-(1R,2R)-cyclohexanediamine) with elemental sulfur. In this complex, three four-coordinate copper ions are bridged by two μ_3-sulfido ions as shown in Figure 1-17. Both Cu-S (2.247(2) Å) and Cu-N (2.028(7) Å) distances are very close to those in the Cu_Z center. Most importantly, the Cu_Z sub cluster defined by Cu2, Cu3, Cu4 and S resembles part of the cores of the $[Cu_3S_2]^{3+}$ cluster.

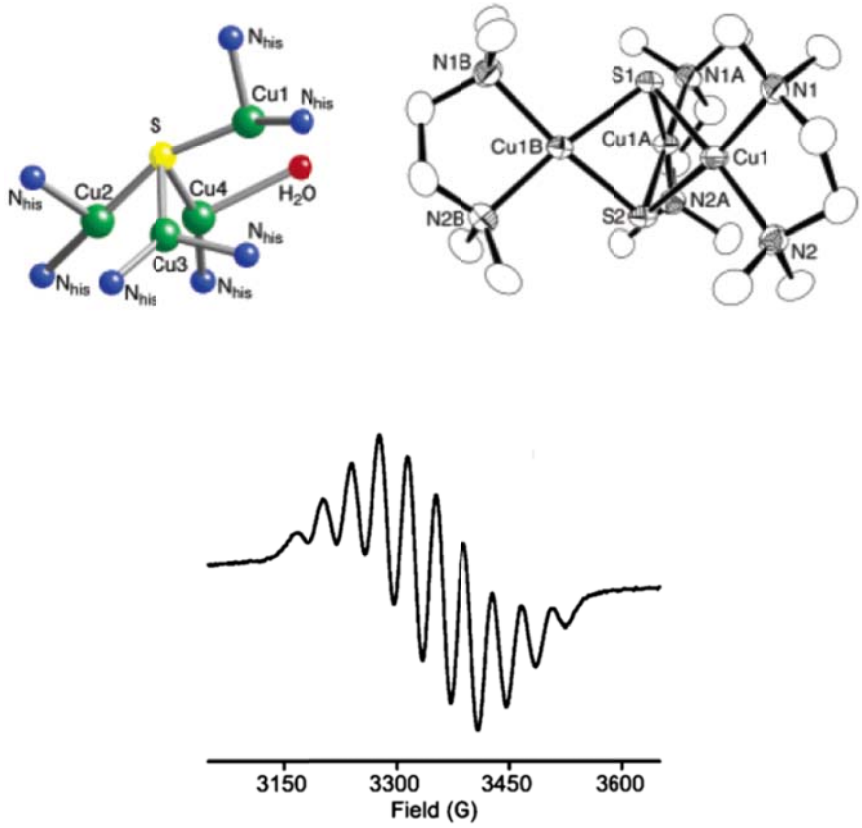

Figure 1-17. Cu_Z site of N_2OR (left side on top) and structure of $[Cu_3(\mu\text{-}S)_2(TMEDA)_3](SBF_6)_3$ (right side on top) and X-band EPR spectrum at room temperature (bottom). Figure is adapted from reference [19].

The cluster can be assigned as a fully delocalized mixed-valence complex supported by spectroscopic data and theoretical calculations. The X-band EPR spectrum exhibits an isotropic signal with a distinctive 10-line hyperfine pattern (Figure 1-17). In summary, this is the best reported model complex that can model part of the structural features of the N_2OR Cu_Z center until now.

1.4.2. Reaction of Cu(II) Precursors with Sulfide Reagents

The reaction of Cu(II) precursors with sulfide reagents is another effective method to obtain Cu-S clusters. Copper-sulfur clusters supported by N-donor supporting ligands have been synthesized and characterized by Tolman's group with this strategy.[20] The synthesis of these complexes involved the reaction between Cu(II) precursor $[LCu^{II}Cl]_n$ and $(TMS)_2S$ as shown in Figure 1-18.

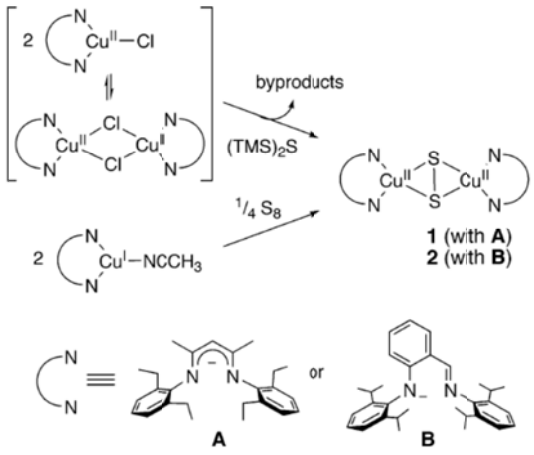

Figure 1-18. Synthesis of Cu-S clusters. Scheme is adapted from reference [20].

The crystal structure of complexes $[(LCu)_2(\mu\text{-}S_2)](L=A)$ **a** and $[(LCu)_2(\mu\text{-}S_2)](L=B)$ **b** are shown in Figure 1-19. In both complexes, the copper ion is four-coordinate with two N donors from the supporting ligand and two S donors from S_2^{2-}. The Cu-Cu distances are similar (3.799(5) Å for complex **a** and 3.8446(16) Å for **b**), and the S-S distances (2.2007 Å for **a** and 2.165 Å for **b**) are longer than other reported dicopper-sulfur complexes.[15-16]

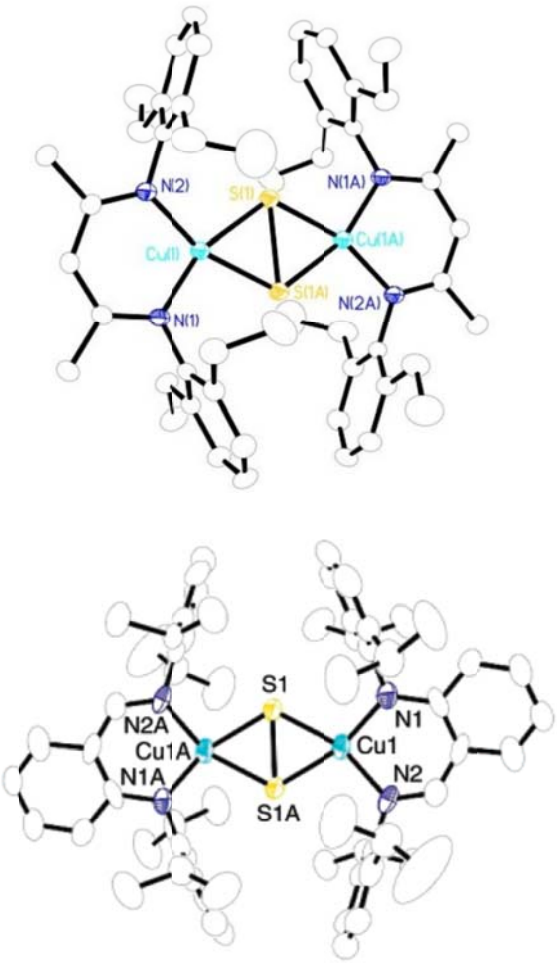

Figure 1-19. Crystal structures of complex **a** (top) and **b** (bottom). Figure is adapted from reference [20]

Recently, Tolman's group synthesized and characterized Cu-S clusters with different nuclearities through metathesis reactions.[21] Novel copper sulfur clusters with varying nuclearity were synthesized by the reaction of $Cu^{II}X_2$ (X = Cl^- or $CF_3SO_3^-$), supporting ligand TMCHD (TMCHD= N,N,N',N'-tetraethyl-trans-(1R,2R)-cyclohexanediamine) and Li_2S or Na_2S as shown in Figure 1-20.

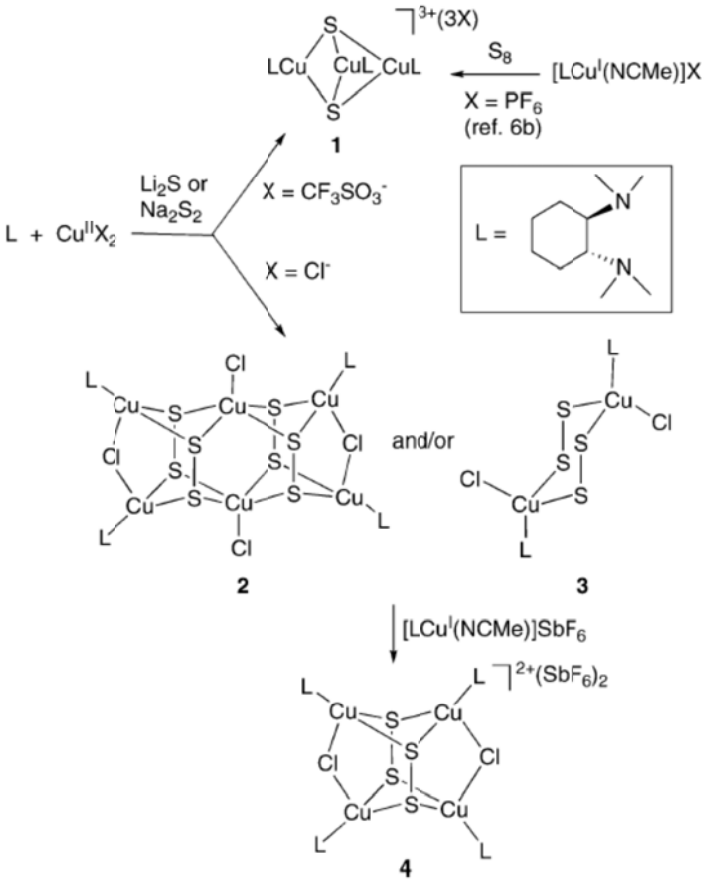

Figure 1-20. Synthesis of the copper sulfide clusters. Figure is adapted from reference [21].

The X-ray crystal structures of copper sulfur clusters **1**, **2**, **3**, **4** are shown in

Figure 1-21. Complex $[(TMCHD)_3Cu_3(\mu\text{-}S)_2]^{3+}$ **(1)** is a trinuclear copper sulfide cluster. Each copper is four-coordinate with two N donors from the ligand TMCHD and two S donors from S_2^{2-}, forming a square planar geometry. The Cu-S distance is about 2.24-2.26 Å. In the novel copper sulfur cluster $[(TMCHD)_4Cu_6(\mu\text{-}S_2)_4Cl_4]$ **(2)**, there are six copper ions with a distorted square-pyramidal geometry. Four of them are ligated by a TMCHD ligand, the other two copper ions are bridged by four S_2^{2-} ligands and one chloride. Each S_2^{2-} coordinates with four different copper ions. The Cu-S and S-S distances are about 2.31-2.38 Å, 2.00 Å, respectively.

Complex $[(TMCHD)_2Cu_2(\mu\text{-}S_2)_2Cl_2]$ **(3)** was synthesized by mixing ligand TMCHD, $CuCl_2$ and Na_2S_2 reagents, which is similar to the previously reported complex $[(TMCHD)_2Cu_2(\mu\text{-}S_2)_2](CF_3SO_3)_2$ with a short S-S bond distances of 1.955 Å and 1.953 Å.[22] Each copper is five-coordinate with two N donors from TMCHD and two S donors from S_2^{2-}, and one chloride.

Complex $[(TMCHD)_4Cu_4(\mu\text{-}S_2)_2Cl_2]^{2+}$ **(4)** was synthesized by the addition of four equivalents of $[(TMCHD)Cu^{I}(CH_3CN)]SbF_6$ into the pre-formed mixture of TMCHD, $CuCl_2$ and Li_2S. The coordination mode of each copper is the same as complex **3**. Two chloride ions function as a bridging ligand and ligate with four copper ions. The average S-S bond distance is 1.99 Å.

In summary, four copper-sulfide clusters were synthesized and characterized through metathesis reactions. These studies represent good progress towards the synthesis of Cu-S clusters and finally reached the N_2O reduction goal.

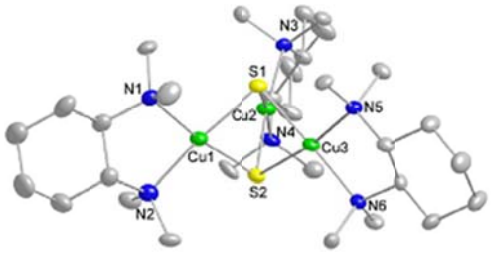

$[(TMCHD)_3Cu_3(\mu\text{-}S)_2]^{3+}$

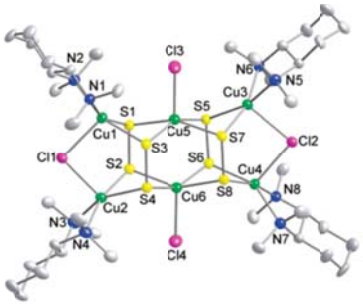

$[(TMCHD)_4Cu_6(\mu\text{-}S_2)_4Cl_4$

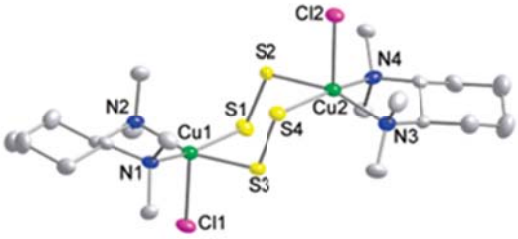

$[(TMCHD)_2Cu_2(\mu\text{-}S_2)_2Cl_2]$

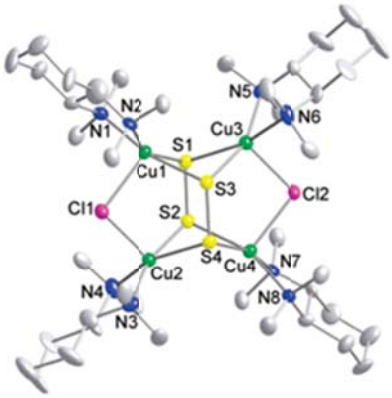

$[(TMCHD)_4Cu_4(\mu\text{-}S_2)_2Cl_2]^{2+}$

Figure 1-21. Crystal structures of Cu-S clusters $[(TMCHD)_3Cu_3(\mu\text{-}S)_2]^{3+}$ **(1)**, $[(TMCHD)_4Cu_6(\mu\text{-}S_2)_4Cl_4]$ **(2)**, $[(TMCHD)_2Cu_2(\mu\text{-}S_2)_2Cl_2]$ **(3)** and $[(TMCHD)_4Cu_4(\mu\text{-}S_2)_2Cl_2]^{2+}$ **(4)**. Figure is adapted from reference [21].

1.4.3. N_2O Reactivity with Transition Metals and Frustrated Lewis Pairs

N_2O is also a potentially strong and environmentally benign oxidant. However it remains underutilized due to its high kinetic stability. So, the poor ligand properties if N_2O have made it a rarity for a well-characterized metal-N_2O adduct. Since the first metal-N_2O complex was reported by Armor and Taube in 1969, which

is thought to be a linear Ru-NNO complex based on spectroscopic and computational studies,[23] there were few metal-N_2O complexes reported. Recently, Dr. Chang reported the synthesis and characterization of a well-defined vanadium-N_2O complex supported by X-ray analysis as shown in Figure 1-22.[24] In this complex, the NNO ligand coordinates in a linear fashion within the apical pocket of the (tpa^{Mes})V platform. The coordination mode of N_2O is assigned as N-bound to the metal based on the observed interatomic distances and DFT calculations.

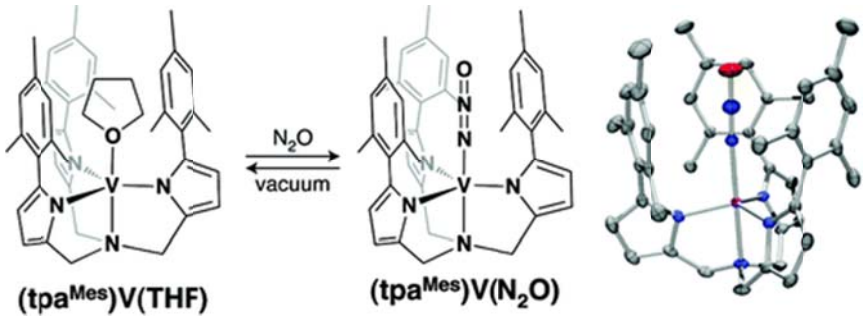

Figure 1-22. Synthesis and crystal structure of (tpa^{Mes})V(N_2O). Figure is adapted from reference [24].

Recently, some phosphine-activated N_2O adducts have been reported with various Lewis acids. In these reports, they developed the concept of "frustrated Lewis pairs" (FLPs).[25] These systems contain sterically hindered acids and bases that are precluded from classical Lewis acid-base adduct formation. The reactivity of N_2O with these FLPs shows that the N_2O molecule coordinates with the Lewis acid and basic components in a P-N-N-O-B mode. The reaction of frustrated Lewis pairs consisting of an equimolar amount of the sterically demanding Lewis base tBu_3P and the Lewis acidic boranes R_2BR' with N_2O in a bromobenzene solution led

to the formation of novel zwitterionic species over 12 hours at room temperature as shown in Figure 1-23.

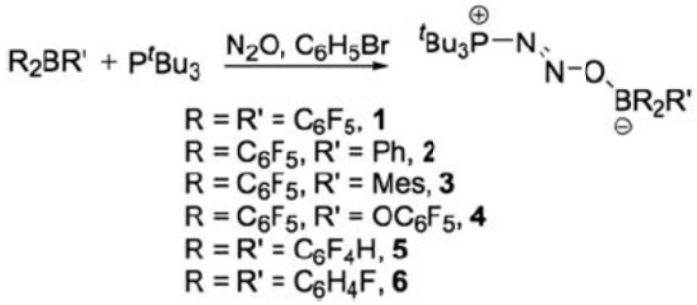

Figure 1-23. Synthetic method for the generation of **1-6**. Figure is adapted from reference [25].

The robustness of the $R_3P(N_2O)$ moiety allows the synthesis of otherwise inaccessible N_2O adducts by the exchange reaction of the borane for stronger Lewis acid such as $[Cp_2ZrMe]^+$ as shown in Figure 1-24.[25] This method to synthesized N_2O transition metal adducts helps chemists to understand the N_2O binding and reduction in both synthetic and biological systems.

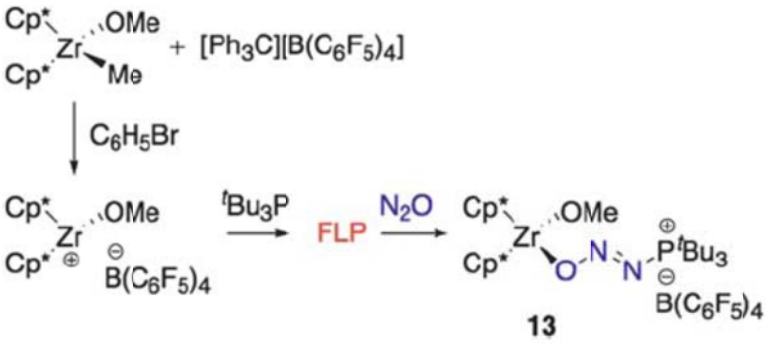

Figure 1-24. Activation of N_2O employing a zr/P FLP yielding **13**. Figure is adapted from reference [25].

1.4.4. N_2O Reactivity Studies of Cu-S Cluster

The terminal goal for modeling chemistry of the Cu_z center is to explore the N_2O reactivity with synthetic Cu-S model complexes. Recently, Tolman's group reported the reduction of nitrous oxide to nitrogen gas by a mixed-valence tricopper-disulfido cluster.[26] The cluster was synthesized by the reaction of Na_2S_2 with [LCu(CH_3CN)X] (L= 1,4,7-trimethyltriazacyclononane, X= $O_3SCF_3^-$ or SbF_6^-). The crystal structure of the cationic portion of the cluster is shown in Figure 1-25. The complex reacts with excess N_2O under a He atmosphere at -80 ^oC to yield N_2, as determined by GC/MS. Although it is a disulfide-bridged cluster that is different from the sulfide-bridged Cu_z active center, the key properties are modeled, such as the copper center being supported by N-donor ligands and similar UV-Vis absorption features. Most importantly, this complex exhibits N_2O reactivity and forms N_2. This report brings the model chemistry studies of Cu_Z center to a new level and represents impressive progress in this research field.

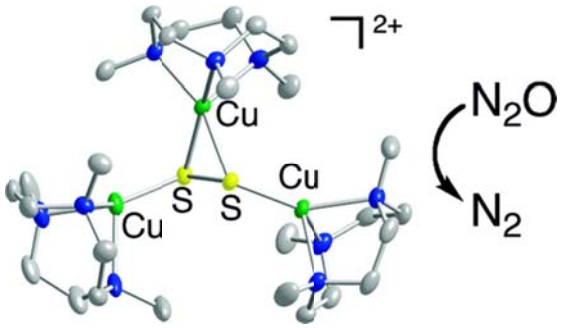

Figure 1-25. Structure of the tricopper-disulfido cluster and reactivity with N_2O. Figure is adapted from reference [26].

1.5. Previous Work by the Houser Group Relevant to Cu_Z Modeling Chemistry

1.5.1. Pyridylmethylamide Ligand System and Their Copper Chemistry

In our efforts to synthesize Cu-S complexes to model the Cu_Z active center in nitrous oxide reductase, we explored a series of pyridylmethylamide ligands HL^R, (R = null, Ph, Me_3, Ph_3), and their copper chemistry. The synthesis of the ligands is shown in Figure 1-26.

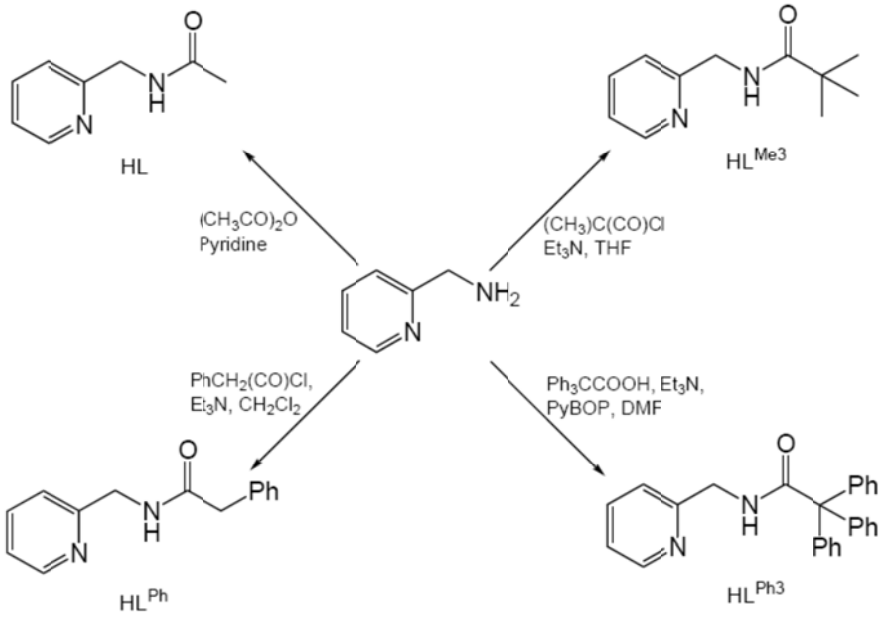

Figure 1-26. Design and synthesis of pyridylmethylamide ligand system.

These ligands bind with the copper ion with different coordination modes depending on the amide nitrogen protonation or deprotonation. For example, the neutral HL ligand chelates with the copper ion and forms a mononuclear complex, $[Cu(HL)_2](ClO_4)_2$. However, the deprotonated amidate binds with the copper ion and forms highly symmetrical octanuclear copper complex, $[Cu_8L_8(OH)_4](ClO_4)_4$.

The crystal structure of both complexes is shown in Figure 1-27.[27]

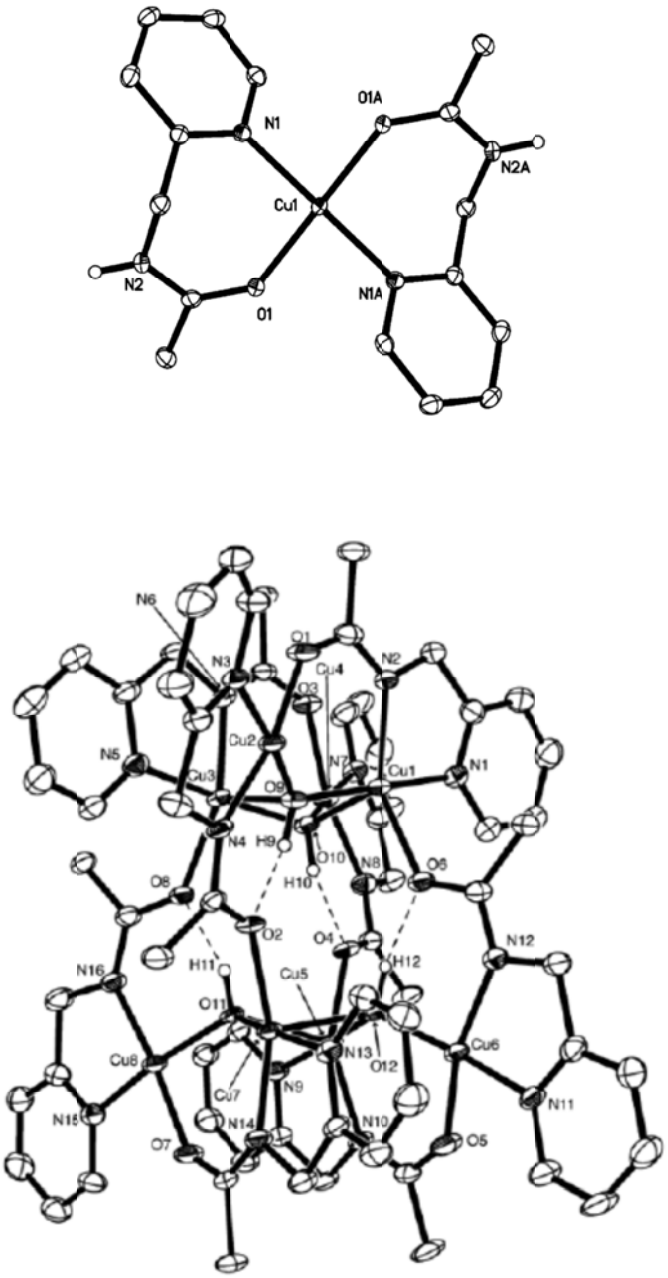

Figure 1-27. X-ray crystal structure of $[Cu(HL)_2](ClO_4)_2$ (top) and $[Cu_8L_8(OH)_4](ClO_4)_4$ (bottom). Figure is adapted from reference [27].

In addition, the substituents linked to the amide play a role in the coordination mode and the nuclearity of the copper complexes. For example, tetranuclear copper cluster $[Cu_4(L^{Ph})_4(OH)_2]^{2+}$ (Figure 1-28) was synthesized with the ligand HL^{Ph}. The more sterically hindered ligands HL^{Me3} and HL^{Ph3} react with copper and form binuclear complexes $[Cu_2(HL^{Me3})_2(OMe)_2]^{2+}$ and $[Cu_2(HL^{Ph3})_2(OMe)_2]^{2+}$ (Figure 1-29), respectively. [28]

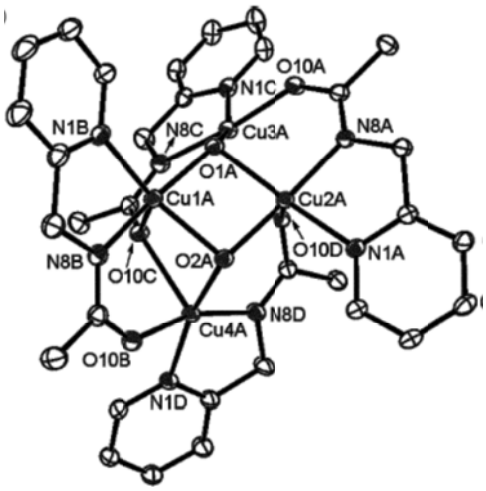

Figure 1-28. X-ray structure of $[Cu_4(L^{Ph})_4(OH)_2]^{2+}$. Figure is adapted from reference [28].

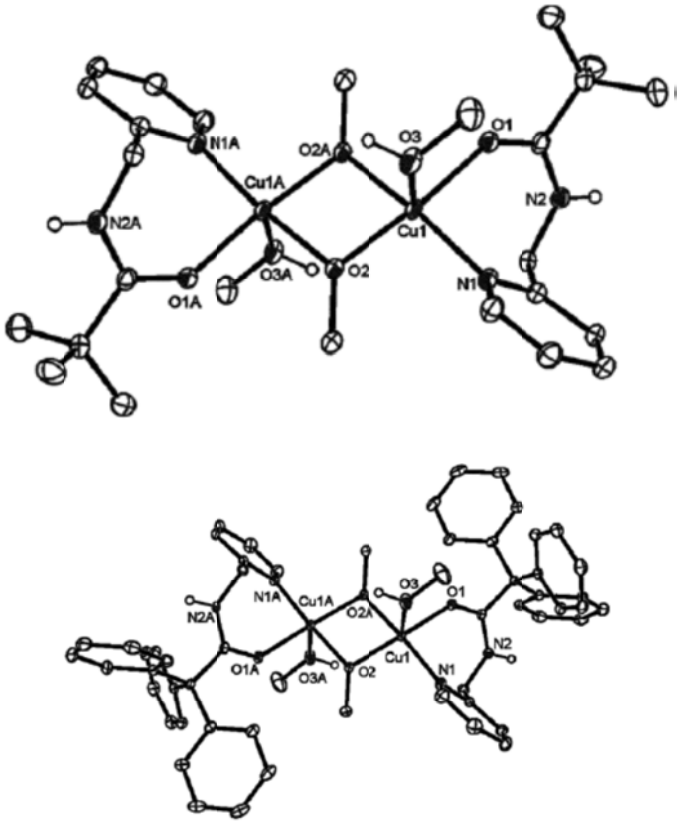

Figure 1-29. X-ray structures of $[Cu_2(HL^{Me3})_2(OMe)_2]^{2+}$ (top) and $[Cu_2(HL^{Ph3})_2(OMe)_2]^{2+}$ (bottom). Figure is adapted from reference [28].

1.5.2. Cu-S Clusters

A new family of pyridylguanidine ligands was developed (Figure 1-30) with strong binding capability to the copper ion. Figure 1-31 shows the structures of both complexes. They are isostructural dicopper disulfide complexes with slight differences in the bond parameters.[29] The central core Cu_2S_2 moieties display a very similar structure as other reported copper disulfide complexes.[17]

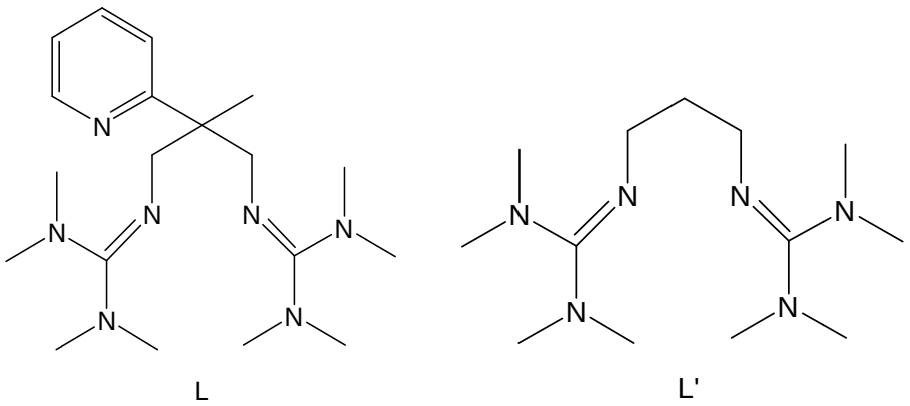

Figure 1-30. Structure of pyridylguanidine ligands.

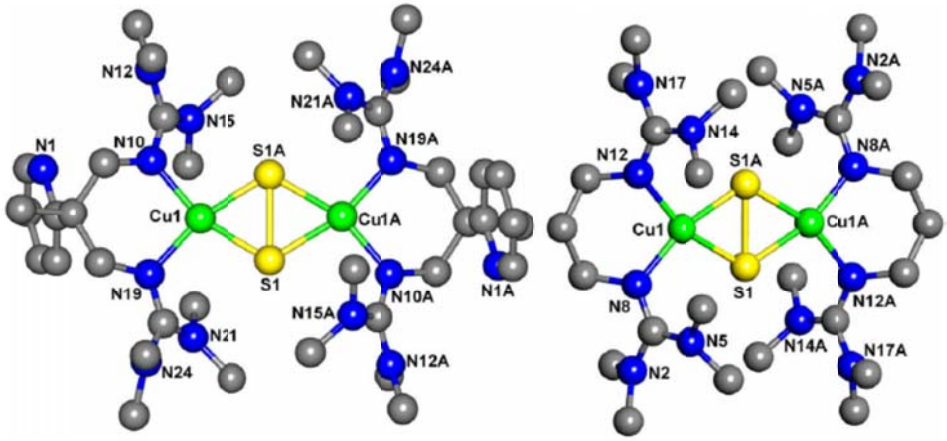

Figure 1-31. X-ray structures of $[Cu_2(L)_2(S_2)](PF_6)_2$ (left) and $[Cu_2(L')_2(S_2)](PF_6)_2$ (right). Figure is adapted from reference [29].

Lei Yang synthesized two naked Cu-S clusters $[Cu_{16}S_{10}]^{4-}$ and $[Cu_{12}S_8]^{4-}$ by the reaction of a mixed-valence copper precursor $[Cu_2(L1)_2]OTf$ (HL1 = 2-phenyl-N-(2-pyridylmethyl)acetamide; OTf = trifluoromethanesulfonate) with (nBu$_4$N)SH and NaSH, respectively.[30] The ratio for the synthesis of both clusters is listed in equation 1-1 and 1-2. The excess SH^- was necessary to reduce the copper(II) to copper(I) in the clusters. The structures of both clusters are shown in Figure 1-32. Unlike

$[Cu_{12}S_8]^{4-}$ where all S^{2-} ligands are μ_3-, $[Cu_{16}S_{10}]^{4-}$ consists of both μ_3- and μ_4-sulfido ligands. Eight μ_3-sulfido atoms decorate the eight triangular faces with an average Cu-S bond distances of 2.16(2) Å and an average Cu-S-Cu bond angle of 79.2(9)^o (slightly smaller than the average Cu-μ_3-S-Cu angle of 82(3)^o in $Na_4[Cu_{12}S_8]$). Two μ_4-sulfido atoms cap the top and bottom points of the cluster with Cu-S bond distances from 2.146(13) to 2.182(11) Å and an average Cu-S-Cu angle of 77.7(6)^o. More details about the characterization and ESI-MS will be covered in Chapter 2.

$$8[Cu_2(L1)_2]OTf + 24(n\text{Bu}_4\text{N})SH \longrightarrow (n\text{Bu}_4\text{N})_4[Cu_{16}S_{10}] \quad (1\text{-}1)$$

$$6[Cu_2(L1)_2]OTf + 18NaSH \longrightarrow Na_4[Cu_{12}S_8] \quad (1\text{-}2)$$

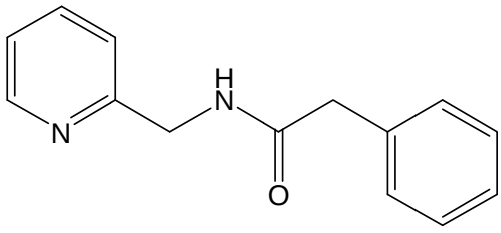

HL1

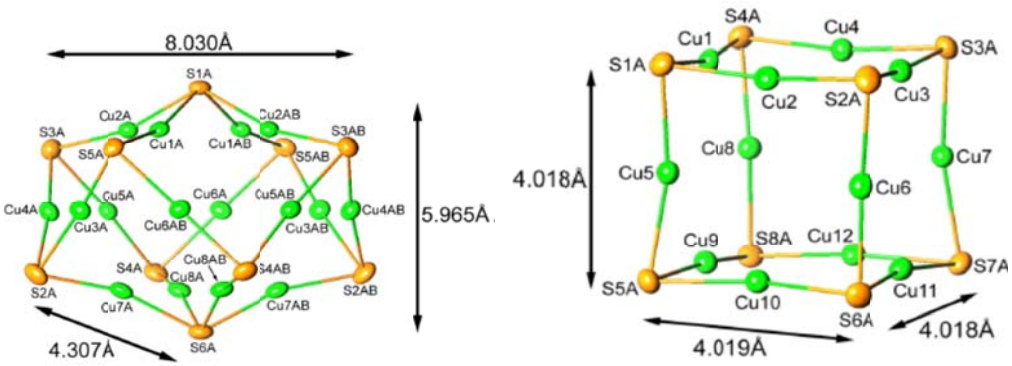

Figure 1-32. X-ray structures of $[Cu_{16}S_{10}]^{4-}$ (left) and $[Cu_{10}S_8]^{4-}$ (right). Figure is adapted from reference [30].

In summary, the unprecedented μ_4-sulfido bridged tetranuclear copper structural features and provocative mechanism of the Cu_Z center in N_2OR have attracted much interest. The terminal goal for the modeling chemistry of this center is to synthesize a series of Cu-S clusters with similar structural and spectroscopic features as the Cu_Z center. Many Cu-S complexes have been synthesized and characterized with X-ray crystal analysis. All of this research also has enriched the Cu-S chemistry study corresponding to well-developed Cu-O_2 chemistry.

From the previous work done by our group, substituted (pyridylalkyl) amide ligands are good candidates to construct polynuclear copper complexes and clusters that would be the template into which the inorganic sulfide could be inserted. This is the main principle to synthesize Cu-S complexes to achieve the goal of the modeling chemistry of Cu_Z center. The copper chemistry of these ligands will be covered in this dissertation.

1.6. References

1. (a) Karlin, K. D., Metalloenzymes, Structural Motifs, and Inorganic Models. *Science* **1993,** *261* (5122), 701-708; (b) Tolman, W. B., Using synthetic chemistry to understand copper protein active sites: a personal perspective. *J Biol Inorg Chem* **2006,** *11* (3), 261-271.

2. Chen, P.; Gorelsky, S. I.; Ghosh, S.; Solomon, E. I., N2O reduction by the mu(4)-sulfide-bridged tetranuclear Cu-Z cluster active site. *Angew Chem Int Edit* **2004,** *43* (32), 4132-4140.

3. Kirn, J.; Rees, D. C., Crystallographic structure and functional implications of the nitrogenase molybdenum-iron protein from Azotobacter vinelandii. *Nature* **1992,** *360* (6404), 553-560.

4. Einsle, O.; Tezcan, F. A.; Andrade, S. L. A.; Schmid, B.; Yoshida, M.; Howard, J. B.; Rees, D. C., Nitrogenase MoFe-Protein at 1.16 Å Resolution: A Central Ligand in the FeMo-Cofactor. *Science* **2002,** *297* (5587), 1696-1700.

5. (a) Berks, B. C.; Page, M. D.; Richardson, D. J.; Reilly, A.; Cavill, A.; Outen, F.; Ferguson, S. J., Sequence-Analysis of Subunits of the Membrane-Bound Nitrate Reductase from a Denitrifying Bacterium - the Integral Membrane Subunit Provides a Prototype for the Diheme Electron-Carrying Arm of a Redox Loop. *Mol Microbiol* **1995,** *15* (2), 319-331; (b) Berks, B. C.; Richardson, D. J.; Reilly, A.; Willis, A. C.; Ferguson, S. J., The Napedabc Gene-Cluster Encoding the Periplasmic Nitrate Reductase System of Thiosphaera-Pantotropha. *Biochem J* **1995,** *309*, 983-992; (c) Berks, B. C.; Richardson, D. J.; Robinson, C.; Reilly, A.; Aplin, R. T.; Ferguson, S. J., Purification and Characterization of the Periplasmic Nitrate Reductase from

Thiosphaera-Pantotropha. *Eur J Biochem* **1994,** *220* (1), 117-124.

6. (a) Fülöp, V.; Moir, J. W. B.; Ferguson, S. J.; Hajdu, J., The anatomy of a bifunctional enzyme: Structural basis for reduction of oxygen to water and synthesis of nitric oxide by cytochrome cd1. *Cell* **1995,** *81* (3), 369-377; (b) Nurizzo, D.; Cutruzzolà, F.; Arese, M.; Bourgeois, D.; Brunori, M.; Cambillau, C.; Tegoni, M., Conformational Changes Occurring upon Reduction and NO Binding in Nitrite Reductase from Pseudomonas aeruginosa†,‡. *Biochemistry-Us* **1998,** *37* (40), 13987-13996.

7. Sakurai, N.; Sakurai, T., Isolation and Characterization of Nitric Oxide Reductase from Paracoccus halodenitrificans†. *Biochemistry-Us* **1997,** *36* (45), 13809-13815.

8. Ravishankara, A. R.; Daniel, J. S.; Portmann, R. W., Nitrous Oxide (N_2O): The Dominant Ozone-Depleting Substance Emitted in the 21st Century. *Science* **2009,** *326* (5949), 123-125.

9. (a) Berks, B. C.; Ferguson, S. J.; Moir, J. W. B.; Richardson, D. J., Enzymes and associated electron transport systems that catalyse the respiratory reduction of nitrogen oxides and oxyanions. *Bba-Bioenergetics* **1995,** *1232* (3), 97-173; (b) Zumft, W. G., Cell biology and molecular basis of denitrification. *Microbiol Mol Biol R* **1997,** *61* (4), 533-616.

10. Brown, K.; Djinovic-Carugo, K.; Haltia, T.; Cabrito, I.; Saraste, M.; Moura, J. J. G.; Moura, I.; Tegoni, M.; Cambillau, C., Revisiting the catalytic Cu_Z cluster of nitrous oxide (N_2O) reductase - Evidence of a bridging inorganic sulfur. *J Biol Chem* **2000,** *275* (52), 41133-41136.

11. Paraskevopoulos, K.; Antonyuk, S. V.; Sawers, R. G.; Eady, R. R.; Hasnain, S. S., Insight into catalysis of nitrous oxide reductase from high-resolution structures of resting and inhibitor-bound enzyme from Achromobacter cycloclastes. *J Mol Biol* **2006,** *362* (1), 55-65.

12. Richardson, D.; Felgate, H.; Watmough, N.; Thomson, A.; Baggs, E., Mitigating release of the potent greenhouse gas N_2O from the nitrogen cycle – could enzymic regulation hold the key? *Trends in Biotechnology* **2009,** *27* (7), 388-397.

13. Chen, P.; DeBeer George, S.; Cabrito, I.; Antholine, W. E.; Moura, J. J. G.; Moura, I.; Hedman, B.; Hodgson, K. O.; Solomon, E. I., Electronic Structure Description of the μ_4-Sulfide Bridged Tetranuclear Cu_Z Center in N_2O Reductase. *J Am Chem Soc* **2002,** *124* (5), 744-745.

14. Ghosh, S.; Gorelsky, S. I.; Chen, P.; Cabrito, I.; Moura; MouraMoura, I.; Solomon, E. I., Activation of N_2O Reduction by the Fully Reduced μ_4-Sulfide Bridged Tetranuclear Cu_Z Cluster in Nitrous Oxide Reductase. *J Am Chem Soc* **2003,** *125* (51), 15708-15709.

15. Helton, M. E.; Chen, P.; Paul, P. P.; Tyeklár, Z.; Sommer, R. D.; Zakharov, L. N.; Rheingold, A. L.; Solomon, E. I.; Karlin, K. D., Reaction of Elemental Sulfur with a Copper(I) Complex Forming a trans-μ-1,2 End-On Disulfide Complex: New Directions in Copper−Sulfur Chemistry. *J Am Chem Soc* **2003,** *125* (5), 1160-1161.

16. Chen, P.; Fujisawa, K.; Helton, M. E.; Karlin, K. D.; Solomon, E. I., Spectroscopy and Bonding in Side-On and End-On Cu_2S_2 Cores: Comparison to Peroxide Analogues. *J Am Chem Soc* **2003,** *125* (21), 6394-6408.

17. Helton, M. E.; Maiti, D.; Zakharov, L. N.; Rheingold, A. L.; Porco, J. A.;

Karlin, K. D., A μ-η2 : η2-disulfide dicopper(II) complex from reaction of S_8 with a copper(I) precursor: Reactivity of the bound disulfur moiety. *Angew Chem Int Edit* **2006,** *45* (7), 1138-1141.

18. Brown, E. C.; Bar-Nahum, I.; York, J. T.; Aboelella, N. W.; Tolman, W. B., Ligand Structural Effects on Cu_2S_2 Bonding and Reactivity in Side-On Disulfido-Bridged Dicopper Complexes. *Inorg Chem* **2006,** *46* (2), 486-496.

19. Brown, E. C.; York, J. T.; Antholine, W. E.; Ruiz, E.; Alvarez, S.; Tolman, W. B., $[Cu_3(\mu\text{-}S)_2]^{3+}$ Clusters Supported by N-Donor Ligands: Progress Toward a Synthetic Model of the Catalytic Site of Nitrous Oxide Reductase. *J Am Chem Soc* **2005,** *127* (40), 13752-13753.

20. Brown, E. C.; Aboelella, N. W.; Reynolds, A. M.; Aullón, G.; Alvarez, S.; Tolman, W. B., A New Class of (μ-η2:η2-Disulfido)dicopper Complexes: Synthesis, Characterization, and Disulfido Exchange. *Inorg Chem* **2004,** *43* (11), 3335-3337.

21. York, J. T.; Bar-Nahum, I.; Tolman, W. B., Structural Diversity in Copper−Sulfur Chemistry: Synthesis of Novel Cu/S Clusters through Metathesis Reactions. *Inorg Chem* **2007,** *46* (20), 8105-8107.

22. York, J. T.; Brown, E. C.; Tolman, W. B., Characterization of a Complex Comprising a $\{Cu_2(S_2)_2\}^{2+}$ Core: Bis(μ-S_2^{2-})dicopper(III) or Bis(μ-$S_2^{\cdot-}$)dicopper(II) ? *Angewandte Chemie International Edition* **2005,** *44* (47), 7745-7748.

23. Armor, J. N.; Taube, H., Formation and reactions of $[(NH_3)_5RuN_2O^{2+}]$. *J Am Chem Soc* **1969,** *91* (24), 6874-6876.

24. Piro, N. A.; Lichterman, M. F.; Harman, W. H.; Chang, C. J., A Structurally Characterized Nitrous Oxide Complex of Vanadium. *J Am Chem Soc* **2011,** *133* (7),

2108-2111.

25. Neu, R. C.; Otten, E.; Lough, A.; Stephan, D. W., The synthesis and exchange chemistry of frustrated Lewis pair-nitrous oxide complexes. *Chemical Science* **2011,** *2* (1), 170-176.

26. Bar-Nahum, I.; Gupta, A. K.; Huber, S. M.; Ertem, M. Z.; Cramer, C. J.; Tolman, W. B., Reduction of Nitrous Oxide to Dinitrogen by a Mixed Valent Tricopper-Disulfido Cluster. *J Am Chem Soc* **2009,** *131* (8), 2812-2814.

27. Mondal, A.; Li, Y.; Khan, M. A.; Ross, J. H.; Houser, R. P., Supramolecular copper hydroxide tennis balls: Self-assembly, structures, and magnetic properties of octanuclear $[Cu_8L_8(OH)_4]^{4+}$ clusters (HL = N-(2-pyridylmethyl)acetamide). *Inorg Chem* **2004,** *43* (22), 7075-7082.

28. Chaudhuri, U. P.; Whiteaker, L. R.; Yang, L.; Houser, R. P., Multinuclear copper complexes of pyridylmethylamide ligands. *Dalton T* **2006,** (15), 1902-1908.

29. Chaudhuri, U. P.; Powell, D. R.; Houser, R. P., New examples of μ-η2:μ2-disulfido dicopper(II,II) complexes with bis(tetramethylguanidine) ligands. *Inorg Chim Acta* **2009,** *362* (7), 2371-2378.

30. Yang, L.; Wang, Z. D.; Powell, D. R.; Houser, R. P., A $[Cu_{16}S_{10}]^{4-}$ cluster containing μ3- and μ4-sulfido ligands. *Dalton T* **2009,** (23), 4439-4441.

CHAPTER 2

SYNTHESIS AND CHARACTERIZATION OF COPPER COMPLEXES WITH PYRIDYLALKYLAMIDE LIGANDS AND INVESTIGATION OF THEIR REACTIVITY WITH SULFUR OR SULFIDE REAGENTS

2.1. Introduction

Although much work has been done for the modeling chemistry of the Cu_Z active center, some unanswered questions about this novel Cu_4S cluster still exist. Such as no X-ray crystal structures of a N_2O adduct have been reported based on Cu-S complexes, and no synthesis of a structurally accurate and spectroscopically similar model complex. Both of them are big challenge for the chemist in this field. In addition, the proposed mechanism by Solomon based on computational studies is found to conflict with some new reported results from the Tolman group.[1] All of these reasons led us and others to investigate the synthetic modeling chemistry of the Cu_Z active site.

One of the main goals of model chemistry of the Cu_Z site is to synthesize low molecular weight Cu-S complexes with similar structural and spectroscopic features as the Cu_Z center. The most widely used and efficient method of obtaining Cu-S complexes is to use Cu(I) precursors reacting with elemental sulfur, followed by the formation and crystallization of Cu-S complexes. A good example of an end-on bound μ-1,2-disulfido dicopper(II) complex was reported in Karlin's group by the reaction of Cu(I) complex with elemental sulfur.[2] Recently, more Cu-S complexes were reported by Tolman's group and Karlin's group with the same synthetic strategy.[3-4] The second important method is to use the reaction between the Cu(II) precursors and sulfide reagents. Recently, Tolman and coworkers reported a series of multinuclear Cu-S model complexes with this synthetic approach.[5]

These reported Cu-S complexes have some similar structural features with the

Cu_Z center. But none of them shows reactivity towards nitrous oxide. Until 2009, Tolman's group reported a trinuclear Cu-S cluster, which reacts with excess N_2O under a He atomosphere at -80^oC slowly and generates N_2 as determined by GC-MS. This complex models key properties structurally and shows the reactivity towards N_2O relevant to the Cu_Z center. This cluster represents the most impressive progress towards the model chemistry studies of the Cu_Z center.[1] Inspired to obtain potential and better model complexes, we aimed to synthesize Cu-S complexes based on our ligand platform.

In our group, we focus on modeling the chemistry of the Cu_Z center using a series of pyridylmethylamide ligands with different substituents on the amide side arm (HL^R; R = H, Me_3, Ph and Ph_3 etc).[6,7,8] Changing the substituents or running the reaction with or without base resulted in different coordination modes of the ligands bound to the copper ions. An octanuclear copper(II) complex, $[Cu_8L_8(OH)_4](ClO_4)_2$, has been reported, which was well characterized by X-ray crystallography, EPR, electronic absorption spectra and magnetism.[6] Recently, some other multinuclear copper complexes, $[Cu_4(L^{Ph})_4(OH)_2](ClO_4)_2$, $[Cu_2(HL^{Me3})_2(OMe)_2](OTf)_2$ and $[Cu_2(HL^{Ph3})_2(OMe)_2](OTf)_2$, with a series of pyridylmethylamide ligands were also reported.[7]

In this thesis, as an extension to our main research, replacement of simple non-coordinating alkyl by the introduction of the coordinating phenol leads to a new family of pyridylalkyamide ligands as shown in Figure 2-1. The introduction of phenol group increases the coordination donor number of the ligand and also the phenolate O can act as a bridging group to connect two metal centers, which leads to

the formation of polynuclear copper complexes. These polynuclear copper complexes can be used as templates for the synthesis of the Cu_Z model complexes. The second reason for the introduction of the phenol group is related to the water derived O present in the Cu_Z center. The design and synthesis of the ligands will be described in 2.2. Then 2.3 and 2.4 will focus on Cu(I) and Cu(II) chemistry with the ligand system, followed by the reactivity studies of the Cu complexes with elemental sulfur or sulfide reagents in 2.5. In this part, the structural and spectroscopic studies of the $[Cu_{16}S_{10}]^{4-}$ cluster will be presented. Conclusions will be drawn from the copper chemistry study of the ligand system in 2-6.

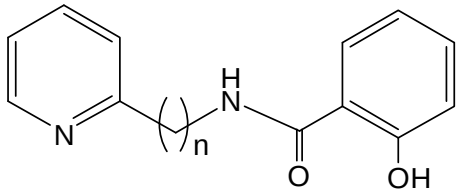

HL^{PhOH} (n=1); $HL^{PhOH'}$ (n=2)

Figure 2-1. Pyridylalkylamide Ligands.

2.2. Synthesis of Pyridylalkylamide Ligands

The copper chemistry of the pyridylmethyl ligand system with different substituents connected with an amide group has been well investigated in our group. In order to synthesize multinuclear copper complexes as precursors to obtain copper sulfide clusters as models for the Cu_Z active site in N_2OR, we introduced one phenol group into the ligands 2-hydroxyphenyl-N-(2-pyridylmethyl)acetamide (HL^{PhOH}) and 2-hydroxyphenyl-N-(2-pyridylethyl)acetamide ($HL^{PhOH'}$), which are different only in

the number of carbon atoms connecting the pyridyl group to the amide group. Both ligands were synthesized by the modified condensation reaction between salicylic acid and the corresponding 2-pyridylalkyl amine in the presence of coupling reagents DCC and HOBT, as shown in Figure 2-2.[6]

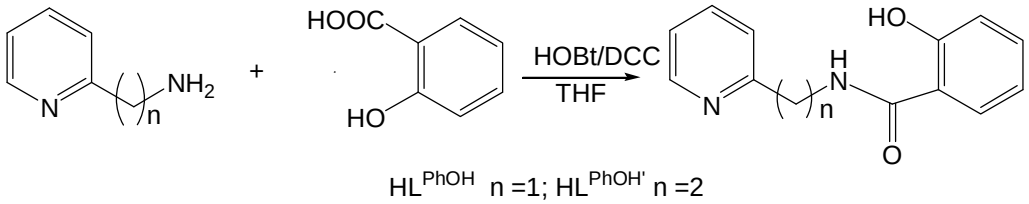

Figure 2-2. Synthesis of pyridylalkylamide ligands HL^{PhOH} and $HL^{PhOH'}$.

2.3. Copper(I) Complexes

2.3.1. $[Cu(HL^{PhOH})_2(CH_3CN)]BF_4$ ***(1)***

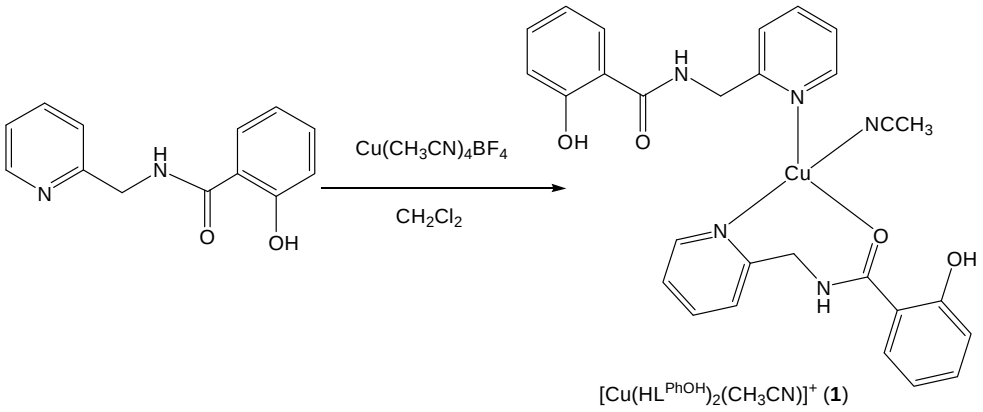

Figure 2-3. Synthesis of $[Cu(HL^{PhOH})_2(CH_3CN)]BF_4$ **(1)**

Complex $[Cu(HL^{PhOH})_2(CH_3CN)]BF_4$ **(1)** was obtained by mixing $[Cu(CH_3CN)_4]BF_4$ with ligand HL^{PhOH} in CH_2Cl_2 solvent. The resulting light yellow solution was filtered and vapor diffusion of diethyl ether into the filtrate resulted in the formation light yellow crystals suitable for X-ray analysis. The representation of the X-ray crystal structure is shown in Figure 2-4. X-ray analysis indicated that **1** is a mononuclear copper complex and the copper ion is four coordinate with two pyridyl N and one carbonyl O from the neutral HL^{PhOH} ligands, and the fourth position is occupied by one N atom from a CH_3CN molecule. One ligand coordinates to the copper ion in a bidentate mode through the pyridyl N and carbonyl O, while the other acts as a monodentate ligand by coordinating only via the pyridyl N.

The coordination geometry of four-coordinate complexes can be complicated, especially when the structure is an intermediate state between tetrahedral and square planar. So, how can we describe the difference of four coordinate copper complexes? Recently, Lei Yang in our group proposed a simple geometry index for four-coordinate complexes, τ_4 (equation 2-1),[9] which is similar to Addison and Reedijk's five-coordinate τ_5 index.[10] The formula is simply the sum of angles α and β- the two largest θ angles in the four-coordinate species - subtracted from 360º, all divided by 141º. The value of τ_4 ranges from 1.00 for a perfect tetrahedral geometry to 0.00 for a perfect square planar geometry. The value in the range of 0 to 1.00 can be described by intermediate structures, trigonal pyramidal or seesaw. For complex **1**, the value of τ_4 is 0.72. So, the geometry of this complex can best be described as a seesaw structure.

$$\tau_4 = \frac{360-(\beta+\alpha)}{141} \qquad (2\text{-}1)$$

The average Cu-N distance of 1.937 Å (see Table 2-1) is consistent with other reported copper(I) complexes. There are hydrogen bonding interactions between the amide N-H groups and the neighboring BF_4^- anions as shown in the packing structure (Figure 2-4). The intermolecular hydrogen bonding can be a driving force to stabilize the complex in the solid state.

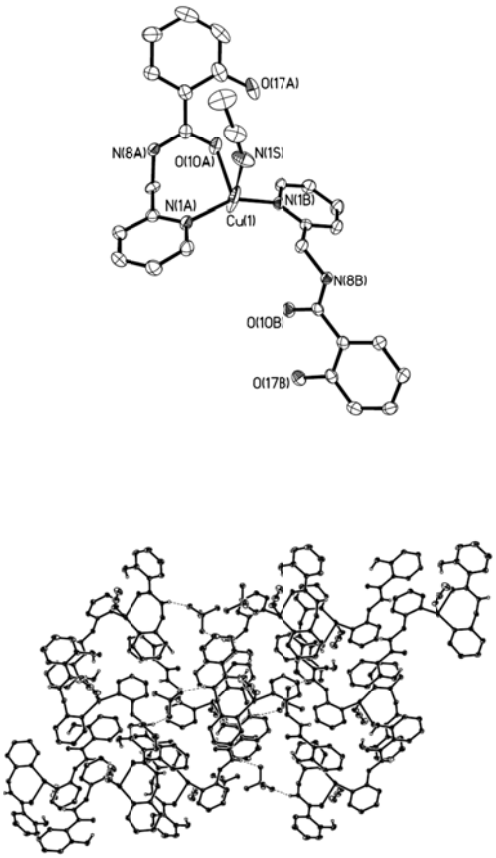

Figure 2-4. X-ray crystal structure (top) and packing diagram (bottom) for complex $[Cu(HL^{PhOH})_2(CH_3CN)]BF_4$ **(1)** with thermal ellipsoids at the 50% probability level. All H atoms have been omitted for clarity.

Table 2-1. Selected bond distances (Å) and angles (deg) for complex **1**.

Bond Lengths (Å)		Bond Angles (deg)	
Cu(1)-N(1B)	1.931(3)	N(1B)-Cu(1)-N(1A)	148.49(16)
Cu(1)-N(1A)	1.944(4)	N(1A)-Cu(1)-O(10A)	104.10(13)
Cu(1)-O(10A)	2.259(3)	N(1B)-Cu(1)-O(10A)	95.81(12)
Cu(1)-N(1S)	2.357(9)	N(1B)-Cu(1)-N(1S)	109.6(3)
		N(1A)-Cu(1)-N(1S)	97.0(3)
		O(10A)-Cu(1)-N(1S)	82.9(3)

2.2.2. [Cu(HL$^{PhOH'}$)$_2$]BF$_4$ ***(2)***

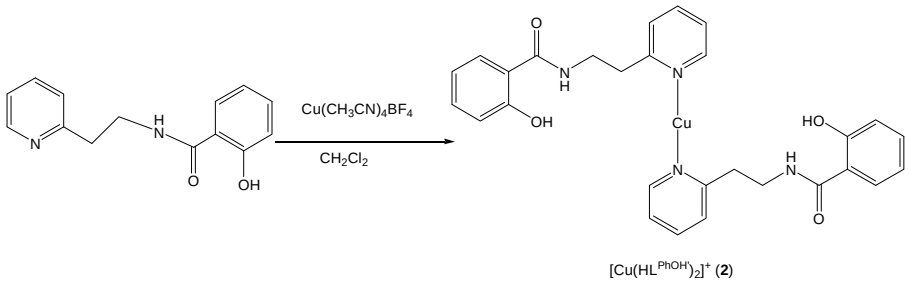

Figure 2-5. Synthesis of [Cu(HL$^{PhOH'}$)$_2$]BF$_4$ **(2)**

When a similar ligand HL$^{PhOH'}$ (see Figure 2-5) was used to replace HL^{PhOH} and reacted with [Cu(CH$_3$CN)$_4$]BF$_4$ in a 2:1 ratio, a new complex, [Cu(HL$^{PhOH'}$)$_2$]BF$_4$ **(2)** was obtained. It has different structural features and coordination geometry comparing to complex **1**. It is a mononuclear, linear, two-

coordinate complex in which the copper is coordinated by two pyridyl N from two $HL^{PhOH'}$ ligands. The Cu(1A)-N(1A) distance of 1.8872 Å is similar to previously reported Cu(I) complexes with N donor-containing ligands.[11] The bond angle of N(1A)-Cu(1A)-N(1AA) is 178.45(9)°, close to a linear geometry. The crystal structure and packing structure of this complex is shown in Figure 2-6. The longer distance (3.140 Å) between the Cu and the carbonyl O indicate very weak interactions, which is a huge difference compared to complex **1**. In complex **1**, the copper ion is coordinated by one carbonyl O, and forms a Cu-O bond with a distance of 2.259 Å, which can be attributed to the differences between ligand HL^{PhOH} and $HL^{PhOH'}$. The addition of one more CH_2 group between the pyridyl ring and the amide N limits the formation of the Cu-O bond interaction. There are also hydrogen bonding interactions between amide N-H groups and the neighboring BF_4^- anions as shown in the packing structure.

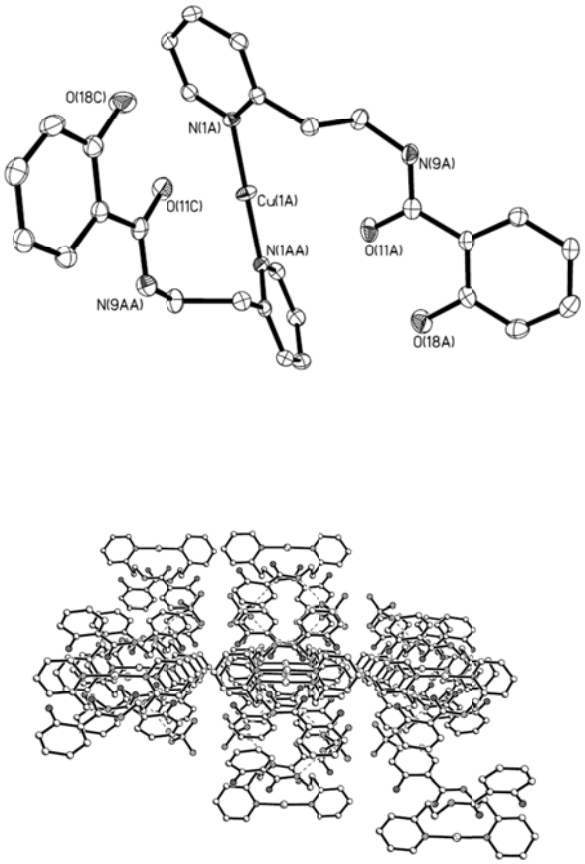

Figure 2-6. X-Ray crystal structure (top) and packing diagram (bottom) for complex $[Cu(HL^{PhOH'})_2]BF_4$ **(2)** with thermal ellipsoids at the 50% probability level. All H atoms have been removed for clarity.

Table 2-2. Selected bond distance (Å) and angle (deg) for complex **2**.

Bond Lengths (Å)		Bond Angles (deg)	
Cu(1A)-N(1A)	1.8872(16)	N(1A)-Cu(1A)-N(1AA)	178.45(9)°
Cu(1A)-N(1AA)	1.8872(16)		

2.4. Copper(II) Complexes

2.4.1. Mononuclear [Cu(HL^{PhOH})$_2$Cl$_2$] ***(3)***

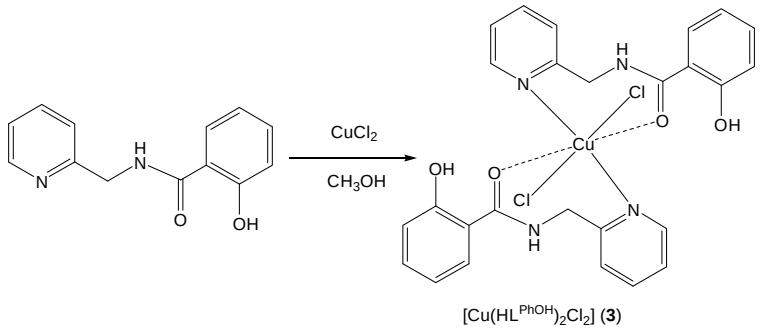

Figure 2-7. Synthesis of [Cu(HL^{PhOH})$_2$Cl$_2$] **(3)**

Addition of a solution of HL^{PhOH} in CH_3OH to a stirring blue solution of $CuCl_2$ in CH_3OH resulted in the formation of a green mixture with some precipitates. After the mixture was stirred for 2 hours, the blue filtrate was obtained by the filtration. Vapor diffusion of diethyl ether into the filtrate led to the formation of blue crystals suitable for X-ray analysis. The crystal structure of [Cu(HL^{PhOH})$_2$Cl$_2$] **(3)** reveals a mononuclear copper complex that consists of one copper, two neutral ligands and two Cl^- anions. The copper is six-coordinate with two pyridyl N atoms, two O atoms and two chloride ions, forming a distorted octahedral geometry. The Cu-N distance in complex **3** is 2.0408(15) Å. The longer Cu-O distance (2.5557(14) Å) indicates weak interaction between Cu and carbonyl O atoms. The complex was synthesized without a base to deprotonate the ligand, so both amide N and phenol O atoms do not coordinate to the copper ion. No crystals were obtained when the reaction was run in the presence of a base (e.g. Et_3N). In the packing structure, there is intramolecular hydrogen bonding between the carbonyl O and OH from the phenol

group with a O1···O2 distance of 2.695 Å and an O1-H···O2 bond angle of 144°. There is intermolecular hydrogen bonding between the Cl and NH amide groups, with a N···Cl distance of 3.261 Å and a N-H···Cl bond angle of 156°.

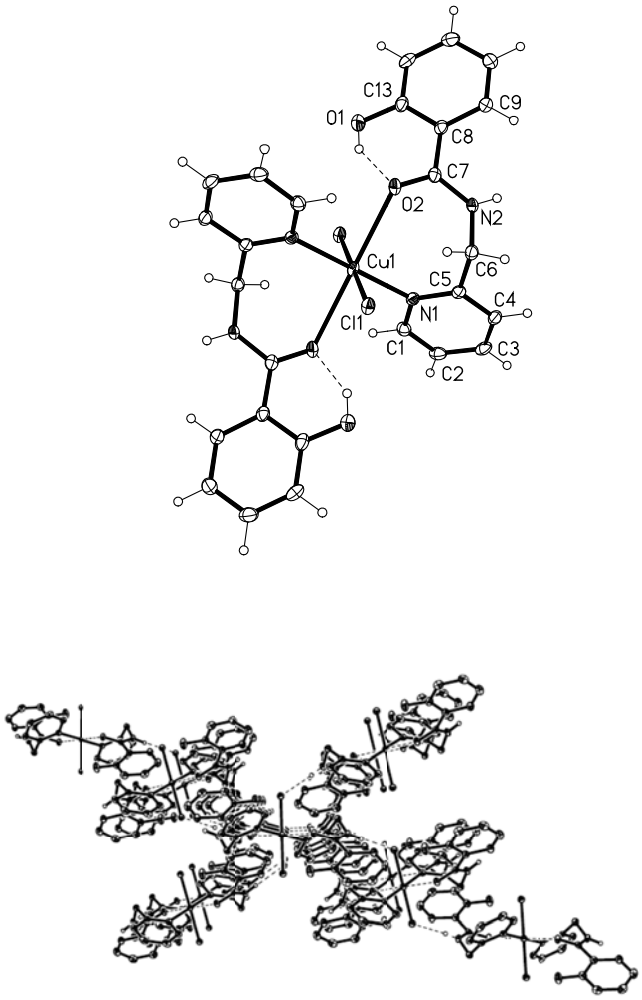

Figure 2-8. X-Ray crystal structure (top) and packing diagram (bottom) for complex $[Cu(HL^{PhOH})_2Cl_2]$ **(3)** with thermal ellipsoids at the 50% probability level.

Table 2-3. Selected bond distance (Å) and bond angle (deg) of complex **3**.

Bond Lengths (Å)		Bond Angles (deg)	
Cu(1)-N(1)	2.0408(15)	N(1)-Cu(1)-N(1A)	180.0
Cu(1)-Cl(1)	2.3062(6)	N(1)-Cu(1)-Cl(1)	91.33(4)
Cu(1)-O(2)	2.5557(14)	N(1A) -Cu(1)-Cl(1)	88.67(4)

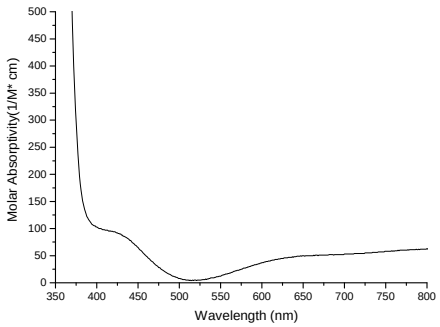

Figure 2-9. UV-Vis spectrum of complex **3** in CH_3OH solvent.

The electronic absorption spectrum of complex **3** in CH_3OH was collected, and it is typical of a copper(II) complex with pyridylamidate ligands, as shown in Figure 2-9. The absorption band at 430 nm can be assigned as a ligand to metal charge transfer transition (LMCT).

2.4.2. Tetranuclear [$Cu_4(L^{PhO})_4$] **(4)**

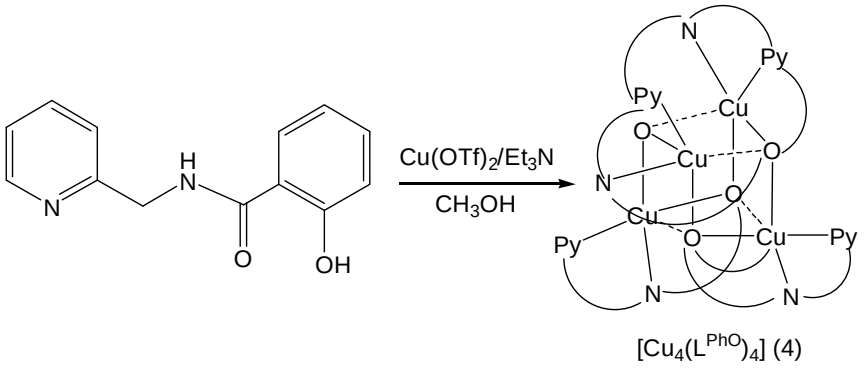

Figure 2-10. Synthesis of [$Cu_4(L^{PhO})_4$] **(4)**

Addition of solid $Cu(OTf)_2$ into a stirred solution of HL^{PhOH} in CH_3OH in the presence of Et_3N resulted in the formation of a dark green solution. After filtration, vapor diffusion of diethyl ether into the filtrate produced dark green crystals suitable for X-ray analysis. The X-ray crystal structure of [$Cu_4(L^{PhO})_4$] is shown in Figure 2-11. Crystallographic analysis shows that [$Cu_4(L^{PhO})_4$] consists of four copper(II) atoms and four fully deprotonated ligands, $(L^{PhO})^{2-}$. Each copper ion is four-coordinate with one N(py), one N(amide), and O(phenolate) from one ligand, and the fourth coordination site is occupied by one oxygen from the second ligand, forming a square planar geometry. This geometry is supported by a τ_4 value of 0.04, close to zero for perfect square planar geometry.[9] Each copper is bridged by one μ_2-phenolato atom.

The Cu_4O_4 core structure forms a partial cube. Four Cu(II) and four O atoms occupy the alternating vertices of the cube. Four copper atoms are bridged by four oxygen atoms. The Cu-N and Cu-O bond lengths range from 1.8892(16) to

1.9948(16) Å and from 1.9451(13) to 1.9906(13) Å, respectively. The *trans* angles of the copper centers are in the range of 175.67-179.20°, which support the slightly distorted square-planar geometry assignment. The phenolate-bridged Cu···Cu distances are in the range from 3.279 Å (Cu1B···Cu1C) to 3.291 Å (Cu1A···Cu1B), while the unbridged Cu···Cu distances are 3.218 Å (Cu1A···Cu1C) or 3.288 Å (Cu1B···Cu1D). In addition, the weak interactions in the apical position of each copper center are evident from the long Cu···O (phenolato) distances. Both distances are very close, with the Cu···O (phenolato) distances in the apical positions of 3.727 Å (Cu1A···O17D) and 3.690 Å (Cu1B···O17A). Strong π···π interactions are found between the aromatic pyridyl ring and the phenolate aromatic ring, with centroid-centroid distances of 3.426 Å and 3.727 Å.

Other hydroxo or alkoxo-bridged tetranuclear copper complexes have been reported with similar cubane-like structures.[12] In most cases, the copper is five-coordinate with N or O from a variety of organic ligands. $[Cu_4(L^{PhO})_4]$ is the first four-coordinate phenolate-bridged tetranuclear copper complex with a distorted open cubane-like geometry.

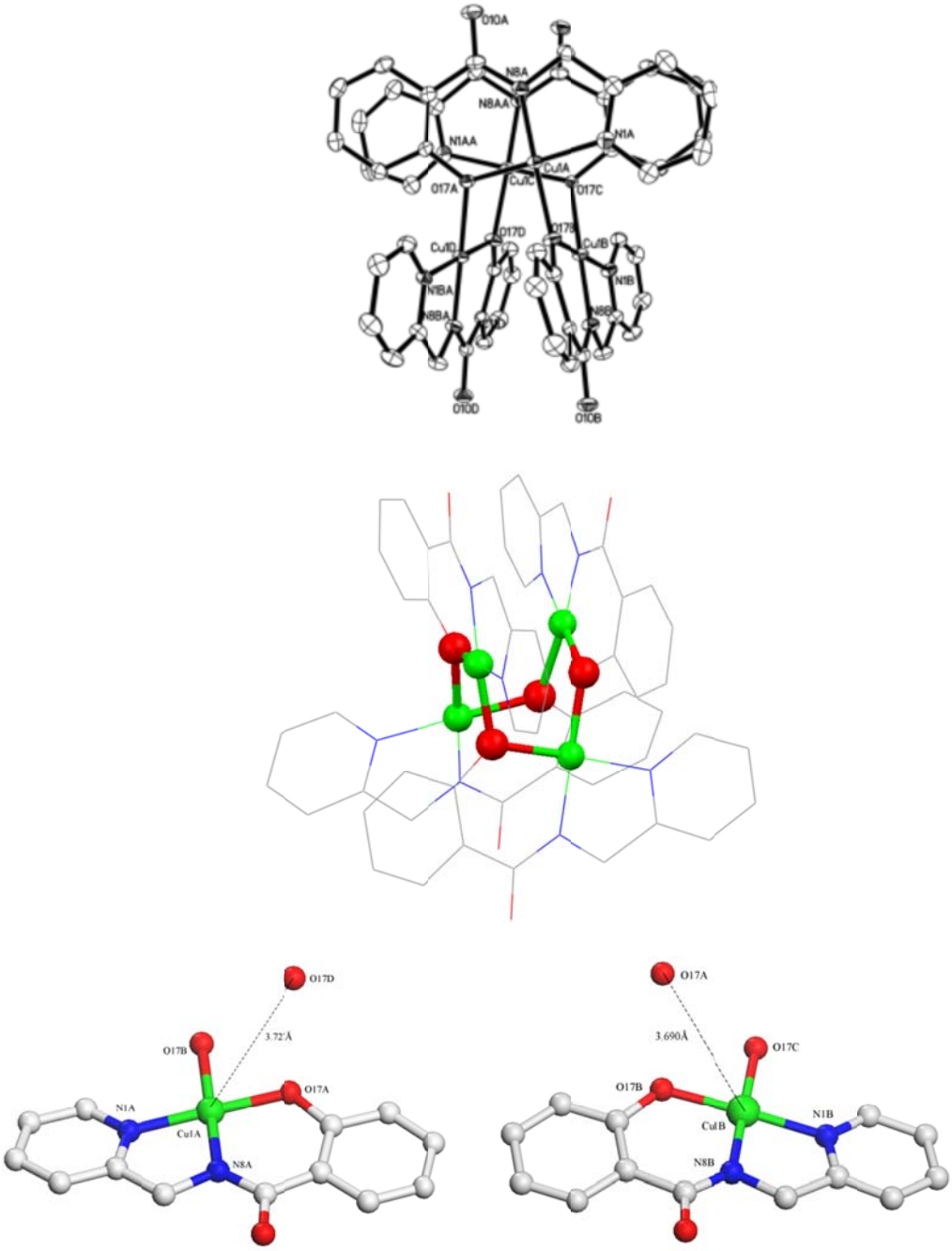

Figure 2-11. X-Ray crystal structure (top) and core cubane structure (middle) for complex $[Cu_4(L^{PhO})_4]$ **(4)**. Bottom: the coordination environment of the copper centers and the corresponding Cu···O distances. All H atoms have been omitted for clarity.

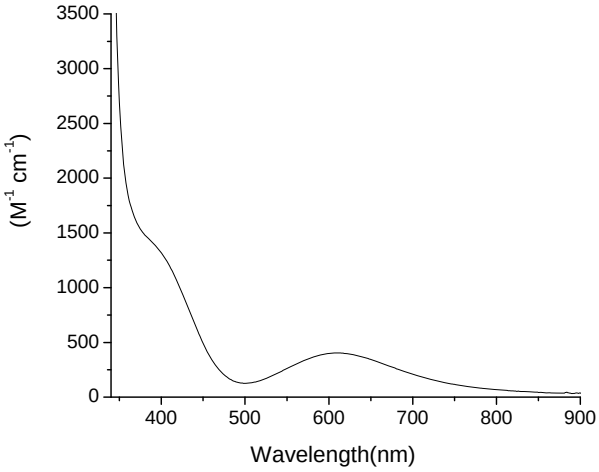

Figure 2-12. Electronic absorption spectrum of complex **4** in CH_3OH.

The electronic absorption spectrum of complex **4** in CH_3OH was collected, and is typical of a copper(II) complex with pyridylamidate ligands as shown in Figure 2-12. The absorption band at 400 nm can be assigned as ligand-to-metal charge transfer transition (LMCT), and a weak absorption band at 611 nm can be assigned as a *d-d* transition.

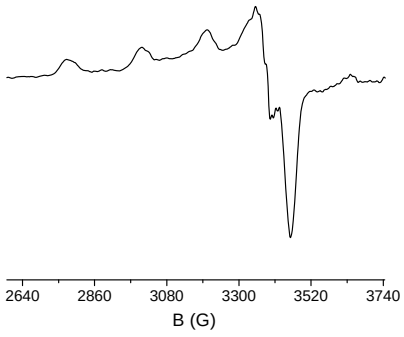

Figure 2-13. EPR spectrum of complex **4** in CH_3OH at 77K.

The X-band EPR spectrum of complex **4** dissolved in MeOH was measured at 77K, and indicated a typical four-line hyperfine feature due to the interaction of electron spin (S=1/2) with the nuclear spin of copper (I = 3/2). The anisotropic spectra morphology ($g_{\parallel}>g_{\perp}>g_e$ = 2.0023) as shown in Figure 2-13 is typical of a square planar copper(II) complex. The ESI-MS data for the cluster in MeOH reveals the presence of the complex in solution. The peak at m/z = 601.90 matches with the cluster plus two sodium ions, $\{[Cu_4(L^{PhO})_4] + 2Na\}^{2+}$, and the peak at m/z = 1181.06 corresponds to the cluster plus one sodium ion, $\{[Cu_4(L^{PhO})_4] + Na\}^{+}$.

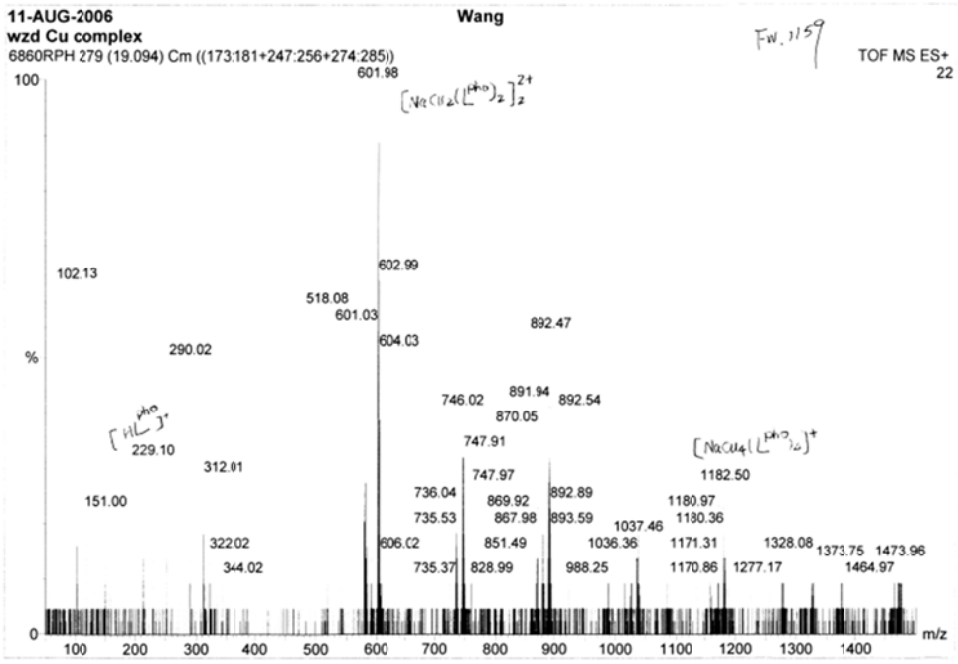

Figure 2-14. ESI-MS of $[Cu_4(L^{PhO})_4]$ **(4)** in MeOH.

Many factors contribute to the magnetic properties of the Cu_4O_4 series of cluster complexes, like Cu···O and Cu···Cu distances, Cu-O-Cu bond angles, and

the geometry of the copper center. Cu-O-Cu bond angles have proven to be the main factor in determining the magnetic properties. The magnetic moment (μ_{eff}) was measured on solution of **4** by the Evans method, with a value of 1.813 BM/Cu, which indicates no antiferromagnetic interactions between the copper atoms comparing with other reported Cu_4O_4 clusters due to the larger Cu-O-Cu bond angles (112.8-113.2°).[13]

Table 2-4. Selected bond distances (Å) and angle (deg) for complex **4**.

Bond Lengths (Å)		Bond Angles (deg)	
Cu(1A)-N(8A)	1.8892(16)	N(8A)-Cu(1A)-O(17A)	94.36(6)
Cu(1B)-N(8B)	1.8916(16)	N(8A)-Cu(1A)-O(17B)	175.67(6)
Cu(1A)-O(17A)	1.9451(13)	O(17A)-Cu(1A)-O(17B)	85.42(5)
Cu(1B)-O(17B)	1.9619(14)	N(8A)-Cu(1A)-N(1A)	84.60(7)
Cu(1A)-O(17B)	1.9906(13)	O(17A)-Cu(1A)-N(1A)	178.95(6)
Cu(1B)-O(17A)	1.9833(16)	O(17B)-Cu(1A)-N(1A)	95.63(6)
Cu(1A)-N(1A)	1.9948(16)	N(8B)-Cu(1B)-O(17B)	93.57(6)
Cu(1B)-N(1B)	1.9910(16)	N(8B)-Cu(1B)-N(1B)	84.32(7)

2.4.3 Binuclear $[Cu_2(L^{PhO'})_2(CH_3OH)_2]$ **(5)**

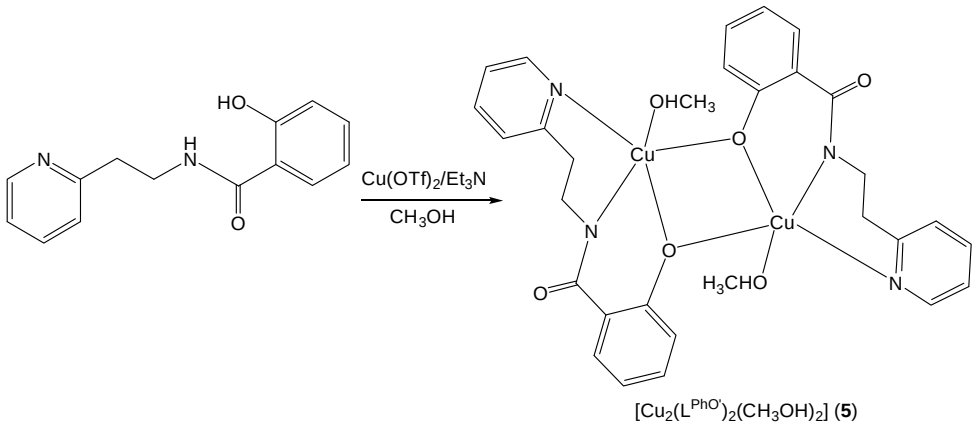

Figure 2-15. Synthesis of $[Cu_2(L^{PhO'})_2(CH_3OH)_2]$ **(5).**

Binuclear $[Cu_2(L^{PhO'})_2(CH_3OH)_2]$ **(5)** was obtained with the same synthetic method as complex **4** using the $HL^{PhOH'}$ ligand to replace HL^{PhOH}. Comparing with complex **4**, the structure of complex **5** is totally different, with a binuclear copper structure that consists of two copper ions and two deprotonated ligands, $(L^{PhO'})^{2-}$. Each copper is five-coordinate with two N donors (pyridyl and amidate), one O donor (phenolate) from one ligand, and one O donor (phenolate) from the second ligand. The fifth coordination site is occupied by a methanol solvent molecule, forming a distorted square pyramid geometry supported by the τ_5 value of 0.180.[10] The Cu-O (MeOH) bond (2.3476(14)) Å is longer than any other Cu-O (1.95-1.98 Å) and Cu-N (1.93-1.99 Å) bond distances, which indicates that the O from methanol occupies the apical position of the square pyramids. The basal positions are occupied by two N and two O from the ligands. The N_2O_2 donor set is almost planar, and the Cu1 and Cu2 centers are displaced from their mean plane by 0.1076 Å and

0.1215 Å toward the corresponding O atom from methanol molecule. The Cu···Cu distance is 3.062 Å. Similar trends are observed in other reported phenolate-bridged dicopper complexes.[14]

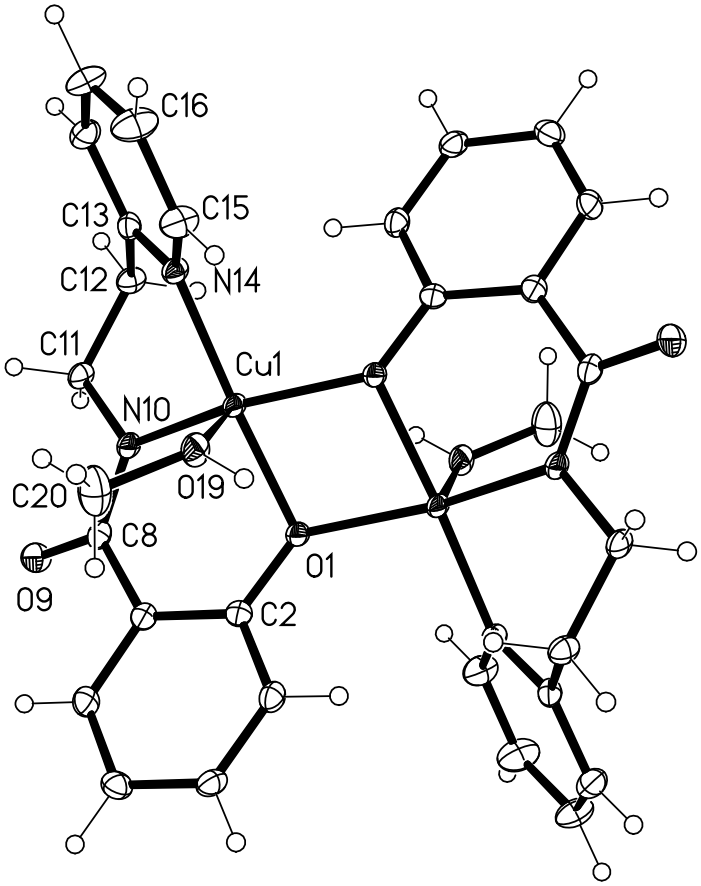

Figure 2-16. X-ray crystal structure of complex $[Cu_2(L^{PhO'})_2(CH_3OH)_2]$ **(5)**, with thermal ellipsoids at the 50% probability level.

The magnetostructural relationship in phenolate-bridged binuclear copper complexes has been widely investigated. The effective magnetic moment (μ_{eff}) of complex **5** is 1.879 BM/Cu, which suggests no antiferromagnetic interaction between the two copper atoms. The X-band EPR spectrum of complex **5** is similar

to complex **4,** and shows a typical axial signal, suggesting dissociation into monomers in solution. The electrospray ionization mass spectra (ESI-MS) of **5** reveals the presence of the compound, with a peak at *m/z* = 607.87 corresponding to $\{[Cu_2(L^{PhO'})_2] + H\}^+$ without the coordinated methanol molecules.

Table 2- 5. Selected bond distances (Å) and angle (deg) for complex **5.**

bond distance (Å)		bond angle (deg)	
Cu1-N10	1.9362(16)	N10-Cu1-O1	91.83(6)
Cu1-O1	1.9530(13)	N10-Cu1-O1#1	158.42(6)
Cu1-O1#1	1.9831(13)	N10-Cu1-N14	93.50(7)
Cu1-N14	1.9954(17)	O1-Cu1-N14	173.74(6)
Cu1-O19	2.3476(14)	N10 -Cu1-O19	86.96(5)
		N14 -Cu1-O19	88.21(6)

2.5. Reactivity Studies of Cu Complexes with Sulfur or Sulfide Reagents

Cu(I) complexes **1** and **2** are relatively stable and can be stored in the glove box under a dinitrogen atomosphere. However, they are easily oxidized by dioxygen when exposed to the air. In order to synthesize Cu-S complexes, we ran the reactions of complexes **1** and **2** with elemental sulfur in the glove box. Unfortunately the reactions resulted in the formation of green mixtures with some black precipitate. After filtration, a turbid light green liquid and some uncharacterized black precipitate were isolated. This method to synthesize Cu-S

complexes did not work well for this ligand system.

Additionally, we tried a second method to synthesize the Cu-S complexes. Tetranuclear Cu(II) complex **4** was used as a precursor to react with tetrabutylammonium hydrogen sulfide, TBASH, leading to the formation of a naked Cu-S cluster $(TBA)_4[Cu_{16}S_{10}]$. This complex does not contain any organic ligand. This cluster was also synthesized by a different synthetic reaction by Lei Yang in our group. The mixed-valence copper complex $[Cu_2(L1)_2]OTf$ (HL1= 2-phenyl-N-(2-pyridylmethyl)acetamide; OTf = trifluoromethanesulfonate) was treated with three equivalents of $(n Bu_4N)SH$ as shown in equation 2-2.

$$8[Cu_2(L1)_2]OTf + 24(nBu_4N)SH \longrightarrow (nBu_4N)_4[Cu_{16}S_{10}] \qquad (2\text{-}2)$$

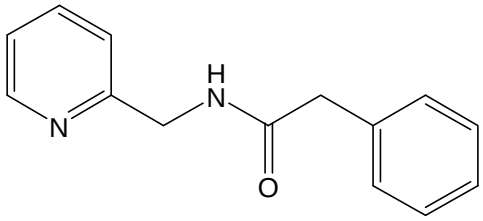

HL1

X-ray analysis reveals that $(TBA)_4[Cu_{16}S_{10}]$ consists of four TBA^+ cations and an unusual $[Cu_{16}S_{10}]^{4-}$ anionic cluster as shown in Figure 2-17.[15] It contains eight μ_3- and two μ_4-sulfido atoms. Each μ_3-sulfido atom binds with three Cu to form triangular faces with an average Cu-S distance of 2.16(2) Å and an average Cu-S-Cu angle of 79.2 (9)°. Two μ_4-sulfido atoms occupy the top and bottom positions of the cluster with an average Cu-S bond distance of 2.17(1) Å and an average Cu-S-Cu angle of 77.7(6)°. The Cu…Cu distances ranges from 2.689(6) to 2.775(7) Å, which are slightly shorter than those reported in a $[Cu_{12}S_8]^{4-}$ cluster.[21] The fully reduced copper(I) oxidation state in the cluster is supported by both charge balance and

spectroscopic evidence. There are no *d-d* transitions in the UV-Vis spectrum, and $(TBA)_4[Cu_{16}S_{10}]$ is EPR silent. The negative mode ESI-MS indicates the thermodynamic stability of the cluster in CH_3CN solution. The only recognizable peak at *m/z*=1359.7 can be assigned as the partially oxidized form of the cluster $\{Na[Cu^{II}_2Cu^{I}_{14}S_{10}]\}^-$ (sodium is presumably from the instrument) as shown in Figure 2-18. [16]

The $(TBA)_4[Cu_{16}S_{10}]$ cluster was synthesized based on two different copper precursors: A mixed-valent copper dimer and a tetranuclear copper(II) complex, respectively. Both methods involve the redox reaction of copper and hydrogen sulfide. The mixed-valence copper or copper(II) starting materials were reduced to copper(I) and the hydrogen sulfide was oxidized to form disulfide species. Different stoichiometries were attempted in the synthesis of the cluster, we can only isolate and crystalize the cluster with ratio of hydrogen sulfide to copper close to 1.5 as shown in our proposed reaction in equation 2-3.

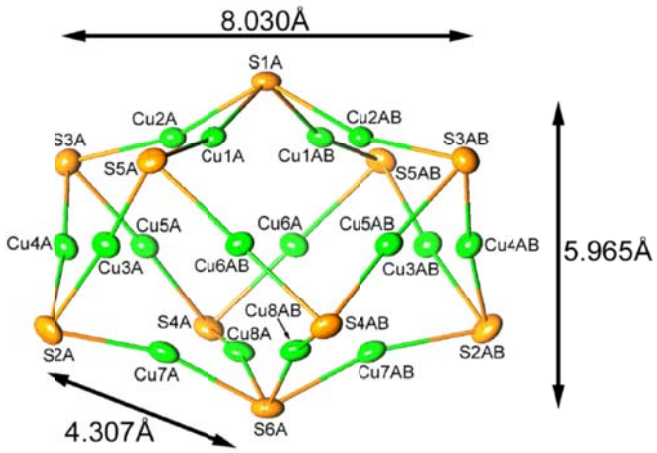

Figure 2-17. X-ray structure of the $[Cu_{16}S_{10}]^{4-}$ portion of the cluster with gyroelongated square dipyramid with thermal ellipsoids at 30% probability level. Figure is adapted from the reference 15

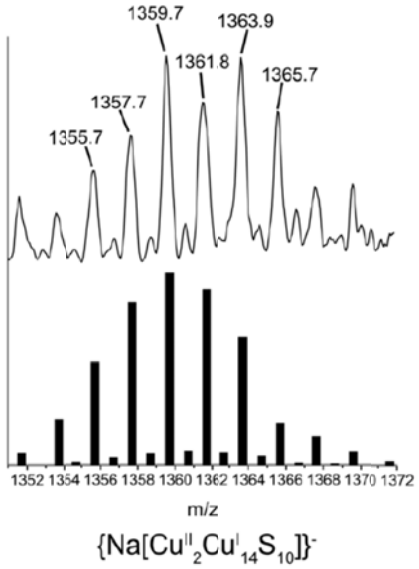

Figure 2-18. Experimental (top) and calculated (bottom) isotope patterns of $(TBA)_4[Cu_{16}S_{10}]$ in ESI-MS negative mode. Figure is adapted from reference 15 .

According to the different stoichiometries we attempted in the synthesis of the cluster from the $[Cu_4L^{PhO}{}_4]$ as a starting material, it is likely that excess hydrogen sulfide was needed to reduce copper(II) to copper(I). We proposed the reasonable reaction as shown in equation 2-3.

$$4[Cu_4L^{PhO}{}_4] + 26TBASH \xrightarrow{CH_3CN} TBA_4[Cu_{16}S_{10}] + 16L^{PhO2-} + 8HSSH + 22TBA^+ + 10H^+ \quad (2\text{-}3)$$

This naked Cu-S cluster could be a good candidate for the low molecular weight model complex of the Cu_Z active site from the nitrous oxide reductase. There are two μ_4-sulfido bridged four-copper units partially similar to the Cu_4S cluster in the Cu_Z center. The average Cu-S bond distances are 2.176 Å for $[Cu_{16}S_{10}]^{4-}$ and 2.178 Å in the enzyme. The molecular geometry of the Cu_4S is square pyramidal for $[Cu_{16}S_{10}]^{4-}$ and see-saw in the Cu_Z active center. So, the $[Cu_{16}S_{10}]^{4-}$ cluster partly models the structural features of the Cu_Z site. Since it is very difficult to obtain scalable crystals for the N_2O reactivity studies, our lab is still exploring other synthetic methods to obtain $(TBA)_4[Cu_{16}S_{10}]$ with higher yields, followed by N_2O reactivity studies.

2.6. Conclusions

In this chapter, the design and synthesis of two new pyridylalkylamide ligands HL^{PhOH} and $HL^{PhOH'}$ as an extension to previous work in our lab was described. With these two ligands in hand, we synthesized and characterized a series of Cu complexes, which included both Cu(I) complexes and Cu(II) complexes. The reactions between other Cu(I) precursors and elemental sulfur was proved to be an effective strategy to obtain Cu-S complexes in the literature. So, we investigated the reaction of complex $[Cu(HL^{PhOH})_2(CH_3CN)]BF_4$ (1) and $[Cu(HL^{PhOH'})_2]BF_4$ (2) with elemental sulfur. Both reactions produced uncharacterizable black precipitate. The isolation of any stable powders from these reactions was unsuccessful, which led to negative results from this synthetic strategy.

Two polynuclear copper(II) complexes were synthesized and characterized: $[Cu_4(L^{PhO})_4]$ (4) and $[Cu_2(L^{PhO'})_2(CH_3OH)_2]$ (5).In both complexes, each ligand has two N donors and one phenolate O donor available to coordinate with the copper ions. The different part is the alkyl (methyl or ethyl) linker between the pyridine and amine group, which has some important effects on the nuclearity of the copper complex formed. In the tetranuclear copper complex 4 , the ligand HL^{PhOH} forms five-member rings between the copper and two nitrogen donor atoms, while in the binuclear copper complex it forms a six-member ring between the copper and two nitrogen donor atoms. In addition, the coordination mode of the copper is different: complex 4 is four-coordinate with square planar geometry of each copper, while

complex 5 is five-coordinate with distorted square pyramid geometry of the copper. All of these differences show the effects of ligand flexibility on the nuclearity and the coordination modes of the copper centers.

Some polynuclear copper complexes have been reported in our group based on pyridylmethylamide ligands. One octanuclear copper complex was obtained by the reaction of copper perchlorate or copper triflate with HL ligand (HL = N-(2-pyridylmethyl)acetamide). It contains eight copper and eight deprotonated ligands and four hydroxide bridging anions. In this complex, all N and O donors are involved in the coordination. Comparing with my tetranuclear copper complex 4, HL^{PhOH} has N_2O_2 donors, the carbonyl O does not coordinate with the copper center. The phenolate O has priority over carbonyl O to coordinate with the copper center.

As we know, Cu_Z center is a tetranuclear copper sulfur cluster. Our complex 4 is also a tetranuclear cluster. If one sulfide is inserted into complex 4, a potential structural model can be obtained for the Cu_Z center. We focused on the reactivity study of complex 4 with different sulfide or hydrogen sulfide reagents based on our proposed design. Reaction of Complex 4 with Li_2S in methanol at -20^oC led to the formation of brown yellow solution and downy black product. Then we changed to CH_3CN solvent to run the same reaction at room temperature, which resulted in the formation of green precipitate with poor solubility. In addition, we also did the reaction of complex 4 with NaHS in DMF solvent. Crystallization of the filtrate from the reaction failed to produce a Cu-S complex. Only when we did the reaction of complex 4 with (nBu$_4$N)SH with a specific stoichiometry. A a naked $[Cu_{16}S_{10}]^{4-}$ cluster isolated and crystallized. This cluster was also synthesized and characterized

by Lei Yang in our group from the reaction of a mixed-valence dimer and (nBu$_4$N)SH.

Our cluster (nBu$_4$N)$_4$[Cu$_{16}$S$_{10}$] only consists of copper and sulfur. We thought that the cluster might be synthesized from simpler starting materials. All reactions we attempted by treating simple Cu(I) or Cu(II) salts with (nBu$_4$N)SH or NaSH in appropriate ratios led to the formation of insoluble copper sulfide precipitates. This is the only set of condition to obtain the cluster except the previous reported method by Lei Yang in our group. So, the pre-organization of the copper ions in either the dimer or the tetramer appears to favor the formation of the cluster. The structural comparison of our naked cluster with the Cu$_Z$ center reveals some similarity of Cu-S bond distances and the presence of a common μ_4-sulfide bridged tetracopper unit. Unfortunately we cannot investigate the N_2O reactivity studies of the cluster due to its lower yield and instability. Our studies still enrich the synthetic model chemistry of the Cu$_Z$ center.

2.7. Experimental

General. All chemical reagents were purchased from commercial suppliers and used without further purification, unless otherwise stated. All solvents used were doubly purified using alumina colunms in a MBraun solvent purification system (MB-PBS). In addition, all Copper(I) complexes were prepared in a glove box. [Cu(CH$_3$CN)$_4$]BF$_4$ was synthesized according to previously reported procedures.[17] ^{1}H NMR spectra were recorded on a Varian 300 MHz spectrometer with deuterated

solvent as an internal standard. Elemental analysis were conducted by Atlantic Microlabs, Norcross, GA. FTIR spectra were collected on NEXUS 470 FTIR spectrometer with the KBr pellet technique. Mass spectra were recorded on a Q-TOF quadrupole time-of-flight mass spectrometer with an electrospray ionization (ESI) source. X-Band EPR spectra of the complexes were recorded using Bruker EMX spectrometer in dichloromethane, acetonitrile, or DMSO at 77K in frozen solutions. Solution magnetic moment measurements were measured using the Evans method.[18]

2-Hydroxyphenyl-N-(2-pyridylmethyl) acetamide HL^{PhOH}: The synthesis of HL^{PhOH} was synthesized by a modified method based on a published report.[8] A solution of salicylic acid (3.0 g, 21.75 mmol) in anhydrous THF (10 mL) was added to a solution of 2-aminomethyl pyridine (2.352 g, 21.75 mmol) in the presence of HOBt (2.94 g, 21.75 mmol) in anhydrous THF (30 mL) at -10 ºC. To this solution, DCC·H_2O (4.488 g, 21.75 mmol) dissolved in a small volume of THF (5 mL) was added drop wise over 10 min. The resulting mixture was stirred at -10 ºC for 1 h, allowed to warm to room temperature, and then stirred for another 20 h. The DCU precipitate was removed by filtration, the filtrate was concentrated under reduced pressure. Finally, the ligand was purified by silica chromatography, producing HL^{PhOH} as a white solid in good yield. Yield: 3.2 g, 64%. Calcd for $C_{13}H_{12}N_2O_2$: C, 68.41; H, 5.30; N, 12.27. Found: C, 68.15; H, 5.53; N, 12.19. ^{1}H NMR (300MHz, CH_2Cl_2-*d*); δ 4.60 (d, 2H), 7.28-7.80 (m, 8H), 8.02 (s, 1H) ppm. FTIR (KBr): 3360, 3057, 3024, 2928, 2850, 2664, 2564, 1638, 1598, 1568, 1538, 1454, 1307, 1241,

1012, 774, 758, 639, 611, 530, 507, 416 cm^{-1}.

2-Hydroxyphenyl-N-(2-pyridylethyl) acetamide $HL^{PhOH'}$: The synthesis of $HL^{PhOH'}$ is similar to the ligand HL^{PhOH} with 2-aminoethyl pyridine as starting material instead of 2-aminomethyl pyridine. Yield: 3.50 g, 70%. Calcd for $C_{14}H_{14}N_2O_2$: C, 69.42; H, 5.79; N, 11.60. Found: C, 68.83; H, 5.92; N, 11.28. ^1H NMR (300 MHz, CH_3CN-*d*); δ 3.15 (d, 2H), 3.78 (d, 2H), 7.27-7.77 (m, 8H), 7.92 (s, 1H) ppm. FTIR (KBr): 3362, 3077, 2927, 2850, 2654, 2572, 1638, 1603, 1541, 1479, 1439, 1311, 1292, 1217, 1099, 1007, 767, 746, 637, 613, 528, 528, 515 cm^{-1}.

$[Cu(HL^{PhOH})_2(CH_3CN)]BF_4$] (1): A solution of $[Cu(CH_3CN)_4]BF_4$ (0.0788 g, 0.25mmol) in CH_3CN was added to a solution of HL^{PhOH} (0.114 g, 0.50 mmol) in CH_3CN, giving a light yellow solution. The reaction solution was stirred for 2h. After filtration, a clear, light yellow solution was isolated. Vapor diffusion of diethyl ether into the filtrate formed light yellow crystals Yield: 0.097 g, 60%. FTIR (KBr): 3502, 2361, 2337, 1653, 1558, 1384, 1260, 883 cm^{-1}.

$[Cu(HL^{PhOH'})_2]BF_4$ (2): A solution of $[Cu(CH_3CN)_4]BF_4$ (0.0788 g, 0.25 mmol) in CH_3CN was added to a solution of $HL^{PhOH'}$ (0.121 g, 0.50 mmol) in CH_3CN, giving a light yellow solution. The solution was stirred for 3h, then after the filtration, it produced a light yellow filtrate. Vapor diffusion of diethyl ether into the filtrate formed light yellow crystals Yield: 0.0982 g, 62%. FTIR (KBr): 3424, 1733, 1606, 1540, 1083, 1033, 521 cm^{-1}.

$[Cu(HL^{PhOH})_2Cl_2]$ (3): A solution of $CuCl_2$ (0.034 g, 0.25 mmol) in methanol was added to a solution of HL^{PhOH} (0.117 g, 0.50 mmol) in methanol, forming the blue solution with a green precipitate. After filtration of the mixture, the blue filtrate was isolated and vapor diffusion of diethyl ether resulted in blue crystals of $[Cu(HL^{PhOH})_2Cl_2]$ Yield: 0.094 g, 64%. Anal. Calcd for $C_{26}H_{24}Cl_2CuN_4O_4$: C, 52.79; H, 4.06; N, 9.48. Found: C, 52.89; H, 4.08; N, 9.34. FTIR (KBr): 3281, 1633, 1597, 1539, 1482, 1336, 1303, 1206, 957, 754, 677, 613, 545 cm^{-1}. UV-Vis [CH_3OH, λ_{max}, nm (ε, $mol^{-1}cm^{-1}$)]: 400 (106). ESI-MS (CH_3OH): *m/z* = 578.93, $[Cu_2(L^{PhO})(HL^{PhO})]^+$; 290.07, $[Cu(HL^{PhO})]^+$; 229.13, $[HL^{PhOH} + H^+]^+$. EPR (CH_3OH, 77K, 9.454 GHz, 0.63 mW): $g_\perp = 2.045$, $g_\parallel = 2.228$, $A_\parallel = 169$ G. Magnetic moment (Evans method, 293K, DMSO-d_6): 1.683 BM/Cu.

$[Cu_4(L^{PhO})_4]$ (4): A solution of $Cu(OTf)_2$ (0.0905 g, 0.25 mmol) in methanol was added to a solution of HL^{PhOH} (0.114 g, 0.50 mmol) and triethylamine (0.147 mL, 1 mmol) in methanol, forming a dark green solution. Vapor diffusion of diethyl ether into this solution resulted in the formation of dark green crystals suitable for crystallographic characterization. Yield: 0.0456 g, 62.9%. Anal. Calcd for $C_{52}H_{40}Cu_4N_8O_8 \cdot (CH_4O)_2$: C, 53.02; H, 3.96; N, 9.16. Found: C, 52.86; H, 4.44; N, 9.35. FTIR (KBr): 3750, 3435, 1772, 1733, 1695, 1653, 1599, 1587, 1548, 1444, 1383, 1215, 1162, 1097, 756, 619, 589, 516, 464 cm^{-1}. UV-vis [CH_3OH, λ_{max}, nm (ε, $mol^{-1}cm^{-1}$)]: 390 (1400), 611 (400). ESI-MS (CH_3OH): *m/z* = 601.98, $[NaCu_2(L^{PhO})_2]_2^{2+}$, *m/z* = 1181.06, $[NaCu_4(L^{PhO})_4]^+$. EPR (CH_3OH, 77K, 9.455GHz, 0.25mW): $g_\perp$ =

2.04, $g_{\|}$ = 2.246, $A_{\|}$= 184 G. Magnetic moment (Evans method, 293K, DMSO-d_6): 1.813 BM/Cu.

$[Cu_2(L^{PhO'})_2(CH_3OH)_2]$ (5): A methanolic solution of $Cu(OTf)_2$ (0.0905 g, 0.25 mmol) was added to a solution of $HL^{PhOH'}$ (0.121 g, 0.50 mmol) and triethylamine (0.147 mL, 1 mmol) in the methanol, forming a green solution. Green crystals were obtained by vapor diffusion of diethyl ether into the solution of the complex. Yield: 0.057g, 68%. Anal. Calcd for $C_{30}H_{32}Cu_2N_4O_6$: C, 53.65; H, 4.77; N, 8.34. Found: C, 53.06; H, 4.56; N, 8.30. FTIR (KBr): 3146, 2946, 2842, 1608, 1595, 1574, 1531, 1486, 1447, 1387, 1259, 1147, 1079, 887, 763, 703, 657, 586, 514, 427 cm^{-1}. UV-Vis [CH_3OH, λ_{max}, nm (ε, $mol^{-1}cm^{-1}$)]: 620 (112). ESI-MS (CH_3OH): *m/z* = 628.87, $[NaCu_2(L^{PhO'})_2]^+$, *m/z* = 607.87, $[Cu_2(L^{PhO'})_2 + H^+]^+$; *m/z* = 304.07, $[Cu(HL^{PhO'})]^+$. EPR (CH_3OH, 77K, 9.455 GHz, 0.25 mW): $g_{\perp}$ = 2.05, $g_{\|}$ = 2.257, $A_{\|}$= 176 G. Magnetic moment (Evans method, 293K, DMSO-d_6): 1.879 BM/Cu.

X-ray Crystallography. All single crystals of **1-5** were grown by vapor diffusion of diethyl ether into solutions of the complex. Intensity data for complex **1-5** were collected at 100(2) K using a diffractometer with a Bruker APEX ccd area detector[19] and graphite-monochromated Mo Kα radiation (λ = 0.71073 Å). The cell parameters for all complexes were determined from a non-linear least squares fit of the data. The data of these complexes were corrected for absorption by the semi-empirical method.[20] The structures were solved by direct methods by use of the SHELXTL program, and refined by full-matrix least-squares on F^2 by use of all reflections.[21]

Hydrogen atom positions were initially determined by geometry and refined by a riding model. Non-hydrogen atoms were refined with anisotropic displacement parameters. All crystal data for these complexes are summarized in following tables.

For complex **1**, the solvent site, which contained both acetonitrile and methylene chloride, was disordered. The occupancies of the solvents refined to 0.628(5) for the acetonitrile, and 0.372(5) for the methylene chloride. Restraints on the positional and displacement parameters of the solvent were required. For complex **2**, the structure contains two (half) cations that were found to sit on crystallographic 2-fold rotation axes. The selected crystal was twinned by a 2-fold rotation about the (1 0 0) axis. The ratio of the twin components refined to 0.4123 (6). Restraints of the N-H and O-H distances were required. For complex **3**, the molecule sits on a crystallographic center of symmetry, thus only half of the atoms are unique. One restraint was required to refine the N-H bond. For complex **4**, the molecule was found to sit on a crystallographic 2-fold rotation axis. The two solvent molecules were found near a crystallographic 2/m site and were severely disordered. For complex **5**, the molecule was found to sit on a crystallographic center of symmetry. A restraint on the length of the O-H bond was required.

Table 2-6. Crystallographic data for complexes **1-5**.

	1	**2**	**3**	**4**	**5**
Formula	$C_{27.63}H_{26.63}BCl_{0.74}CuF_4N_{4.63}O_4$	$C_{28}H_{28}B\ Cu\ F_4N_4O_4$	$C_{26}H_{24}Cl_2CuN_4O_4$	$C_{54}H_{48}Cu_4N_8O_{10}$	$C_{30}H_{32}Cu_2N_4O_6$
Fw	664.15	634.89	590.93	1223.16	671.68
Space group	$P2_1/c$	$C2/c$	$P2_1/c$	$C2/c$	$P\bar{1}$
a (Å)	15.661(2)	21.943(5)	11.662(2)	24.617 (5)	7.2285(12)
b (Å)	12.949(2)	17.586(4)	8.0504(16)	17.336(4)	10.3814(16)
c (Å)	14.190(2)	14.607(2)	13.350(3)	13.445(3)	11.0545(18)
α (deg)	90	90	90°	90	67.337(5)
β (deg)	96.749(5)	107.988(8)	101.751(5)	120.791(5)	89.615(5)
γ (deg)	90	90	90°	90	70.128(5)
Z	4	8	2	4	1
V (Å^3)	2857.7(7)	5361.2(19)	1227.1(4)	4929.0(19)	7122.5(2)
ρ_{calcd} (g/cm^3)	1.544	1.573	1.599	1.648	1.565
μ(mm^{-1})	0.903	0.886	1.150	1.733	1.554
$R1$ [I > 2σ(I)]	0.0691	0.0344	0.0282	0.0260	0.0256
wR(F^2 all data)	0.1745	0.0959	0.0777	0.0715	0.0670
GOF on F^2	1.046	1.001	1.005	1.011	1.018

2.8. References

1. Bar-Nahum, I.; Gupta, A. K.; Huber, S. M.; Ertem, M. Z.; Cramer, C. J.; Tolman, W. B., Reduction of Nitrous Oxide to Dinitrogen by a Mixed Valent Tricopper-Disulfido Cluster. *J Am Chem Soc* **2009,** *131* (8), 2812-2814.

2. Helton, M. E.; Chen, P.; Paul, P. P.; Tyeklar, Z.; Sommer, R. D.; Zakharov, L. N.; Rheingold, A. L.; Solomon, E. I.; Karlin, K. D., Reaction of elemental sulfur with a copper(I) complex forming a trans-μ-1,2 end-on disulfide complex: New directions in copper-sulfur chemistry. *J Am Chem Soc* **2003,** *125* (5), 1160-1161.

3. Brown, E. C.; Aboelella, N. W.; Reynolds, A. M.; Aullon, G.; Alvarez, S.; Tolman, W. B., A new class of (μ-η^2:η^2-disulfido)dicopper complexes: Synthesis characterization and disulfido exchange. *Inorg Chem* **2004,** *43* (11), 3335-3337.

4. (a) York, J. T.; Brown, E. C.; Tolman, W. B., Characterization of a complex comprising a complex $\{Cu_2(S_2)_2\}^{2+}$ core: Bis(μ-S_2^{2-})dicopper(III) or bis(μ-S_2(center dot-))dicopper(II)? *Angew Chem Int Edit* **2005,** *44* (47), 7745-7748; (b) Brown, E. C.; York, J. T.; Antholine, W. E.; Ruiz, E.; Alvarez, S.; Tolman, W. B., $[Cu_3(\mu\text{-}S)_2]^{3+}$ clusters supported by N-donor ligands: Progress toward a synthetic model of the catalytic site of nitrous oxide reductase. *J Am Chem Soc* **2005,** *127* (40), 13752-13753; (c) Helton, M. E.; Maiti, D.; Zakharov, L. N.; Rheingold, A. L.; Porco, J. A.; Karlin, K. D., A μ-η2:η2-disulfide dicopper(II) complex from reaction of S_8 with a copper(I) precursor: Reactivity of the bound disulfur moiety. *Angew Chem Int Edit* **2006,** *45* (7), 1138-1141.

5. York, J. T.; Bar-Nahum, L.; Tolman, W. B., Structural diversity in copper-sulfur chemistry: Synthesis of novel Cu/S clusters through metathesis reactions.

Inorg Chem **2007,** *46* (20), 8105-8107.

6. Mondal, A.; Li, Y.; Khan, M. A.; Ross, J. H.; Houser, R. P., Supramolecular copper hydroxide tennis balls: Self-assembly, structures, and magnetic properties of octanuclear $[Cu_8L_8(OH)_4]^{4+}$ clusters (HL = N-(2-pyridylmethyl)acetamide). *Inorg Chem* **2004,** *43* (22), 7075-7082.

7. Chaudhuri, U. P.; Whiteaker, L. R.; Yang, L.; Houser, R. P., Multinuclear copper complexes of pyridylmethylamide ligands. *Dalton T* **2006,** (15), 1902-1908.

8. Yang, L.; Houser, R. P., Copper(I) coordination chemistry of (pyridylmethyl)amide ligands. *Inorg Chem* **2006,** *45* (23), 9416-9422.

9. Yang, L.; Powell, D. R.; Houser, R. P., Structural variation in copper(I) complexes with pyridylmethylamide ligands: structural analysis with a new four-coordinate geometry index, tau(4). *Dalton T* **2007,** (9), 955-964.

10. Addison, A. W.; Rao, T. N.; Reedijk, J.; van Rijn, J.; Verschoor, G. C., Synthesis, structure, and spectroscopic properties of copper(II) compounds containing nitrogen-sulphur donor ligands; the crystal and molecular structure of aqua[1,7-bis(N-methylbenzimidazol-2[prime or minute]-yl)-2,6-dithiaheptane]copper(II) perchlorate. *Journal of the Chemical Society, Dalton Transactions* **1984,** (7), 1349-1356.

11. (a) Sorrell, T. N.; Jameson, D. L., Synthesis, structure, and reactivity of monomeric two-coordinate copper(I) complexes. *J Am Chem Soc* **1983,** *105* (19), 6013-6018; (b) Sanyal, I.; Karlin, K. D.; Strange, R. W.; Blackburn, N. J., Chemistry and structural studies on the dioxygen-binding copper-1,2-dimethylimidazole system. *J Am Chem Soc* **1993,** *115* (24), 11259-11270; (c)

Banthia, S.; Samanta, A., In situ reduction of copper(II) forming an unusually air stable linear complex of copper(I) with a fluorescent tag. *Inorg Chem* **2004,** *43* (22), 6890-6892.

12. (a) Sletten, J.; Sorensen, A.; Julve, M.; Journaux, Y., A Tetranuclear Hydroxo-Bridged Copper(Ii) Cluster of the Cubane Type - Preparation and Structural and Magnetic Characterization of Tetrakis[(2,2'-Bipyridyl)(μ-Hydroxo)Copper(II)] Hexafluorophosphate. *Inorg Chem* **1990,** *29* (25), 5054-5058; (b) Lopez, N.; Vos, T. E.; Arif, A. M.; Shum, W. W.; Noveron, J. C.; Miller, J. S., Structure and Magnetic Properties of a Hydroxo-Bridged Copper(II) Distorted Cubane Stabilized via Supramolecular Hydrogen Bonding with an Ionic Hexafluoroacetylacetonate. *Inorg Chem* **2006,** *45* (11), 4325-4327; (c) Aronica, C.; Chastanet, G.; Pilet, G.; Le Guennic, B.; Robert, V.; Wernsdorfer, W.; Luneau, D., Cubane Variations: Syntheses, Structures, and Magnetic Property Analyses of Lanthanide(III)−Copper(II) Architectures with Controlled Nuclearities‖. *Inorg Chem* **2007,** *46* (15), 6108-6119; (d) Eberhardt, J. K.; Glaser, T.; Hoffmann, R.-D.; Fröhlich, R.; WW; Fröhlich, U., A Tetranuclear Hydroxo-Bridged Copper(II) Complex with PrimaryN-Acylamidines as Ligands: Preparation, Structural, and Magnetic Characterisation. *Eur J Inorg Chem* **2005,** *2005* (6), 1175-1181; (e) Liu, H.; Wang, H.; Wu, H.; Niu, D., Synthesis, structure, and properties of a tetranuclear copper(II) tridentate Schiff-base complex with a pseudo-double-cubane core. *Journal of Coordination Chemistry* **2005,** *58* (15), 1345-1349; (f) Yilmaz, V. T.; Kars, V.; Kazak, C., A Tetranuclear μ3-Alkoxo-bridged Cubane-like Copper(II) Complex Containing 2-(Ethylamino)ethanol and Acetate: Synthesis and Structural

Characterization. *Zeitschrift für anorganische und allgemeine Chemie* **2007,** *633* (2), 351-353.

13. (a) Saimiya, H.; Sunatsuki, Y.; Kojima, M.; Kashino, S.; Kambe, T.; Hirotsu, M.; Akashi, H.; Nakajima, K.; Tokii, T., Antiferromagnetism induced by successive protonation of terminal phenol groups of a bis(μ-phenoxide)-bridged dicopper(ii,ii) complex. *Journal of the Chemical Society, Dalton Transactions* **2002,** (19), 3737-3742; (b) Thompson, L. K.; Mandal, S. K.; Tandon, S. S.; Bridson, J. N.; Park, M. K., Magnetostructural Correlations in Bis(μ_2-phenoxide)-Bridged Macrocyclic Dinuclear Copper(II) Complexes. Influence of Electron-Withdrawing Substituents on Exchange Coupling. *Inorg Chem* **1996,** *35* (11), 3117-3125.

14. (a) Chiari, B.; Piovesana, O.; Tarantelli, T.; Zanazzi, P. F., Out-of-plane coordination and exchange coupling in oxygen-bridged copper(II) dimers. *Inorg Chem* **1988,** *27* (23), 4149-4153; (b) Mandal, S. K.; Thompson, L. K.; Newlands, M. J.; Gabe, E. J.; Nag, K., Structural and magnetic studies on macrocyclic dicopper(II) complexes. Influence of electron-withdrawing axial ligands on spin exchange. *Inorg Chem* **1990,** *29* (7), 1324-1327; (c) Berti, E.; Caneschi, A.; Daiguebonne, C.; Dapporto, P.; Formica, M.; Fusi, V.; Giorgi, L.; Guerri, A.; Micheloni, M.; Paoli, P.; Pontellini, R.; Rossi, P., Ni(II), Cu(II), and Zn(II) Dinuclear Metal Complexes with an Aza−Phenolic Ligand: Crystal Structures, Magnetic Properties, and Solution Studies. *Inorg Chem* **2002,** *42* (2), 348-357.

15. Yang, L.; Wang, Z.; Powell, D. R.; Houser, R. P., A [Cu16S10]4- cluster containing μ_3- and μ_4-sulfido ligands. *Dalton T* **2009,** (23), 4439-4441.

16. Betz, P.; Krebs, B.; Henkel, G., $[Cu_{12}S_8]^{4-}$: A Closed Binary Copper(I)

Sulfide Cage with Cuboctahedral Metal and Cubic Sulfur Arrangements. *Angewandte Chemie International Edition in English* **1984,** *23* (4), 311-312.

17. Kubas, G. J. *Inorg. Synth.* **1979,** *19,* 90-91.

18. Evans, D. F. *J. Chem. Soc.* **1959,** 2003-2005.

19. (a) Data Collection: SMART Software Reference Manual (1998). Bruker-AXS, 5465 E. Cheryl Parkway, Madison, WI 53711-5373 USA. (b) Data Reduction: SAINT Software Reference Manual (1998). Bruker-AXS, 5465 E. Cheryl Parkway, Madison, WI 53711-5373 USA.

20. G. M. Sheldrick (2002). SADABS. Program for Empirical Absorption Correction of Area Detector Data. University of Göttingen, Germany.

21. G. M. Sheldrick (2000). SHELXTL Version 6.10 Reference Manual. Bruker-AXS, 5465 E. Cheryl Parkway, Madison, WI 53711-5373 USA. (b) *International Tables for Crystallography, Vol C,* Tables 6.1.1.4, 4.2.6.8, and 4.2.4.2, Kluwer: Boston (1995).

CHAPTER 3

SYNTHESIS AND CHARACTERIZATION OF COPPER(II) COMPLEXES WITH SUBSTITUTED PYRIDYLBIS(PHENOL) LIGANDS

3.1. Introduction

The synthesis and characterization of mono- and polynuclear copper complexes have attracted much interest due to their relevance in bioinorganic chemistry and possible modeling functions to partially mimic the structural and spectroscopic features of some copper-containing proteins. In our lab, we have developed a series of pyridyl amide ligands and many copper complexes with various nuclearity and oxidation state were reported.[1] More recently, as an extension to our previous pyridyl amide ligands, pyridylbis(acetamide) ligand $H_2pp(ac)_2$ (Figure 3-1) and its trinuclear mixed-valence complex were reported.[1a] Based on the same consideration, we synthesized pyridine and phenol-containing ligands H_2L^{imine}, H_2L^{amine}, and H_4L^{amide} that were found to support copper(II) complexes of varying nuclearity.[2] The diimine ligand H_2L^{imine}, with rigid C=N bonds, formed a mononuclear compound, the more flexible diamine ligand H_2L^{amine} formed a trinuclear complex, whereas the H_4L^{amide} ligand with rigid amide moieties formed a hexanuclear complex. While the pyridyl nitrogen in the mono and trinuclear complexes of H_2L^{imine} and H_2L^{amine} ligand, respectively, does not coordinate to the copper center, it does in the hexanuclear complex of H_4L^{amide} ligand. More recently we extended our ligand system to incorporate the ligand $H_2L^{tBu\text{-}amine}$ that contains the *tert*-butyl substituent on the 3- and 5-positions of the phenol rings (Figure 3-1). Five new iron(III) complexes using the ligands H_2L^{amine} and $H_2L^{tBu\text{-}amine}$ were synthesized and found that based on the type of substituents on the phenol ring the ligand can foster the hydroxo- or oxo- bridged binuclear iron(III) complexes and also depending upon

the type of the metal salt and the solvent used for the synthesis, the ligands can foster the mono- or binuclear iron(III) complexes.[3]

Based on our previous reported copper and iron chemistry studies of this series of pyridylbis(aminophenol) ligands, the pyridyl N shows different coordination modes with the changes of the ligands and the metal. The pyridyl N does not coordinate with copper in both H_2L^{amine} and H_2L^{imine} ligands, while the pyridyl N does coordinate with iron in both ligands. Attracted by what are the factors to determine the coordination mode of the pyridyl N donor, we surmise that steric and electronic effects may play a role in the determination of the coordination mode of pyridyl N. In this chapter, we design several new ligands with the introduction of different substituents in the 3-, 5- or 3- and 5-positions of the phenol ring. We expect to see different coordination modes of pyridyl N with the changes of the substituents. This research also provides insight into the tetradentate versus pentadentate chelating preferences of this ligand system based on the nucleophilicity of the phenol rings.

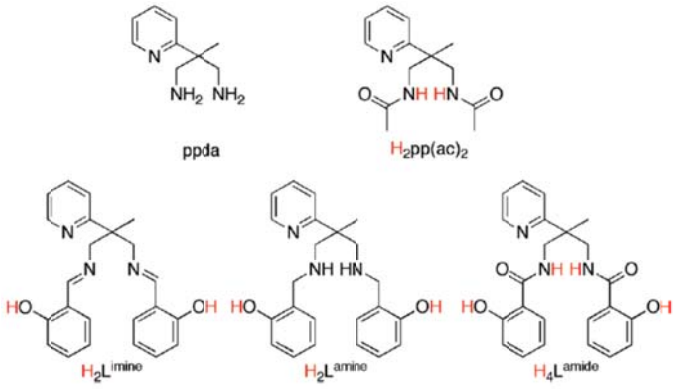

Figure 3-1. Ligand system with ppda backbone. Scheme is adapted from reference [2].

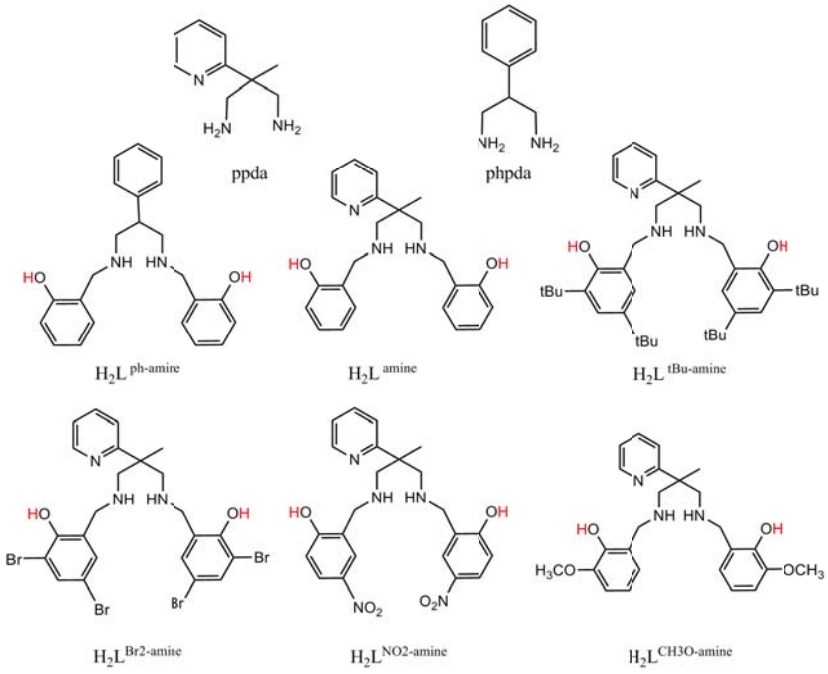

Figure 3-2. Ligand system with substituted pyridylbis(phenol) ligands.

3.2. Synthesis of Substituted Pyridylbis(phenol) Ligands

The ligands $H_2L^{Br2\text{-}amine}$, $H_2L^{CH3O\text{-}amine}$, and $H_2L^{NO2\text{-}amine}$ were prepared by the general procedure as shown in Figure 5-3 in which ppda was condensed with appropriate aldehyde in methanol at 50 °C, followed by reduction with $NaBH_4$ at 0 °C. The amine product was extracted with dichloromethane, dried over anhydrous $MgSO_4$ and isolated after solvent evaporation. All the ligands were synthesized with good yields (> 60%).

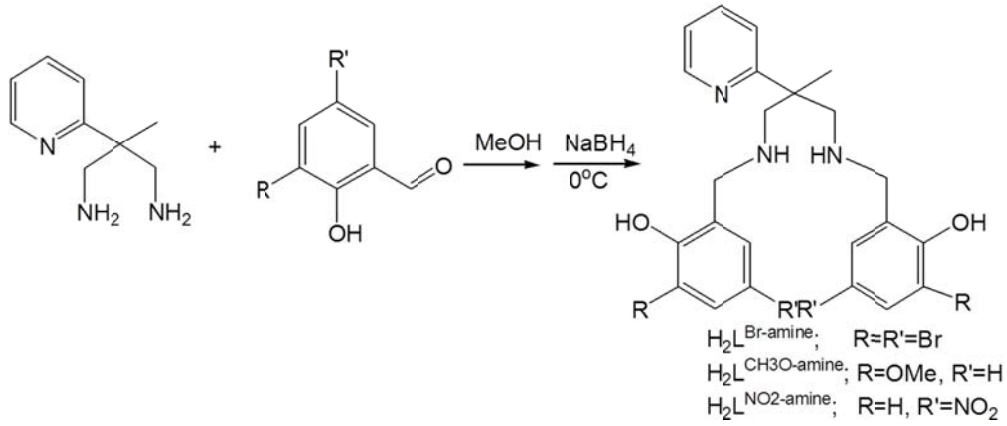

Figure 3-3. Synthesis of the substituted pyridylbis(phenol) ligands.

3.3. Synthesis and Characterization of Copper(II) Complexes

3.3.1. Mononuclear [Cu($L^{Br2\text{-}amine}$)] (6)

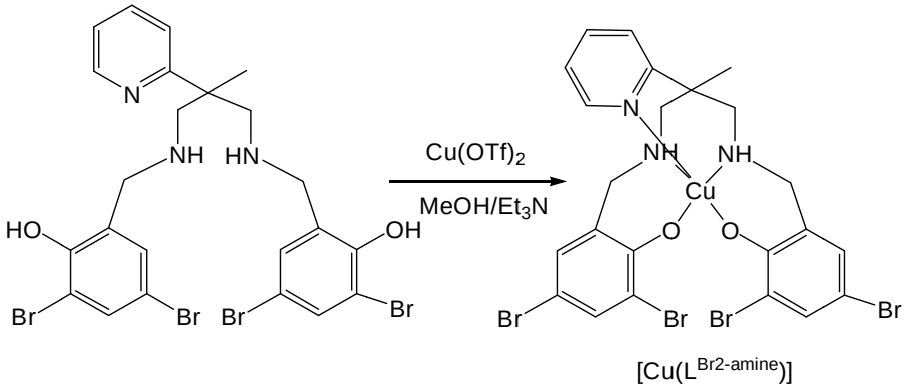

Figure 3-4. Synthesis of [Cu($L^{Br2\text{-}amine}$)] **(6).**

The addition of $Cu(OTf)_2$ in CH_3OH into the stirring $H_2L^{Br2\text{-}amine}$ with the presence of Et_3N resulted in the formation of dark green solution. After the filtration, crystals of [Cu($L^{Br2\text{-}amine}$)] **(6)** were obtained from the slow evaporation of

the filtrate. X-ray analysis revealed that **6** contain a five-coordinate copper(II) ion with slightly distorted square pyramidal geometry having a τ_5 value of 0.107. The copper(II) ion in **6** is coordinated by a N_3O_2 donor atom set that involves two amine N atoms, two deprotonated O atoms and also the pyridyl N atom (Figure 3-5, top). Two amine N atoms and two phenolate O atoms occupy the basal plane and the pyridyl N atom occupies the apical position of the pyramid. The axial Cu-N bond distance (2.324 Å) is longer than the basal planar Cu-N bond distances (1.992 and 2.044 Å). Selected bond lengths (Å) and bond angles (°) are listed in Table 3-1. The solid state structure of this complex consists of three subunits of **6** connected by intermolecular hydrogen bonding (Figure 3-5, bottom). The H···O bond distances are in the range from 2.13 to 2.19 Å. The N-H···O bond distances are in the range of 2.804 to 2.902 Å. The short bond distances show the strong hydrogen bonding between the units.

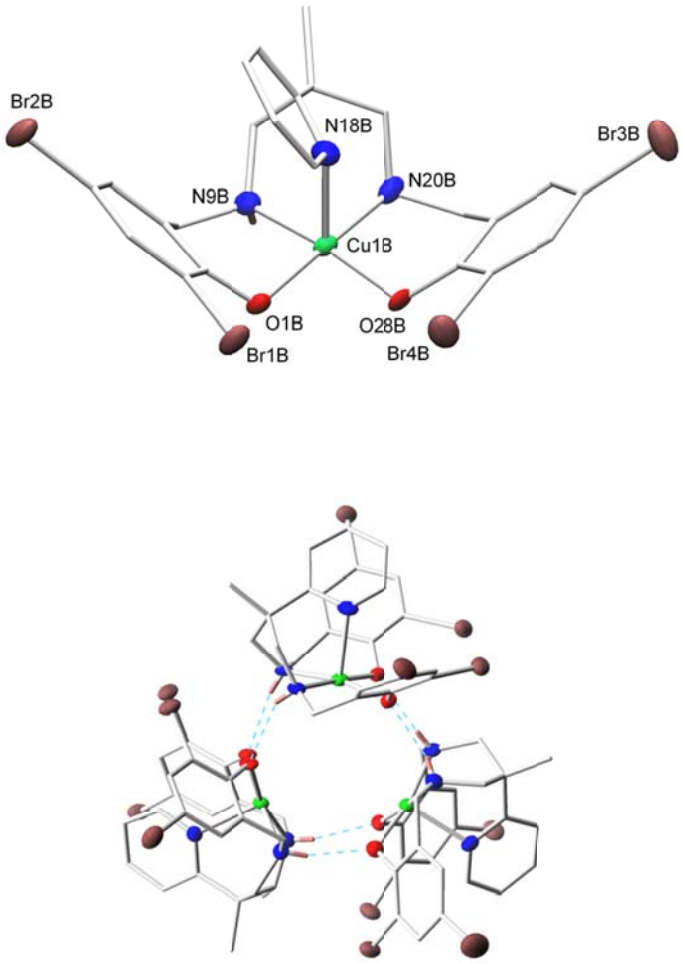

Figure 3-5. X-ray structure of [Cu($L^{Br2\text{-}amine}$)] **(6)** with all H atoms except for amine protons removed for clarity (top). Trimeric unit of **6** showing H-bonding connecting each unit. All H atoms except for amine protons have been removed for clarity (bottom).

Table 3-1. Selected bond lengths (Å) and angles (deg) for **6**.

Cu1B-N20B	1.992(6)	Cu1B-O1B	1.944(4)
Cu1B-N9B	2.044(6)	Cu1B-O28B	1.948(4)
Cu1B-N18B	2.324(5)		
O1B-Cu1B-O28B	89.43(18)	N20B-Cu1B-N9B	84.3(2)
O1B-Cu1B-N20B	174.56(19)	O1B-Cu1B-N18B	95.41(19)
O28B-Cu1B-N20B	93.6(2)	O28B-Cu1B-N18B	93.87(18)
O1B-Cu1B-N9B	91.8(2)	N20B-Cu1B-N18B	88.9(2)
O28B-Cu1B-N9B	168.74(18)	N9B-Cu1B-N18B	97.1(2)

3.3.2. Mononuclear [Cu($L^{NO2\text{-}amine}$)] (7)

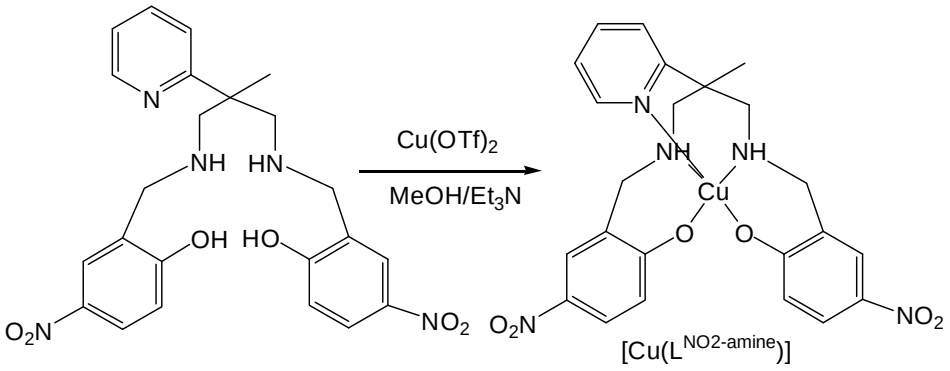

Figure 3-6. Synthesis of [Cu($L^{NO2\text{-}amine}$)] **(7).**

Complex **7** was prepared by the same method as complex **6** using $H_2L^{NO2\text{-}amine}$ to replace $H_2L^{Br2\text{-}amine}$. Similar to **6**, the nitro-substituted ligand $H_2L^{NO2\text{-}amine}$ also formed a mononuclear complex [Cu($L^{NO2\text{-}amine}$)] (**7**). Single crystals of **7** were

obtained by the slow evaporation of a methanol solution of **7.** Like in **6**, the structure of **7** consists of a five-coordinate Cu(II) ion possessing a square pyramidal geometry (τ_5 value of 0.00083, Figure 3-7). The coordination environment consists of two amine N-atoms, one pyridyl N-atom and two deprotonated phenolate O. Like in **6**, the basal plane of the pyramid in **7** is occupied by two amine N and two phenolate O atoms and the apical position is occupied by the pyridyl N atom. The axial Cu-N bond distance (2.224 Å) is longer than the basal planar Cu-N (1.997 and 2.066 Å) bond distances. Selected bond lengths (Å) and bond angles (°) are listed in Table 3-2.

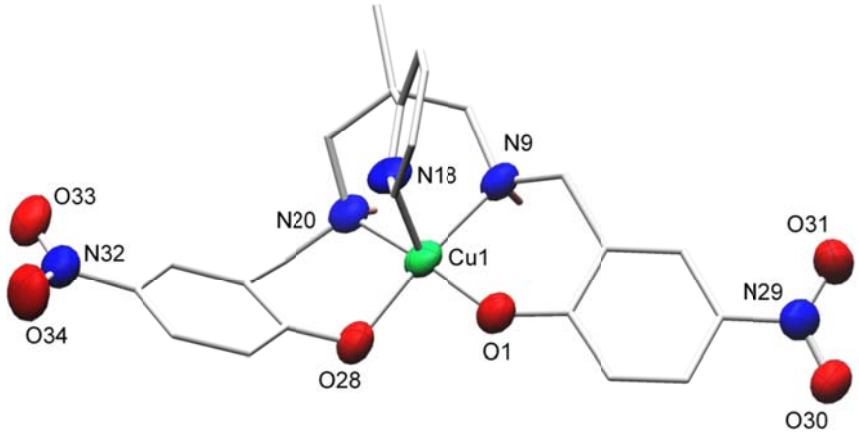

Figure 3-7. X-ray structure of [Cu($L^{NO2\text{-}amine}$)] **(7)** with all H atoms except for amine protons removed for clarity.

Table 3-2. Selected bond lengths (Å) and angles (deg) for **7**.

Cu1-N20	1.997(4)	Cu1-O1	1.931(4)
Cu1-N9	2.066(5)	Cu1-O28	1.975(4)
Cu1-N18	2.224(4)		
O1-Cu1-O28	84.75(16)	N20-Cu1-N9	87.80(18)
O1-Cu1-N20	171.41(17)	O1-Cu1-N18	98.74(16)
O28-Cu1-N20	92.99(17)	O28-Cu1-N18	100.52(17)
O1-Cu1-N9	93.22(17)	N20-Cu1-N18	89.81(17)
O28-Cu1-N9	171.46 (17)	N9-Cu1-N18	87.98(18)

3.3.3. [Cu($L^{MeO\text{-}amine}$) Na($CH_3OH)_2$](ClO_4) (8)

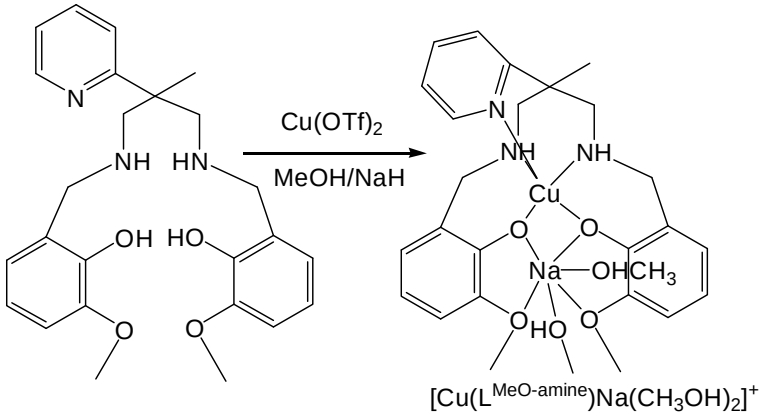

Figure 3-8. Synthesis of [Cu($L^{MeO\text{-}amine}$)Na($CH_3OH)_2$] **(8).**

Multiple attempts to synthesize copper complexes of $H_2L^{MeO\text{-}amine}$ using triethyl amine as a base for phenol deprotonation resulted in the formation of an

uncharacterizable waxy product. However, the reaction of the $H_2L^{MeO\text{-}amine}$ with copper(II) perchlorate in methanol using NaH as a base for hydrogen deprotonation resulted in a heterometallic binuclear copper/sodium compound $[Cu(L^{MeO\text{-}amine})Na(CH_3OH)_2]ClO_4$ (**8**). X-ray quality crystals were obtained by the slow evaporation of a methanol solution of **8**. The X-ray structure of **8** reveals that the bimetallic complex consists of a five-coordinate Cu(II) ion with a square pyramidal geometry

(τ_5 = 0.0053) and a six-coordinate Na^+ ion with distorted octahedral geometry as shown in Figure 3-9. The N_3O_2 donor atom set around Cu is comprised of two amine N atoms, one pyridyl N atom and two deprotonated O atoms. The axial Cu-N bond distance (2.246 Å) is longer than the basal planar Cu-N bond distances (2.028 and 2.041 Å). Selected bond lengths (Å) and bond angles (°) are listed in Table 3-3. The sodium ion is six-coordinate with two phenolate O atoms, two O atoms from the ligand methyl ether groups, and two O atoms from the methanol ligands, forming a distorted octahedral geometry.

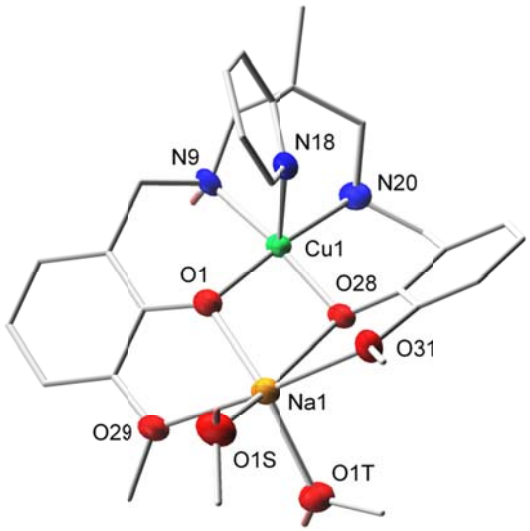

Figure 3-9. X-ray structure of [Cu($L^{MeO\text{-}amine}$)Na($CH_3OH)_2$] **(8)** with all H atoms except for amine protons removed for clarity.

In summary, the three copper complexes with different substituted pyridylbis(phenol) ligands were synthesized and characterized by X-ray analysis. In all three complexes, the copper ion is five-coordinate with three N atoms and two Phenolate O atoms from the corresponding ligand. The bond distances of average Cu-N and Cu-O are in a close value for all three complexes. The pyridyl N does coordinate with the copper center, which is different than the coordination modes of some reported copper complexes with similar ligands.[2] The different coordination behaviors of the pyridyl groups could result from the electronic properties of the substituents on the phenol ring of the ligands. In the copper complex with tert-butyl substituents, the electron donating behavior of the tert-butyl substituents in the diamine ligand increases the electron density in the copper center upon coordination. This repels the pyridyl N- atom away so it does not coordinate with

the copper center. However, in complexes **6** and **7** the electron withdrawing behavior of the bromo and the nitro substituents makes the copper center electron deficient upon coordination. This causes the coordination of the pyridyl N- to the copper center. However, in complex **8** this assumption appears to be contradictory because in spite of the electron donating behavior of the methoxy substituent, the pyridyl N- atom is coordinated to the copper center. The plausible explanation for this anomalous behavior could be that the coordination of the methoxy- substituents to the sodium ion reduces the electron donating behavior of this substituent and makes the copper center still electron deficient and forces the coordination the pyridyl N.

Table 3-3. Selected bond lengths (Å) and angles (deg) for complex **8.**

Cu1-O28	1.923(3)	Cu1-N9	2.028(4)
Cu1-O1	1.950(3)	Cu1-N20	2.041(4)
Cu1-N18	2.246(4)	O1-Na1	2.355(4)
O28-Na1	2.284(4)	O29-Na1	2.574(4)
O31-Na1	2.547(4)	Na1-O1T	2.302(4)
Na1-O1S	2.311(4)		
O28-Cu1-O1	84.46(14)	O28-Na1-O1	68.28(13)
O28-Cu1-N9	170.88(16)	O1T-Na1-O1	150.38(16)
O1-Cu1-N9	92.70(16)	O1S-Na1-O1	100.46(14)
O28-Cu1-N20	92.90(15)	O28-Cu1-N20	65.40(13)
O1-Cu1-N20	170.56(15)	O1T-Na1-O31	87.10(15)
N9-Cu1-N20	88.50(17)	O1S-Na1-O31	92.06(14)
O28-Cu1-N18	98.94(14)	O1-Na1-O31	118.59(14)
O1-Cu1-N18	101.12(14)	O28-Na1-O29	112.49(14)
N9-Cu1-N18	90.10(16)	O1T-Na1-O29	88.39(15)
N20-Cu1-N18	88.24(15)	O1S-Na1-O29	92.99(14)
O28-Na1-O1T	115.66(16)	O1-Na1-O29	64.61(12)
O28-Na1-O1S	141.45(15)	O31-Na1-O29	173.37(14)
O1T-Na1-O1S	92.50(16)		

3.4. Spectroscopic and Electrochemical Studies

Complexes **6-8** exhibit intense ligand to metal charge transfer transitions (LMCT) in the range of 300-425 nm. The *d-d* transitions are in the range of 590-650 nm. The X-band EPR spectra of all three complexes in frozen DMSO or CH_2Cl_2 at 77 K are typical of mononuclear copper(II) complexes with predominantly axial character indicating a d_{x2-y2} ground state, which is consistent with the X-ray analysis.

The redox properties of **6-7** were studied by cyclic voltammetry in acetonitrile. The cyclic voltammograms (CVs) of **6-7** showed quasi-reversible Cu^{II}/Cu^{I} redox waves with $E_{1/2}$ potentials that range from -680 mv for **7** to -897 mV for **6** versus Ag/AgCl, and ΔE values that range from 206 mV for **6** to 210 mV for **7**. The electrochemical behavior of complex **8** was investigated by cyclic voltammetry in CH_2Cl_2 solution. It also showed a quasi-reversible Cu^{II}/Cu^{I} redox wave with a $E_{1/2}$ potential of -954 mV versus Ag/AgCl, and a ΔE value of 367 mV. As can be observed in Table 3-4, the half-wave potentials ($E_{1/2}$) of the complexes become less negative in the order of the ligand sequence as $H_2L^{tBu\text{-}amine} > H_2L^{amine} > H_2L^{Br2\text{-}amine} > H_2L^{NO2\text{-}amine}$. The influence of the ligand on the redox potential of the Cu^{II}/Cu^{I} process clearly indicates the electronic effect of the substituents present on the phenol ring of the ligands. The bromo- and nitro- groups, as electron-withdrawing substituents in **6** and **7** respectively, cause low negative half-wave potentials in these complexes. On the other hand, tert-butyl groups as electron donating substituents cause comparatively high negative half-wave potentials in the complex.

The examination of substituent effects on redox potentials can be explored by

Hammett analysis. The plot of $E_{1/2}$ versus the Hammett parameter [6] for the reduction of Cu(II) complexes is shown in Figure 3-10. The cyclic voltammograms of four compounds in CH_3CN are shown in Figure 3-11. A linear relationship is obtained for the reduction of the copper center with a calculated slope (ρ) of 191 mv, which matches with the proposed explanation for the electronic effects of the substituents. Tert-butyl groups as an electron donating substituent cause comparatively low negative half-wave potentials in these complexes.

Table 3-4. Cyclic Voltammetry Data showing Cu^{II}/Cu^{I} processes in CH_3CN

Complexes	Solvent	$E_{½}$ (mV)	$2\sigma_p$
$[Cu(L^{tBu\text{-}amine})(CH_3OH)]$	CH_3CN	-1055	-0.40
$[Cu_3(L^{amine})_2(CH_3CN)_2](ClO_4)_2$	CH_3CN	-914	0
$[Cu(L^{Br2\text{-}amine})]$ **(6)**	CH_3CN	-897	0.46
$[Cu(L^{NO2\text{-}amine})]$ **(7)**	CH_3CN	-680	1.56

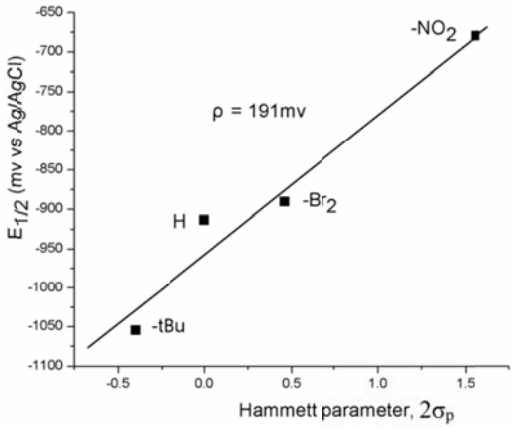

Figure 3-10. Plot of $E_{1/2}$ *vs* the Hammett substituent constants for the reduction of Cu(II) center in series of compounds in CH_3CN.

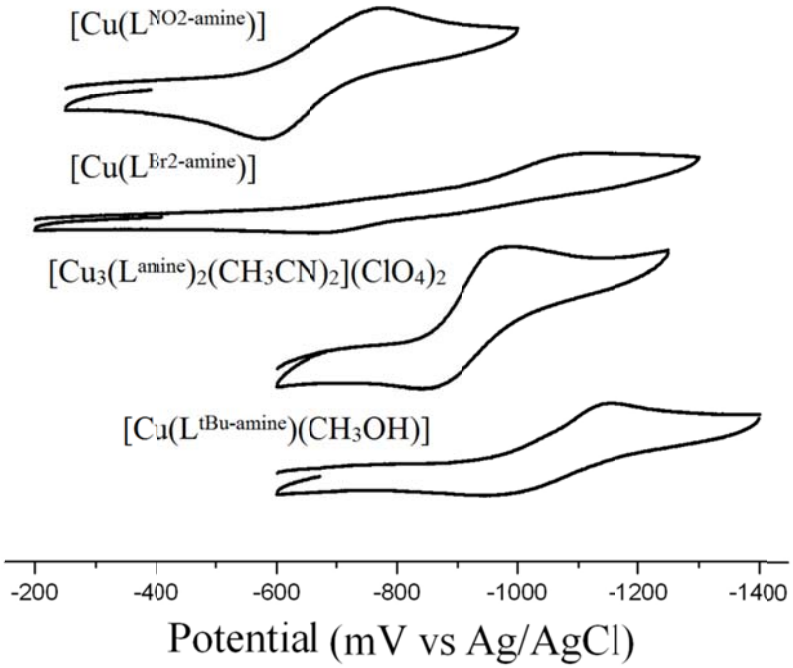

Figure 3-11. Cyclic voltammograms of the compounds in CH_3CN containing 0.1 M NBu_4PF_6 and at a scan rate of 100 mV/s.

3.5. Conclusions

In this chapter, three substituted pyridylbis(aminophenol) ligands: $H_2L^{Br2\text{-}amine}$, $H_2L^{CH3O\text{-}amine}$, and $H_2L^{NO2\text{-}amine}$ were synthesized and fully characterized by ^1H NMR, FT-IR and elemental analysis. The copper chemistry of these ligands was investigated. Two mononuclear copper complexes: $[Cu(L^{Br2\text{-}amine})]$ (6) and $[Cu(L^{NO2\text{-}amine})]$ (7) are obtained and characterized by X-ray analysis. One heterometallic Cu-Na complex $[Cu(L^{MeO\text{-}amine})Na(CH_3OH)_2]$ (8) is also characterized by X-ray crystallography. In all three complexes, the copper center is five coordinate with N_3O_2 donor in a square pyramidal geometry. The pyridyl N does coordinate with

the copper center from an apical position. Comparing with the copper complex [CuL$^{t\text{Bu-amine}}$(CH_3OH)] obtained from the $H_2L^{t\text{Bu-amine}}$ ligand, the pyridyl N does not coordinate with the copper center due to the formation of the hydrogen bonds. In order to interpret different coordination modes of substituted pyridylbis(aminophenol) ligands, we propose the following hypothesis based on the nucleophilicity of the phenol donors[5].

All the ligands based on the 2-methyl-2-(pyridine-2-yl)propane-1,3-diamine (ppda) platform have the same 1,3-propanediamine backbone attached to the methylenephenol groups. The prochiral amine groups coordinate to a copper ion, forming the *meso*-(*s*) and *meso*-(*r*) diastereomers, as shown in Figure 3-12. The six-membered chelate ring can adopt either a chair or boat conformation. The preferred conformations of the *meso*-(*s*) or *meso*-(*r*) diastereomers are highlighted in boxes in Figure 3-12. In the mononuclear [CuL$^{t\text{Bu-amine}}$(CH_3OH)] complex, the pyridyl N does not coordinate with the copper center and instead forms hydrogen bonds with both amine NH groups in the *meso*-(*r*)-chair conformation. In contrast, the pyridyl N does coordinate to the copper center in the *meso*-(*s*)-boat conformation in complexes 6-8. We rationalize that the reason why the *meso*-(*r*)-chair coordination mode is selected in [CuL$^{t\text{Bu-amine}}$(CH_3OH)], while the *meso*-(*s*)-boat coordination mode is selected in complexes 6-8, is based on the electronic properties of the ligands. The complexes with the *meso*-(*r*)-chair coordination mode, {[CuL$^{t\text{Bu-amine}}$(CH_3OH)] and [$Cu_3(L^{amine})_2(CH_3CN)_2$]($ClO_4$)$_2$}, contain the more nucleophilic phenolato groups in ligands $H_2L^{t\text{Bu-amine}}$ and H_2L^{amine}, while the complexes with the *meso*-(*s*)-boat coordination mode (6-8) have less nucleophilic phenolate O due to the

electron withdrawing nature of Br and NO_2 in the case of $H_2L^{Br2\text{-}amine}$ and $H_2L^{NO2\text{-}amine}$. We rationalize that the less nucleophilic phenolato donors ($H_2L^{Br2\text{-}amine}$ and $H_2L^{NO2\text{-}amine}$) make the copper electron deficient and cause preference of the pyridyl N coordination. The more nucleophilic donors (H_2L^{amine} and $H_2L^{tBu\text{-}amine}$) make the copper center more electron rich and hence there is less energetic benefit from the pyridyl N coordination than is gained from the hydrogen bonding formation between the pyridyl N and amine NH groups. The *meso*-(*s*)-boat coordination mode of complex 8 can be attributed to the coordination of methoxy substituents to the sodium ion, which may draw electrons away from the copper center and thus the coordination of the pyridyl N. The Hammett plot also supports the electronic effects that the substituents on these ligands have on the redox potentials of their copper complexes. The more electron-rich copper centers in H_2L^{amine} and $H_2L^{tBu\text{-}amine}$ have larger negative potentials and are hence more difficult to reduce, while the electron deficient copper centers in $H_2L^{Br2\text{-}amine}$ and $H_2L^{NO2\text{-}amine}$ have relatively smaller negative potentials and are thus easier to reduce.

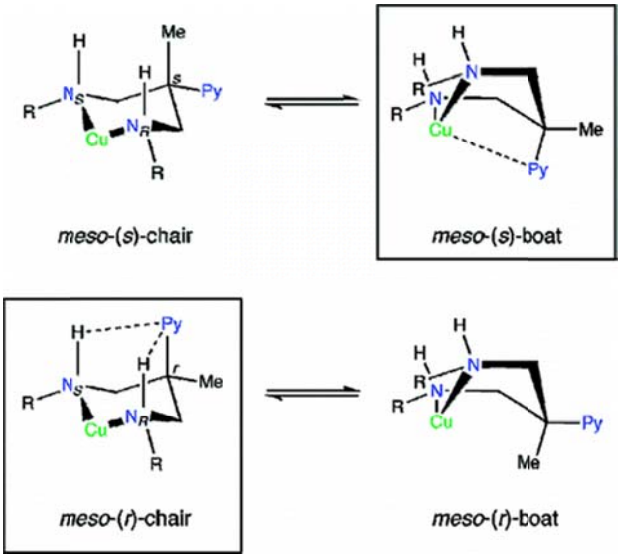

Figure 3-12. Proposed two diastereomers, the figure is adapted from reference [5]

3.6. Experimental

General Procedures. Unless otherwise stated, all reagents were used as received from commercial sources. The starting materials 2-phenylpropane-1,3-diamine (phpda) and 2-methyl-2-(pyridine-2-yl)propane-1,3-diamine (ppda) were synthesized according to the literature procedure.[7] Solvents used were doubly purified using alumina columns in a MBraun solvent purification system (MB-SPS). Infrared spectra were measured from 4000 to 400 cm^{-1} as KBr pellets on a NEXUS 470 FTIR spectrometer. ^{1}H NMR spectra were measured using a Varian 300 MHz instrument. ESI (positive) spectra were measured in Q-TOF quadrupole time-of flight mass spectrometer (Micromass, Manchester, U.K.) containing Z-spray electrospray ionization source (ESI). Elemental analyses were performed by Atlantic Microlab, Norcross, GA. UV-visible spectra of acetonitrile solutions of compound **7** and dichloromethane solutions of compounds **6,** and **8** were measured

using a Shimadzu UV2401PC spectrophotometer in the range 250 to 1000 nm on solution ranging in concentration from 1.0 x 10^{-3} M and 1.0 x 10^{-4} M. Cyclic voltammetry experiments were performed using a BAS 50W potentiometer. A standard three-electrode cell was employed with a glassy-carbon working electrode, a Pt-wire auxiliary electrode, and an Ag/AgCl reference electrode under an inert atmosphere at room temperature. X-Band EPR spectra of the complexes were recorded using Bruker EMX spectrometer in dichloromethane, acetonitrile, or DMSO at 77K in frozen solutions. Solution magnetic moment measurements were measured using the Evans method.[8] Magnetic susceptibility of the complexes in the solid state was measured by using a Johnson Matthey; Fabricated Equipment's Magnetic Susceptibility Balance (MSB – AUTO) with Magnetic field Strength 4.5 kGauss and measurement range ± 1.999 x 10^{-4} to ± 5 x 10^{-10} cgs. The MSB-AUTO possesses a detector which is based on the Evan's design and measures the susceptibility by detecting the force acting upon a suspended magnet. A narrow bore sample tube with 0.400 cm outer diameter and 0.200 cm inner diameter was used. Dry powdered samples were packed by tapping the tube up to the minimum height of 15 mm. Measurements were made at room temperature of 22 ^{o}C. TARE function was used to operate at gain E-6. Mass susceptibility was recorded following the input of the sample length and the sample weight.

Caution! *Perchlorate salts of metal complexes with organic ligands are potentially explosive. Although no difficulty was encountered during the syntheses described herein, they should be prepared in small amounts and handled with caution.*

Preparation of the ligands $H_2L^{Br2\text{-}amine}$, $H_2L^{MeO\text{-}amine}$, and $H_2L^{NO2\text{-}amine}$ The ligands $H_2L^{Br2\text{-}amine}$, $H_2L^{MeO\text{-}amine}$, and $H_2L^{NO2\text{-}amine}$ were prepared by the general procedure in which ppda (0.330 g, 2.00 mmol) was condensed with appropriate aldehyde (4.00 mmol) in 40 mL of methanol at 50 °C. After 2 h, $NaBH_4$ (0.220 g, 6.00 mmol) was added into the solution in small portions at 0 °C. The solution was then stirred at room temperature for 2 h, the solvent was evaporated, and the amine product was extracted with dichloromethane, dried over anhydrous $MgSO_4$ and isolated after solvent evaporation.

6,6'-(2-methyl-2(pyridine-2-yl)propane-1,3diyl)bis(azanediyl)bis(methylene)bis-(2,4-dibromophenol) ($H_2L^{Br2\text{-}amine}$): 3,5-dibromosalicylaldehyde (1.12 g, 4.00 mmol) was used. Yield: 0.826 g, 60%. Anal. Calcd for $C_{23}H_{23}Br_4N_3O_2$: C, 39.9; H, 3.3; N, 6.1. Found: C, 40.4; H, 3.4; N, 5.8. ^{1}H NMR (300 MHz, CD_2Cl_2, 300K) δ 1.46 (s, 3H), 2.91 (d, J = 12 Hz, 2H), 3.06 (d, J = 11.7 Hz, 2H), 3.40 (d, J = 14.4 Hz, 2H), 3.98 (d, J = 14.4 Hz, 2H), 7.10-7.34 (m, 4H), 7.53-7.75 (m, 3H), 8.52 (d, J = 9 Hz, 1H) ppm. FTIR (KBr): 3288 (O-H), 3071 (s, C-H), 2842 (s, C-H), 1589, 1569, 1454 (s, C=N_{py}, C=$C_{aromatic}$), 1384, 1282, 1260, 1152, 1089, 993, 860, 787, 748, 684, 651 cm^{-1}. ESI-MS (MeOH): m/z = 693 $[H_2L^{Br2\text{-}amine} + H]^+$.

6,6'-(2-methyl-2(pyridine-2-yl)propane-1,3diyl)bis(azanediyl)bis(methylene)bis-(2-methoxyphenol) ($H_2L^{MeO\text{-}amine}$): 2-hydroxy-3-methoxybenzaldehyde (0.608 g, 4.00 mmol) was used. Yield: 0.570 g,

65%. Anal. Calcd for $C_{25}H_{31}N_3O_4 \cdot H_2O$: C, 65.9; H, 7.3; N, 9.2. Found: C, 65.6; H, 7.2; N, 8.9. ^{1}H NMR (300 MHz, $CDCl_3$, 300K) δ 1.49 (s, 3H), 2.88 (d, *J* = 11.4 Hz, 2H), 3.14 (d, *J* = 11.7 Hz, 2H), 3.82 (s, 6H), 3.90 (m, 4H), 6.58-6.78 (m, 6H), 7.13-7.64 (m, 3H), 8.50 (d, *J* = 6 Hz, 1H) ppm. FTIR (KBr): 3418 (O-H), 2832 (s, C-H), 1589, 1477 (s, $C{=}N_{py}$, $C{=}C_{aromatic}$), 1328, 1232, 1158, 1074, 769, 732, 621 cm^{-1}. ESI-MS (MeOH): *m/z* = 438 $[H_2L^{MeO\text{-}amine} + H]^+$.

2,2'-(2-methyl-2(pyridine-2-yl)propane-1,3diyl)bis(azanediyl)bis(methylene)bis-(4-nitrophenol) ($H_2L^{NO2\text{-}amine}$): 2-hydroxy-5-nitrobenzaldehyde (0.668 g, 4.00 mmol) was used. Yield: 0.654 g, 70%. Anal. Calcd for $C_{23}H_{25}N_5O_6 \cdot 2CH_3OH$: C, 56.5; H, 6.3; N, 13.2. Found: C, 56.2; H, 5.5; N, 12.6. ^{1}H NMR (300 MHz, CD_2Cl_2, 300K) δ 1.45 (s, 3H), 2.99 (d, *J* = 12 Hz, 2H), 3.14 (d, *J* = 11.7 Hz, 2H), 3.43 (s, 2H), 3.73 (s, 2H), 4.00 (m, 4H), 6.83 (d, 1H); 7.24-7.37 (m, 4H), 7.78-8.08 (m, 3H), 8.53 (d, *J* = 4.2 Hz, 1H) ppm. FTIR (KBr): 3431 (O-H), 2930 (s, C-H), 1593, 1476 (s, $C{=}N_{py}$, $C{=}C_{aromatic}$), 1335, 1284, 1157, 1089, 995, 865, 787, 752, 650 cm^{-1}. ESI-MS (MeOH): *m/z* = 468 $[H_2L^{NO2\text{-}amine} + H]^+$.

Synthesis of the complexes 6-8. A general synthetic route was used for the preparation of complexes **6-8** in which the appropriate Cu(II) salt was added to the solution of respective ligands (0.100 mmol) in methanol. For complexes **6-7,** Et_3N (0.040 mL, 0.30 mmol) and for **8**, NaH (0.072g, 0.30 mmol) was used as a base for phenol deprotonation. In each case, the resulting dark green solution was stirred for 2 h at room temperature and filtered to remove any unreacted solids. The X-ray

quality crystals of complexes **6-8** were obtained after crystallization by appropriate methods.

[Cu($L^{Br2\text{-}amine}$)] (6): $H_2L^{Br2\text{-}amine}$ (0.0693 g, 0.100 mmol) and $Cu(OTf)_2$ (0.036 g, 0.100 mmol) were used. Yield: 0.0527 g, 65%. Anal. calcd for $C_{23}H_{21}Br_4CuN_3O_2 \cdot 1/2CH_2Cl_2$: C, 35.4; H, 2.8; N, 5.3. Found: C, 35.3; H, 2.6; N, 5.4. UV/vis (CH_2Cl_2) [λ_{max}, nm (ε, $M^{-1}cm^{-1}$)]: 306 (10,300), 352 (2,800), 407 (2,380), 648 (180). EPR (9.442 GHz, mod. amp. 10.0 G, DMSO, 77K): $g_{\parallel}$ = 2.350, $g_{\perp}$ = 2.109 , and $A_{\parallel}$ = 169 G. FTIR (KBr): 3107 (s, C-H), 2919 (s, C-H), 2361, 2338, 1652, 1575, 1434 (s, C=N_{py}, C=$C_{aromatic}$), 1398, 1300, 1264, 1155, 1090, 1035, 860, 789, 750, 667, 627 cm^{-1}. ESI-MS (MeOH): *m/z* = 776 [Cu($L^{Br2\text{-}amine}$) + Na]$^+$. Solution magnetic moment (Evans method, 19.8 ^oC, 5.50 x 10^{-3} M, chloroform-d_1): 1.73 μ_B/Cu. Solid state magnetic moment (MSB-Auto, 4.5 kG, 22.0 ^oC): 1.60 μ_B/Cu.

[Cu($L^{NO2\text{-}amine}$)] (7): $H_2L^{NO2\text{-}amine}$ (0.0467 g, 0.100 mmol) and $Cu(ClO_4)_2 \cdot 6H_2O$ (0.0370 g, 0.100 mmol.) were used. Yield: 0.0339 g, 60%. Anal. calcd for $C_{23}H_{23}CuN_5O_6 \cdot 2H_2O$: C, 48.9; H, 4.8; N, 12.4. Found: C, 48.7; H, 4.8; N, 12.4. UV/vis (CH_3CN) [λ_{max}, nm (ε, $M^{-1}cm^{-1}$)]: 404 (29,400), 641 (290 sh). EPR (9.449 GHz, mod. amp. 4.0 G, DMSO, 77K): $g_{\parallel}$ = 2.316, $g_{\perp}$ = 2.10, and $A_{\parallel}$ = 176 G. FTIR (KBr): 3164 (s, C-H), 1652, 1596, 1479 (s, C=N_{py}, C=$C_{aromatic}$), 1437, 1399, 1290, 1182, 1092, 928, 898, 835, 760, 667 cm^{-1}. ESI-MS (MeOH): *m/z* = 529 [Cu($L^{NO2\text{-}amine}$) + H]$^+$. Solution magnetic moment (Evans method, 19.8 ^oC, 5.50 x 10^{-3} M, dimethylsulfoxide-d_6): 1.84 μ_B/Cu. Solid state magnetic moment (MSB-Auto, 4.5

kG, 22.0 ^{o}C): 1.83 μ_B/Cu.

[Cu($L^{MeO\text{-}amine}$)Na(CH_3OH)$_2$](ClO_4) (8): $H_2L^{MeO\text{-}amine}$ (0.044 g, 0.100 mmol) and $Cu(ClO_4)_2 \cdot 6H_2O$ (0.036 g, 0.100 mmol) were used. Yield: 0.0480 g, 70%. Anal. calcd for $C_{27}H_{37}ClCuN_3NaO_{10} \cdot H_2O$: C, 46.0; H, 5.6; N, 6.0. Found: C, 45.3; H, 5.0; N, 6.5. UV/vis (CH_2Cl_2) [λ_{max}, nm (ε, $M^{-1}cm^{-1}$)]: 342 (1,950), 423 (2,210) 594 (450 sh). EPR (9.436 GHz, mod. amp. 5.0 G, CH_2Cl_2, 77K): $g_{\parallel}$ = 2.249, $g_{\perp}$ = 2.086, and $A_{\parallel}$ = 176 G. FTIR (KBr): 2836 (s, C-H), 1595, 1569, 1481 (s, C=N_{py}, C=$C_{aromatic}$), 1361, 1239, 1163, 1079, 960, 791, 747, 623 cm^{-1}. ESI-MS (MeOH): *m/z* = 521 [Cu($L^{MeO\text{-}amine}$) + Na]$^+$. Solution magnetic moment (Evans method, 19.8 ^{o}C, 5.50 x 10^{-3} M, acetonitrile-d_3): 1.59 μ_B. Solid state magnetic moment (MSB-Auto, 4.5 kG, 22.0 ^{o}C): 1.25 μ_B/Cu.

X-ray Crystal Structure Determination. Single crystals of **6,** and **7** were obtained by slow evaporation of methanol solutions of the corresponding compounds, whereas X-ray quality crystals of **6** were isolated by slow evaporation of a dichloromethane solution of **6.** Intensity data for **6 -8** were collected at 100 (2) K using a diffractometer with a Bruker APEX ccd area detector.[9] Data were collected for **6 - 7** using graphite-monochromated Mo Kα radiation (λ = 0.71073 Å), while for **8**, graphite-monochromated Cu Kα radiation (λ = 1.54178 Å) was used. The samples were cooled to 100(2) K. Cell parameters were determined from a non-linear least squares fit of the data. The data were corrected for absorption by the semi-empirical method.[10] The structures were solved by direct methods and refined

by full-matrix least-squares methods on F^2.[11] Hydrogen atom positions of hydrogens bonded to carbons were initially determined by geometry and refined by a riding model. Hydrogens bonded to nitrogens or oxygens were located on a difference map, and their positions were refined independently. Non-hydrogen atoms were refined with anisotropic displacement parameters. Hydrogen atom displacement parameters were set to 1.2 (1.5 for methyl) times the displacement parameters of the bonded atoms.

In **6**, there are three metal complex molecules and two solvent (CH_2Cl_2) sites per asymmetric unit of the cell. Both solvent sites were severely disordered and were best modeled using the Squeeze program. The N-H distances were restrained to be approximately equal. In **7**, the intensity data were truncated to 0.94 Å resolution because data in higher resolution shells all had R(int) > 0.25. The second water site was so disordered that it was best modeled using the Squeeze program. In **8**, the perchlorate anion was disordered, and was modeled with refined occupancies of 0.591(8) and 0.409(8) for the A and B labeled groups. Restraints on the positional and displacement parameters of the perchlorate were required. Crystal data for **6-8** are summarized in Table 3-5.

Table 3-5. Crystallographic data for complexes **6**, **7**, and **8.**

	6· 2/3CH_2Cl_2	**7**· 2H_2O	**8**
formula	$C_{23.67}H_{22.33}Br_4Cl_{1.33}CuN_3O_2$	$C_{23}H_{27}Cu\ N_5O_8$	$C_{27}\ H_{37}\ ClCu\ N_3\ NaO_{10}$
fw	811.23	565.04	685.58
Crystal system	Monoclinic	Orthorhombic	Triclinic
Space group	$P2_1/n$	*Pbca*	$P\bar{1}$
a (Å)	13.626(5)	21.150(5)	10.6796(12)
b (Å)	20.992(8)	10.823(3)	11.1968(12)
c (Å)	29.684(12)	22.675(6)	15.2613(16)
α (deg)	90	90	99.326(8)
β (deg)	91.599(8)	90	104.157(8)
γ (deg)	90	90	114.830(9)
V ($Å^3$)	8487(6)	5190(2)	1531.5(3)
Z	12	8	2
ρ_{calcd} mg/m^3	1.905	1.446	1.487
μ (mm^{-1})	6.577	0.897	2.463
θ (deg)	1.89 to 25.25	2.04 to 22.21	3.13 to 67.15
R1,wR2[I >2δ(I)]	0.0506, 0.1266	0.0595, 0.1572	0.0515, 0.1805
GOF on F^2	1.002	1.017	1.122

3.7. References

1. (a) Yang, L.; Powell, D. R.; Klein, E. L.; Grohmann, A.; Houser, R. P., Delocalized mixed-valence Bi- and trinuclear complexes with short Cu-Cu bonds. *Inorg Chem* **2007,** *46* (17), 6831-6833; (b) Yang, L.; Houser, R. P., Copper(I) coordination chemistry of (pyridylmethyl)amide ligands. *Inorg Chem* **2006,** *45* (23), 9416-9422; (c) Chaudhuri, U. P.; Whiteaker, L. R.; Yang, L.; Houser, R. P., Multinuclear copper complexes of pyridylmethylamide ligands. *Dalton T* **2006,** (15), 1902-1908; (d) Mondal, A.; Li, Y.; Khan, M. A.; Ross, J. H.; Houser, R. P., Supramolecular copper hydroxide tennis balls: Self-assembly, structures, and magnetic properties of octanuclear $[Cu_8L_8(OH)_4]^{4+}$ clusters (HL = N-(2-pyridylmethyl)acetamide). *Inorg Chem* **2004,** *43* (22), 7075-7082; (e) Klein, E. L.; Khan, M. A.; Houser, R. P., Synthesis, characterization, and reactivity of new copper(II) complexes of 2-methylthio-N-(2-pyridylmethyl)acetamide. *Inorg Chem* **2004,** *43* (23), 7272-7274; (f) Chaudhuri, U. P.; Whiteaker, L. R.; Mondal, A.; Klein, E. L.; Powell, D. R.; Houser, R. P., Substituted pyridylmethylamide ligands and their zinc complexes. *Inorg Chim Acta* **2007,** *360* (11), 3610-3618; (g) Yang, L.; Powell, D. R.; Houser, R. P., Structural variation in copper(I) complexes with pyridylmethylamide ligands: structural analysis with a new four-coordinate geometry index, tau(4). *Dalton T* **2007,** (9), 955-964.

2. Shakya, R.; Jozwiuk, A.; Powell, D. R.; Houser, R. P., Synthesis and Characterization of Polynuclear Copper(II) Complexes with Pyridylbis(phenol) Ligands. *Inorg Chem* **2009,** *48* (9), 4083-4088.

3. Shakya, R.; Powell, D. R.; Houser, R. P., Unsupported mu-Oxo- and mu-

Hydroxo-Iron(III) Dimers and Mononuclear Iron(III) Complexes with Pyridylbis(aminophenol) Ligands. *Eur J Inorg Chem* **2009,** (35), 5319-5327.

4. Hansch, C.; Leo, A.; Taft, R. W., A Survey of Hammett Substituent Constants and Resonance and Field Parameters. *Chem Rev* **1991,** *91* (2), 165-195.

5. Shakya, R.; Wang, Z.; Powell, D. R.; Houser, R. P., Tetradentate vs Pentadentate Coordination in Copper(II) Complexes of Pyridylbis(aminophenol) Ligands Depends on Nucleophilicity of Phenol Donors. *Inorg Chem* **2011,** *50* (22), 11581-11591.

6. Hansch, C.; Leo, A.; Taft, R. W. *Chem. Rev.* **1991,** *91,* 165.

7. Friedrich, S.; Schubart, M.; Grade, L. H.; Scowen, I. J.; Edwards, A. J.; Mcpartlin, M. *Chem. Ber./Recl.* **1997,** *130,* 1751-1759.

8. Evans, D. F. *J. Chem. Soc.* **1959,** 2003-2005.

9. (a) SMART Software Reference Manual; Bruker-AXS: Madison, WI, 1998. (b) SAINT Software Reference Maunual; Bruker-AXS: Madison, WI, 1998.

10. Sheldrick, G. M. (2007). SADABS. Program for Empirical Absorption Correction of Area Detector Data. University of Göttingen, Germany.

11. (a) Sheldrick, G. M. SHELXTL Version 6.10 Reference manual; Bruker AXS Inc,: Madison, WI, 2000. (b) International Tables for Crystallography; Kluwer: Boston, 1995; Vol. C.

CHAPTER 4

COPPER COMPLEXES WITH PYRAZINE-CONTAINING PYRIDYLALKYLAMIDE LIGANDS

4.1. Introduction

Coordination polymers can be described as molecular inorganic-organic hybrid compounds with infinite one- two- or three–dimensional networks, which have been widely synthesized and investigated due to their potential application in gas storage and separation,[1] catalysis,[2] magnetism[3] and photochemistry.[4] Remarkable progress has been made in this area. Since the appearance of the phrase, coordination polymers, appeared in the early of 1960s, the number of published papers with the key words, coordination polymers, shows implosive increase. Coordination polymers have played important roles in the porous-materials area.[5] Two central components, connectors and linkers, are required for the construction of coordination polymers. Coordination number and coordination geometry are the two most important characteristics of the connectors and linkers. Transition metal ions such as copper, zinc, iron or silver are often used as versatile connectors in the construction of coordination polymers. With the dependence on the metal and oxidation state, coordination numbers can range from 2 to 7, leading to different geometries, which can be linear, T-shaped, tetrahedral, square planar or octahedral as shown in Figure 4-1.

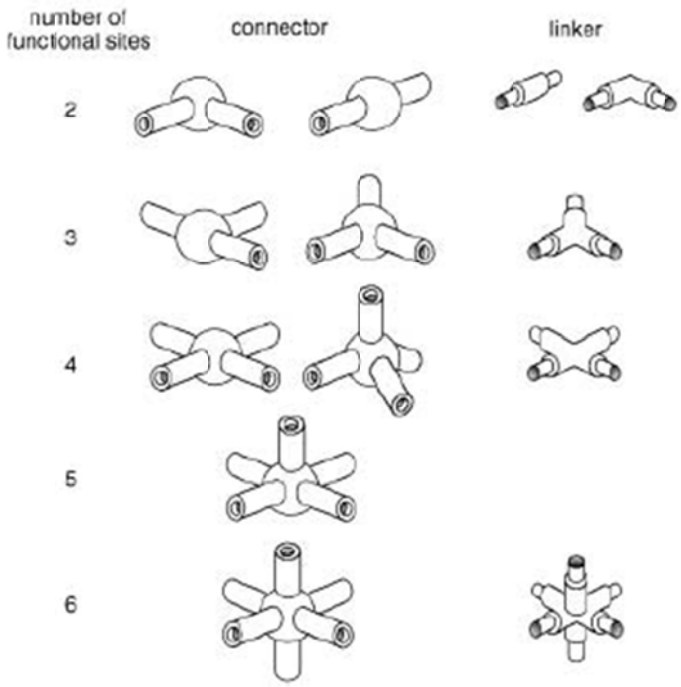

Figure 4-1. Components of coordination polymers. Figure is adapted from reference [5]

Linkers afford a wide variety of linking sites with tuned binding strength and directionality as shown in Figure 4-2. Halides are the smallest and simplest linkers. The most frequently used neutral organic ligands are pyrazine and 4, 4′-bipy. Many reviews about the structural topologies of the frameworks of coordination polymers have been published.[6] The topology of the motif can range from 1D linear or zigzag chain structures, 2D square grid networks to 3D nets. Various combinations of connectors and linkers afford various specific structural motifs to meet the specific function of the coordination polymer as shown in Figure 4-3.

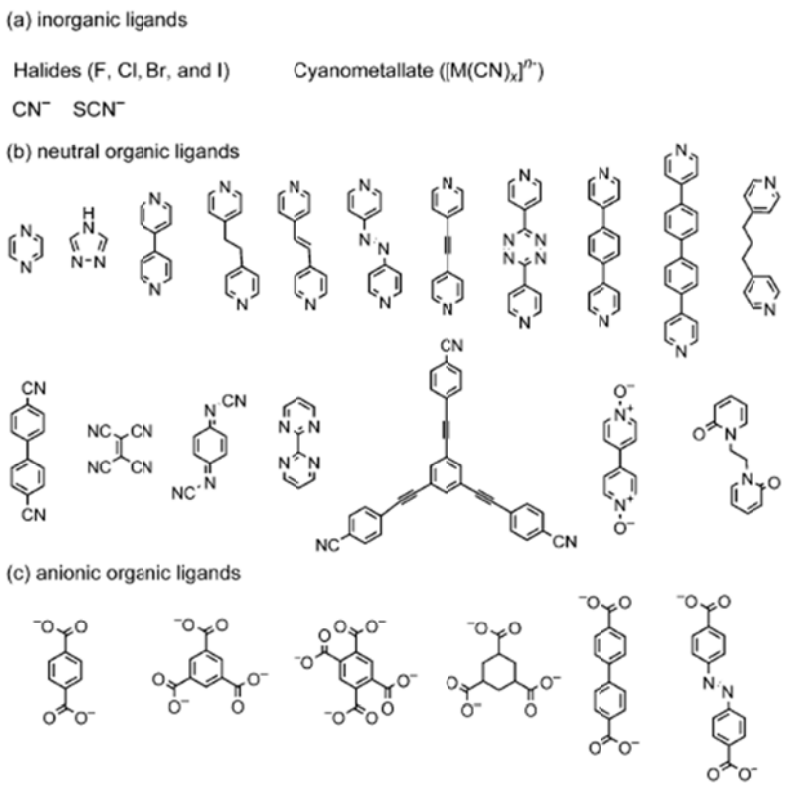

Figure 4-2. Examples of linkers used in coordination polymers. Figure is adapted from reference [5].

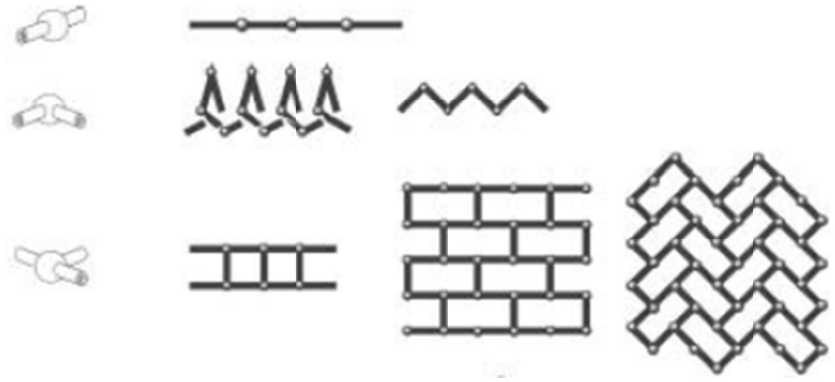

Figure 4-3. The structural framework constructed by using different connectors and linear linkers. Figure is adapted from reference [5]

.

Pyrazine-based ligands play a very important role in coordination chemistry. Bis (tridentate) pyrazine-based diamide ligands have been used to produce tetranuclear metal complexes. In Dr. Sally Brooker's group, they reported the synthesis and characterization of a pyrazine-based diamide ligand H_2L as shown in Figure 4-4.[6] This symmetrical diamide ligand c[7]ontains a central bridging pyrazine unit connected by two tridentate binding pockets. Two amide hydrogens can be deprotonated with the presence of the base, in which the anionic amidate N can coordinate to the metal center. As predicted, the ligand coordinates with the metal center in different modes with or without the base. The 1:1 reaction of Cu $(BF_4)_2 \bullet xH_2O$ with the ligand H_2L in CH_3CN in the absence of the base leads to the formation of a centrosymmetric dimer, $[Cu\ (H_2L)(MeCN)]_2(BF_4)_4$. In this complex, the pyrazine ring does not bridge two Cu(II) ions as only one pyrazine N donor coordinates with the copper(II) ion. With the addition of one equivalent of Et_3N into the reaction, a teranuclear copper(II) complex was synthesized and characterized by X-ray analysis. In this complex, both pyrazine N donors and the deprotonated amidate N atoms are involved in tridentate chelation. This is a rare example of a discrete grid of pyrazine-based amide ligands. Our ligand system, shown in Figure 4-7, is similar and part of the ligand H_2L. The coordination mode of the ligand H_2L should provide hints to the possible bonding modes for my ligand system.

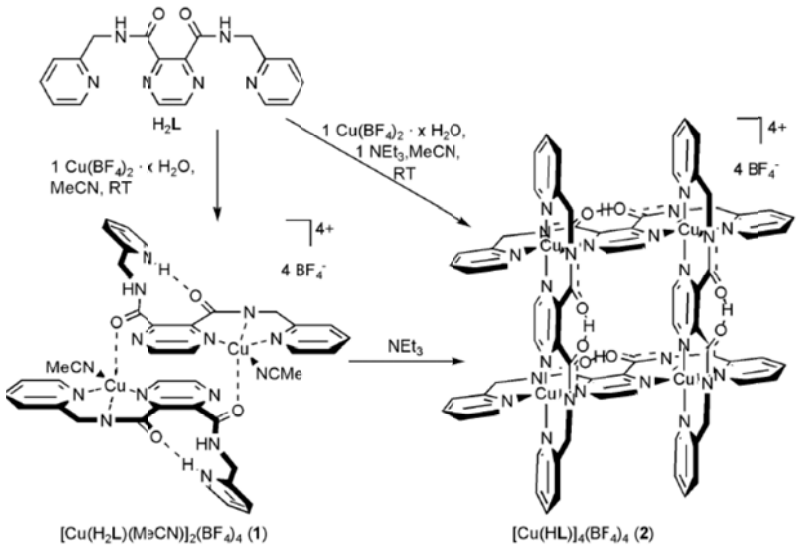

Figure 4-4. The synthesis of binuclear and tetranuclear copper(II) complexes with the bis-terdentate diamide ligand H_2L. Figure is adapted from reference [7].

The Brooker group also reported a homolog of H_2L, ligand H_2L^{Et}, which is an ethylene-linked bis-terdentate ligand. The 1:1 reaction of $Cu(BF_4)_2 \cdot xH_2O$ with H_2L^{Et} in CH_3CN without or with the base lead to the formation of similar tetranuclear copper(II) complex $[Cu_4(H_2L)_2(HL)_2](BF_4)_6$ and $[Cu_4(HL)_4](BF_4)_4$ as shown in Figure 4-5, respectively. From the differences of the synthesized Cu(II) complexes, it is clear that the change from methylene to ethylene bridging arms has a profound effect on the coordination modes of the corresponding Cu(II) complexes. The synthesis and characterization of a tetranuclear nickel(II) complex was also described in the same paper.[7]

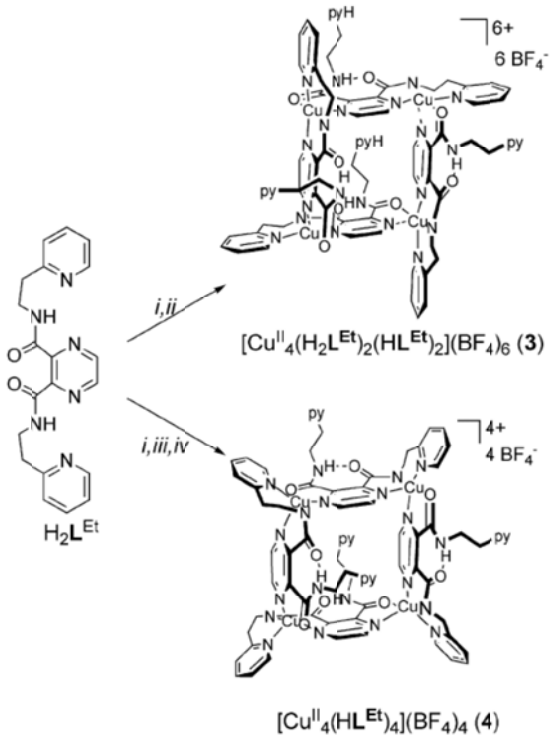

Figure 4-5. Synthesis of tetranuclear copper(II) complexes with the ligand H_2L^{Et}. Figure is adapted from reference [8].

With the same ligand system, Dr. Stoeckli-Evans reported the synthesis and characterization of one binuclear copper(II) complex, and two tetranuclear copper(II) and nickel(II) complexes with multiple anion encapsulations.[9]

Another two homologous pyrazine-based diamide ligands H_2L^1 and H_2L^2 as shown in Figure 4-6, are linkage isomers of the previous ligands H_2L and H_2L^{Et}. No tetranuclear copper(II) complexes of H_2L^1 and H_2L^2 were synthesized, but one tetranuclear cobalt(III) grid type complex was reported.[10] The reaction of $Cu(BF_4)_2 \cdot 4H_2O$ with both ligands prefers to produce dicopper(II) complexes.[11]

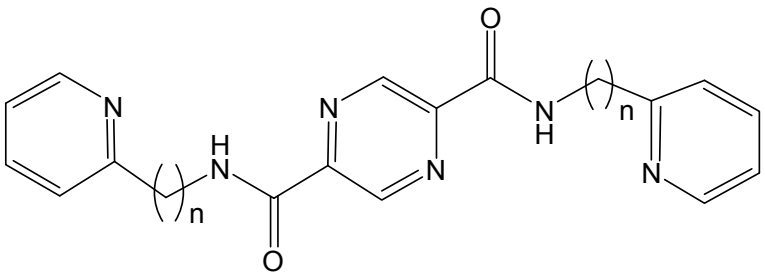

n=1: H_2L^1; n=2: H_2L^2

Figure 4-6. Pyrazine-based bis(tridentate) diamide ligands H_2L^1 and H_2L^2 used in reference [10].

As an analog to the previously mentioned bis(tridentate) two-alkylpyridine arm amide ligands, single-alkylpyridine arm amide ligands HL^{Pz} and $HL^{Pz'}$, were prepared as shown in Figure 4-7.[12] In this ligand system, the pyrazine nitrogen out of the back of the ligand is spare, which means that this pyrazine N could act as a linker atom to coordinate with the second metal to form coordination polymers. Some research has been done with this ligand system. Recently, Hubin and co-workers reported the structure of a trimetallic mixed–valence cobalt complex of the ligand HL^{Pz}.[12] Cobalt and silver complexes of this ligand system were reported by Brooker and co-workers.[13]

Motivated to see how the copper chemistry will be changed by the introduction of the pyrazine substituent and in collaboration with the Hubin research group, we set out to investigate HL^{Pz} and $HL^{Pz'}$. The ligands HL^{Pz} and $HL^{Pz'}$ still share the same common pyridylalkylbenzamide platform as in chapter 2. One pyrazine ring is introduced into the platform as the substituent, and so two more potential N-donors are available for the coordination to the metal ions. .. Two N donor atoms from the pyrazine increase the coordination mode of the ligand. Only one N donor or both N

donors coordinate with the copper ions in different reaction conditions. So, the copper chemistry of both ligands is expected to be abundant and interesting.

In addition to the pyridyl N, deprotonated amide N and in-sphere pyrazine N have the potential to coordinate with copper center and form the cap to further react with the sulfide reagents. Metathesis reactions were proved to be a successful method for the synthesis of Cu-S clusters by mixing the copper salts, suitable ligands and sulfide reagents. Tolman's group reported several Cu-S clusters based on the reaction of CuX2 (X= Cl^-, or $CF_3SO_3^-$), bidentate *N,N,N′,N′*-tetramethylethylenediamine (Me_4eda) ligand, and Li_2S or Na_2S_2. So, we set the goal to synthesize Cu-S clusters based on metathesis reactions using our pyrazine-based amide ligands.

We also plan to investigate the coordination polymer chemistry, in which HL^{Pz} and $HL^{Pz'}$ acting as tridentate terminal ligands to react with different bridging ligands as linkers.

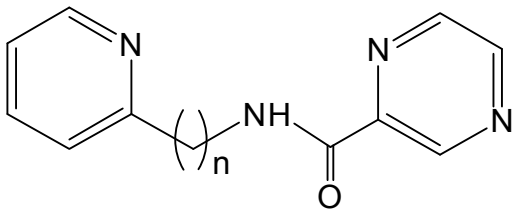

HL^{Pz}(n=1); $HL^{Pz'}$ (n=2)

Figure 4-7. Pyrazine-based amide ligands used in the synthesis of **9-13**.

4.2. Synthesis of Pyrazine-based Amide Ligands

The synthesis of the ligands HL^{Pz} and $HL^{Pz'}$ followed the reported method as shown in Figure 4-5.[12] Both ligands were synthesized by dissolving pyrazine-2-carboxylic acid methyl ester into methanol and adding 2-aminomethylpyridine or 2-aminoethylpyridine dissolved in methanol. The solutions were refluxed overnight and then dried down to off-white powders. The resulting products were dissolved in a minimal amount of warmed solvent and then cooled to produce colorless crystals. The ligands were fully characterized by IR, ^{1}H-NMR and ESI-MS.

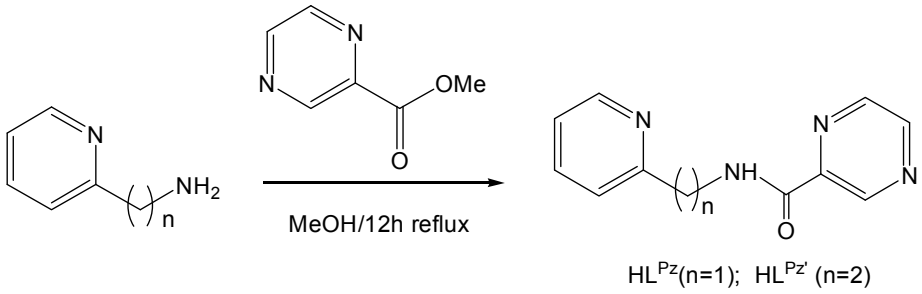

Figure 4-8. Synthesis of the pryazine-based ligand HL^{Pz} and $HL^{Pz'}$.

Both ligands bear one pyridyl and one pyrazine ring connected by an amide functional group. Generally, pyridylamide ligands exhibit two main coordination modes depending on the state of the amide group: the neutral amide state and the deprotonated amidate state. The neutral amide mostly coordinates with the metal center by the pyridyl N atom only or both pyridyl N atom and the amide carbonyl O atom. With the presence of a base in the reaction, the deprotonated amidate N atom also coordinates with the metal ions. The difference between HL^{Pz} and $HL^{Pz'}$ is that

HL^{Pz} is methylene-linked to the amide and $HL^{Pz'}$ is ethylene-linked to the amide. The change of the linking group has a profound effect on the coordination modes with the metal center. This fact will be confirmed by the following discussion in this chapter.

4.3. Copper(I) Complex: $[Cu(HL^{Pz})Cl]_n$ (9)

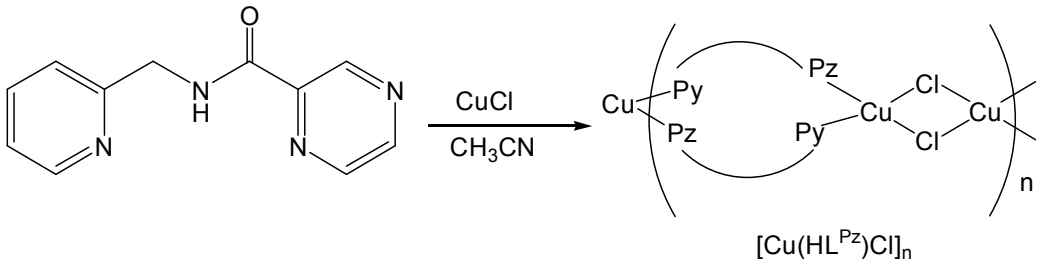

Figure 4-9. Synthesis of $[Cu(HL^{Pz})Cl]_n$ **(9).**

Complex $[Cu(HL^{Pz})Cl]_n$ **(9)** was prepared by the reaction of CuCl with ligand HL^{Pz} in CH_3CN. The red crystals of **9** were obtained by vapor diffusion of diethyl ether into the yellow filtrate from the reaction solution. X-ray analysis of complex **9** reveals that it consists of a series of Cu_2Cl_2 dimers bridged by two HL^{pz} ligands, and forms an infinite 1-D chain structure as shown in Figure 4-10. The copper atom is bound to two nitrogen donors (comprised of one pyridine nitrogen and one pyrazine nitrogen atom) and two Cl anions with Cu···Cl distances of 2.3289(9) Å and 2.4680(11) Å, respectively. The Cu-N bond lengths are 2.008 Å and 2.071 Å, which are longer than some reported chloral-bridged copper(I) complexes by Lei Yang in our group.[14] The average Cu-Cl (2.398 Å) and Cu-N (2.040 Å) bond distances are comparable with values in other Cu_2Cl_2 complexes with diamond core structures.

The smaller Cu-Cl-Cu bond angle (77.17°) and the larger Cl-Cu-Cl bond angle (102.83°) lead to a slightly shorter Cu···Cu bond distance (2.994 Å) than the reported range of 2.997 to 3.150 Å.[15] The Cu atom displays distorted trigonal-pyramidal geometry supported by $\tau_4 = 0.73$.[16] The outside pyrazine N acts as a bridging donor to bind with copper and forms the chain structure. In our lab, Lei Yang reported the synthesis and characterization of a series of chloral-bridged mono or binuclear copper (I) complexes with (pyridylmethyl)amide ligands.[14] Different structural topologies result from the difference of the (pyridylmethyl)amide ligand with different substituent groups on the amide. In this case, the pyrazine ring connects with the amide group. The pyrazine N coordinates with the second copper atom and leads to the formation of the 1D chain structure. The packing structure of **9** shows the formation of 1D ladder structure as shown in Figure 4-11. Selected bond lengths and bond angles for **9** are listed in Table 4-1.

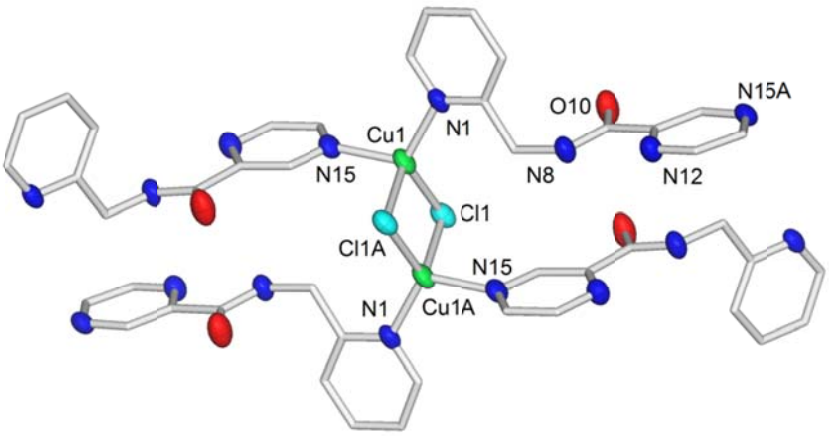

Figure 4-10. X-ray crystal structure for complex $[Cu(HL^{Pz})Cl]_n$ **(9)**. All H atoms have been omitted for clarity.

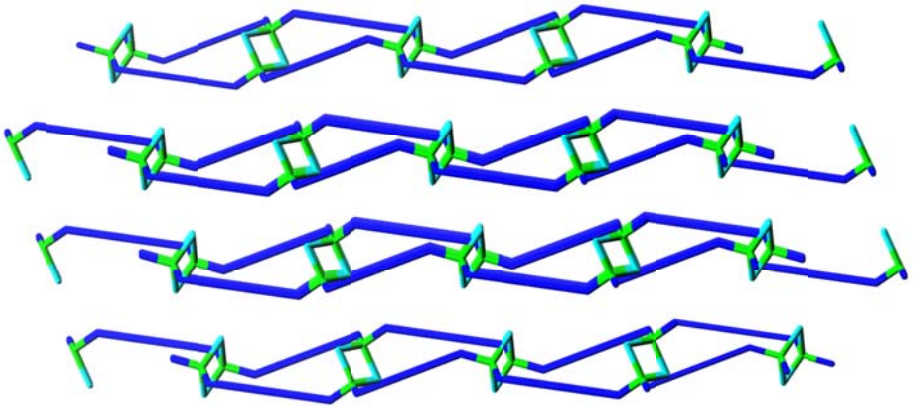

Figure 4-11. 1D ladder structure of $[Cu(HL^{Pz})Cl]_n$ **(9)**.

Table 4-1. Selected bond distances (Å) and bond angles (deg) for complex **9.**

Cu1-N1	2.008(2)	Cu**1**-Cl1	2.4680(11)
Cu1-N15	2.071(2)	Cl1-Cu1A	2.3289(9)
Cu1-Cl1A	2.3289(9)	Cu**1**-Cu1A	2.9936(9)
N1-Cu1-N15A	113.42(8)	N1-Cu1-Cl1A	125.46(6)
N15-Cu1-Cl1A	105.38(6)	N1-Cu1-Cl1	105.57(6)
N15A-Cu1-Cl1	100.99(6)	Cl1A-Cu1-Cl1	102.83(3)
N1-Cu1-Cu1A	132.27(6)	N15A1-Cu1-Cu1A	111.32(6)
Cl1A-Cu1-Cu1A	52.50(3)	Cl1-Cu1-Cu1A	49.334(19)

4.4. Copper(II) complexes

*4.4.1. Mononuclear [Cu(L^{Pz})(py)$_2$][OTf]•H_2O **(10)***

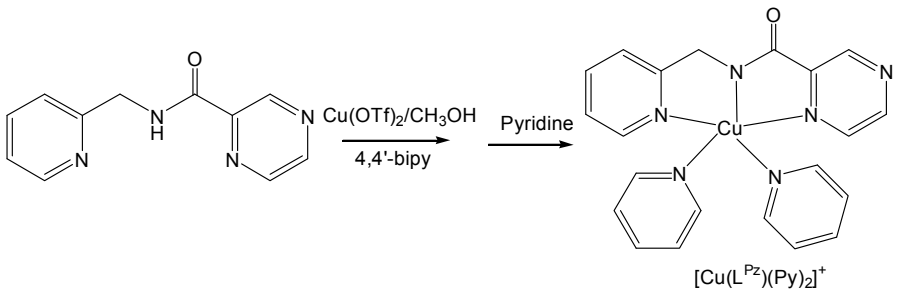

Figure 4-12. Synthesis of $[Cu(L^{Pz})(Py)_2]^+$ **(10)**.

With the goal to obtain coordination polymers, the choice of the bridging ligand plays a very important role in the construction of the geometry and topology of the polymers. 4,4'-bipyridine as a bidentate neutral bridging ligand has been widely used in the synthesis of coordination polymers.[5] Addition of a solution of $Cu(OTf)_2$ in CH_3OH to a stirred methanol solution of HL^{Pz} in the presence of basic Et_3N resulted in the formation of a blue solution. Following the addition of 4,4'-bipyridine to this solution, a purple precipitate was obtained. The solubility of the purple precipitate was checked in different solvents, such as CH_2Cl_2, CH_3CN and CH_3OH. While it was insoluble in these solvent, it dissolved in pyridine very well. A blue filtrate was obtained after filtration to remove insoluble impurities, and vapor diffusion of diethyl ether into the filtrate produced green needle-shaped crystals of **10**. X-ray analysis of complex **10** reveals that it is a mononuclear copper (II) complex, which is composed of one deprotonated ligand L^{Pz} and two pyridine solvent molecules as shown in Figure 4-13. The 4,4'-bipyridine from the reaction

was replaced by the strong pyridine solvent ligands during the crystallization process.

The copper ion in **10** is five-coordinate, with three N donors from the ligand and two N donors from pyridine molecules, forming a square pyramidal geometry supported by $\tau_5 = 0.173$.[15a] The apical Cu-N17 distance of 2.232(5) Å is longer than the average Cu-N distance (2.005 Å) in the square planar bonds. Selected bond distances (Å) and bond angles (deg) of complex **10** are shown in Table 4-2. The electronic absorption spectrum of complex **10** in CH_3OH was collected, and is typical of copper(II) complexes with pyridylamidate ligands. The absorption band at 320 nm can be assigned as ligand to metal charge transfer transition (LMCT) and a weak absorption band at 642 nm assigned as a *d-d* transition.

The X-band EPR spectrum of complex **10** displays typical axial signals with four-line hyperfine features with $S = 1/2$ due to the interaction of the electron spin and the copper nucleus spin. $g_{\parallel} = 2.254 > g_{\perp} = 2.045 > 2.003$ shows the d_{x2-y2} ground state of the five-coordinate copper(II) complex.

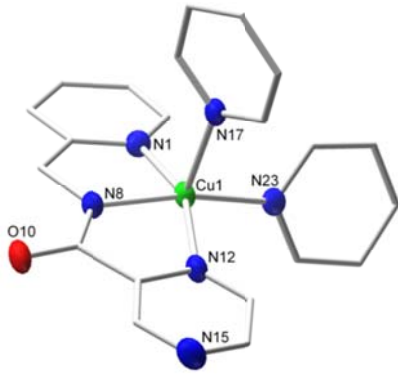

Figure 4-13. X-ray crystal structure for complex $[Cu(HL^{Pz})(Py)_2]^+$ **(10)**. All H atoms have been omitted for clarity

Table 4-2. Selected bond distances (Å) and bond angles (deg) for complex **10.**

Cu1-N8	1.917(5)	Cu1-N23	1.979(5)
Cu1-N1	2.057(5)	Cu1-N12	2.067(5)
Cu1-N17	2.232(5)		
N8-Cu1-N23	167.28(19)	N8-Cu1-N1	81.4(2)
N23-Cu1-N1	96.60(19)	N8-Cu1-N12	80.23(19)
N23-Cu1-N12	98.25(18)	N1-Cu1-N12	156.93(18)
N8-Cu1-N17	98.71(18)	N23-Cu1-N17	93.99(18)
N1-Cu1-N17	102.81(18)	N12-Cu1-N17	93.67(18)

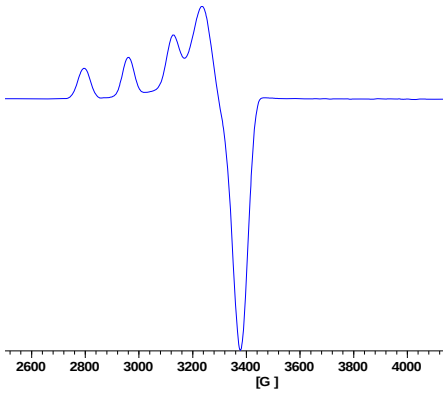

Figure 4-14. EPR spectrum of complex **10** in CH_3OH at 77K.

4.4.2. Binuclear $[Cu_2(L^{Pz})_2(4,4'\text{-bipy})(OTf)_2]$ **(11)**

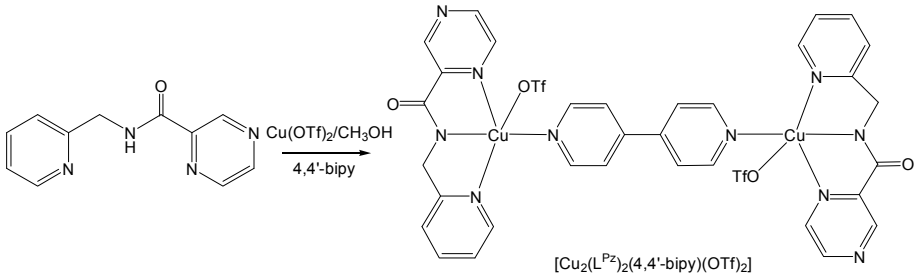

Figure 4-15. Synthesis of $[Cu_2(L^{Pz})_2(4,4'\text{-bipy})(OTf)_2]$ **(11)**.

Binuclear complex $[Cu_2(L^{Pz})_2(4,4'\text{-bipy})(OTf)_2]$ (**11**) was prepared with the same reaction as complex **10** using a different method. A solution of 4,4′-bipyridine in CH_3OH was layered on the blue solution from the reaction solution of $Cu(OTf)_2$ and deprotonated L^{Pz-}, from which purple crystals of **11** suitable for X-ray analysis were obtained. From the IR analysis, the purple precipitate obtained in the synthesis of complex **10** should be the same as the complex **11**. X-ray analysis of complex **11** shows that it is a binuclear copper(II) complex as shown in Figure 4-16. The copper center is five-coordinate with three N atoms from the ligand and one N atom from the bridging 4,4′-bipyridine ligand. The fifth apical position is occupied by the O from the triflate anion, forming a slightly distorted square pyramidal geometry (τ_5 = 0.143).[17] So, the copper ion does not coordinate with the 4-$N_{pyrazine}$ atom of the ligand and does not form a coordination polymer. The deprotonated L^{pz-} acts as a terminal tridentate ligand and 4,4′-bipy acts as a bridging ligand to bind with the copper atoms. The 4,4′-bipy ligand is slightly distorted as shown in the crystal structure to fit the geometry of the copper ions. The 4,4′-bipy rings are twisted away

from co-planarity by about 30°. The average Cu-N distance is typical for Cu(II) complexes. The apical Cu-O distance (2.3867 Å) is longer than the normal Cu-O bond distance.

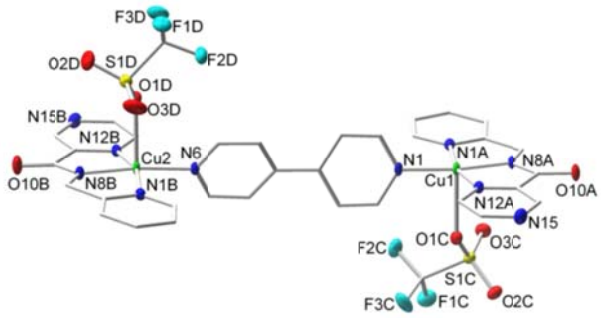

Figure 4-16. X-ray crystal structure for complex $[Cu_2(L^{Pz})_2(4,4'\text{-bipy})(OTf)_2]$ **(11)**. All H atoms have been omitted for clarity.

Table 4-3. Selected bond distances (Å) and bond angles (deg) for complex **11.**

Cu1-N8A	1.901(2)	Cu1-N1	1.972(2)
Cu1-N1A	2.005(2)	Cu1-N12A	2.023(2)
Cu1-O1C	2.3525(18)	Cu2-N8B	1.901(2)
Cu2-N6	1.968(2)	Cu2-N1B	2.017(2)
Cu2-N12B	2.028(2)	Cu2-O1D	2.3867(18)
N8A-Cu1-N1	172.56(9)	N8A-Cu1-N1A	82.70(9)
N1-Cu1-N1A	98.09(9)	N8A-Cu1-N12A	82.05(9)
N1-Cu1-N12A	96.40(8)	N1A-Cu1-N12A	163.95(9)
N8A-Cu1-O1C	93.63(8)	N1-Cu1-O1C	93.49(8)
N1A-Cu1-O1C	100.49(8)	N12A-Cu1-O1C	85.45(8)
N8B-Cu2-N6	173.62(9)	N8B-Cu2-N1B	82.30(9)
N6-Cu2-N1B	96.69(9)	N8B-Cu2-N12B	82.34(9)
N6-Cu2-N12B	97.73(9)	N1B-Cu2-N12B	162.88(9)
N8B-Cu2-O1D	92.77(8)	N6-Cu2-O1D	93.57(8)
N1B-Cu2-O1D	105.54(8)	N12B-Cu2-O1D	82.72(7)

4.4.3. Coordination Polymer [Cu (L^{Pz})(N_3)]$_n$ **(12)**

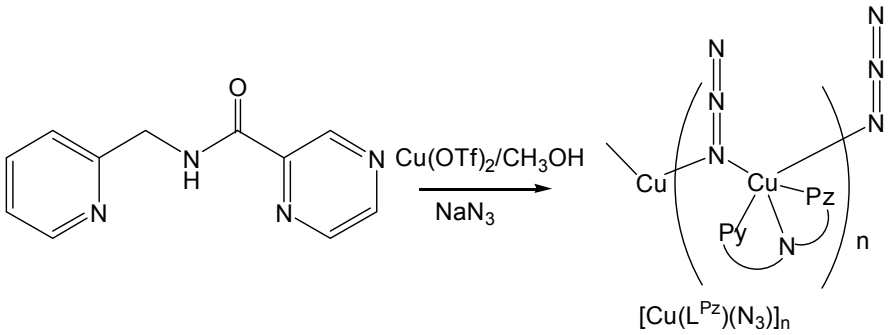

Figure 4-17. Synthesis of $[Cu(L^{Pz})(N_3)]_n$ **(12)**.

Low-dimensional coordination polymers have attracted much interest due to their fascinating magnetic properties.[5] The selection of appropriate bridging ligands to transmit the exchange interactions between the paramagnetic centers becomes very important. The azide anion is one of the most widely used bridging ligands due to its versatile coordination modes. μ_2-1, 3 (end-to-end, EE) and μ_2-1,1 (end-on, EO) are the two most common coordination modes. From many reported azide-bridged transition metal complexes and their magnetic studies, the relationship of the magnetism of the complexes and the bridging modes of the azide anion is illustrated. Azide anion can mediate ferromagnetic (FO) couplings in the EO mode and antiferromagnetic (AF) couplings in the EE mode although there is some reported exceptions.[15b] Due to its various binding modes, various discrete clusters,[15c] one-dimensional chains two-dimensional sheets[18] and three-dimensional networks[19] [20] have been reported with different ancillary ligands.

Complex $[Cu(L^{Pz})(N_3)]_n$ **(12)** was obtained by the layer crystallization method.

We used azide to replace 4,4'-bipyridine as the linker for the construction of coordination polymer **12**. X-ray analysis of complex **12** shows that it is an azido-bridged (EO) one dimension polymer as shown in Figure 4-18. In this complex, the copper center is five coordinate with three N donors from the ligand HL^{Pz} and two N atoms from the N_3^- anionic bridging ligand, resulting in the formation of square pyramidal geometry (τ_5 = 0.073). Three N donors of the ligand and one N donor from the azide anion comprise the basal plane, and the axial position is occupied by the N from the bridging azide. The bridging EO azido anions are bound to two Cu(II) atoms with Cu-N distances of 1.973 Å and 2.533 Å, and the Cu-N17-Cu angle is 136.52°. The intrachain Cu···Cu distance is 4.191 Å, which is longer than the reported Cu complexes with N_3^- in an EO mode. [25] The 3D packing structure of **12** is shown in Figure 4-19. Three layers are shown packed closely, with two different directions of the azide groups. Each layer forms a separate 1D chain structure.

The X-band EPR spectrum of complex **12** displays typical axial signals with four-line hyperfine features with S =1/2 due to the interaction of the electron spin and the copper nucleus spin. $g_{\parallel}$ = 2.248 > $g_{\perp}$ = 2.037 > 2.003 shows the d_{x2-y2} ground state of this five-coordinate copper(II) complex. In solutions of **12** dissolved in CH_3OH, the coordination polymer dissociates and forms monomers (*m/z* = 341 $[Cu(L^{Pz})N_3 + Na]^+$), dimmers (*m/z* = 659 $\{[Cu(L^{Pz})N_3]_2 + Na\}^+$) and trimers (*m/z* = 977 $\{[Cu(L^{Pz})N_3]_3 + Na\}^+$) as shown in ESI-MS.

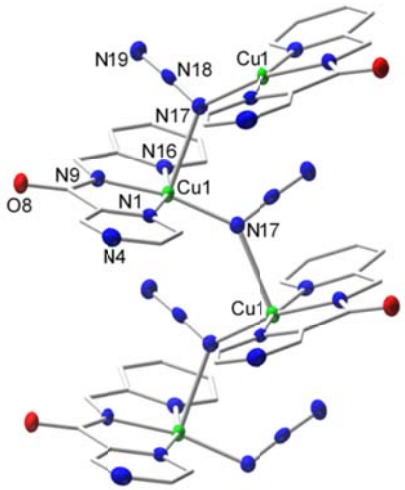

Figure 4-18. X-ray crystal structure of complex $[Cu(L^{Pz})(N_3)]_n$ **(12)**. All H atoms have been omitted for clarity.

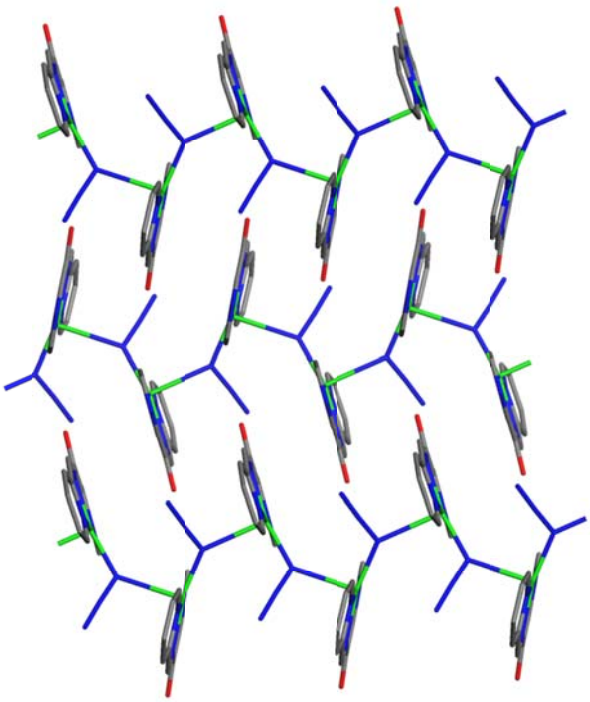

Figure 4-19. Packing structure of complex $[Cu(L^{Pz})(N_3)]_n$ **(12)**.

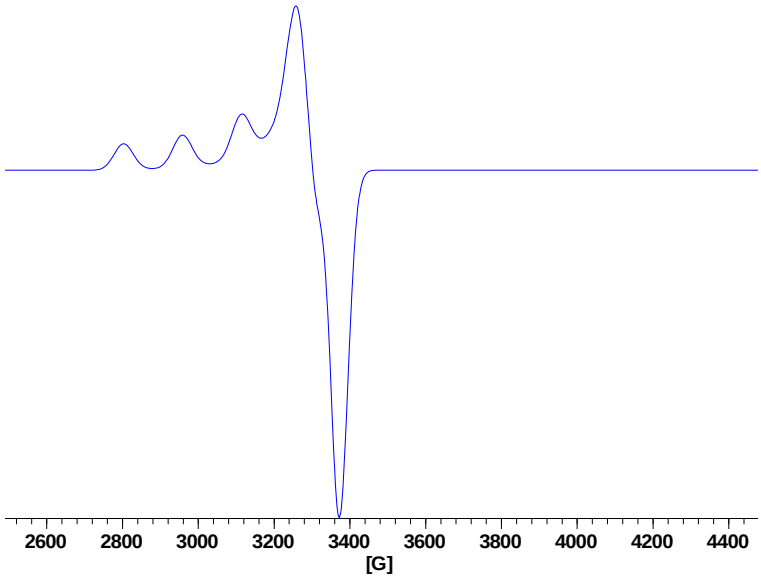

Figure 4-20. EPR spectrum of complex **12** in CH_3OH at 77K.

Table 4-4. Selected bond distances (Å) and bond angles (deg) for complex **12.**

Cu1-N9	1.911(3)	Cu1-N17	1.973(3)
Cu1-N16	2.013(3)	Cu1-N1	2.013(3)
N9-Cu1-N17	168.11(10)	N9-Cu1-N16	82.16(10)
N17-Cu1-N16	100.69(10)	N9-Cu1-N1	81.54(9)
N17-Cu1-N1	95.35(9)	N16-Cu1-N1	163.69(10)

4.4.4. Coordination Polymer [Cu ($L^{Pz'}$)(N_3)]$_n$ ***(13)***

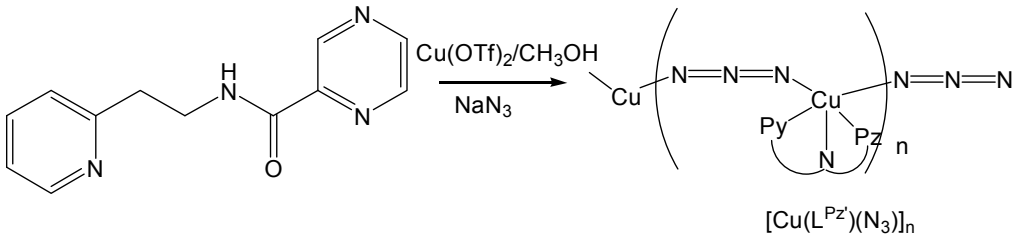

Figure 4-21. Synthesis of [Cu ($L^{Pz'}$)(N_3)]$_n$ (**13**).

Complex [Cu($L^{Pz'}$)(N_3)]$_n$ **(13)** was synthesized by the same method as complex **12**, except that a different ligand, $HL^{Pz'}$, was used instead of HL^{Pz}. The crystal structure of complex **13** is similar to complex **12**. It is also an azido-bridged one dimensional coordination polymer as shown in Figure 4-22. In complex **13**, the copper center is five coordinate with three N from the ligand $HL^{Pz'}$, and two N from the N_3^- anionic bridging ligand, forming a distorted square pyramidal geometry. Three N donors from the ligand and one azido N donor comprise the basal plane, the axial position is occupied by the N donor from the azide anion with the longer Cu-N_{azido} distance of 2.470 Å. The coordination of mode of the azido ligand is different than in complex **12**. The bridging EE azido anions are bound to Cu(II) with Cu-N distances of 1.993 Å and 2.470 Å. The difference of the two ligands HL^{Pz} and $HL^{Pz'}$ have important effects on the coordination bridging mode of the azide anion ligand. The 3D packing structure of complex **13** is shown in Figure 4-23. Layer 1 and layer 2 are shown packed closely with overlap of the two pyridyl rings. The π···π interactions are found between the two aromatic pyridyl rings. The distance of layer 2 and layer 3 is longer than layer 1 and 2 or layer 3 and 4. Each layer is a 1D zigzag

structure bridged by an azide in end-to-end mode.

The X-band EPR spectrum of complex **13** display typical axial signal with four-line hyperfine features with S =1/2 due to the interaction of the electron spin and the copper nucleus spin. $g_{\parallel}$ = 2.249 > $g_{\perp}$ = 2.037 > 2.003 shows the d_{x2-y2} ground state of five-coordinate copper(II) complex. The solution behavior of **13** is the same as **12**, with peaks for the monomers (*m/z* = 355 $[Cu(L^{Pz'})N_3 + Na]^+$), dimers (*m/z* = 687 $\{[Cu(L^{Pz'})N_3]_2 + Na\}^+$) and trimers (*m/z* = 1019 $\{[Cu(L^{Pz'})N_3]_3 + Na\}^+$) found in ESI-MS.

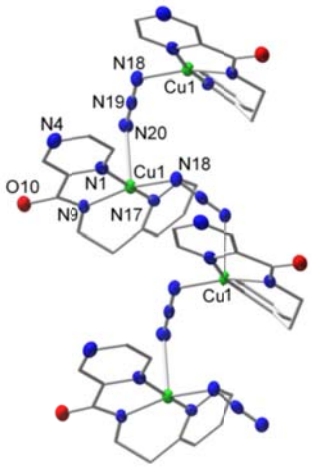

Figure 4-22. X-ray crystal structure of complex $[Cu(L^{Pz'})(N_3)]_n$ **(13).** All H atoms have been omitted for clarity.

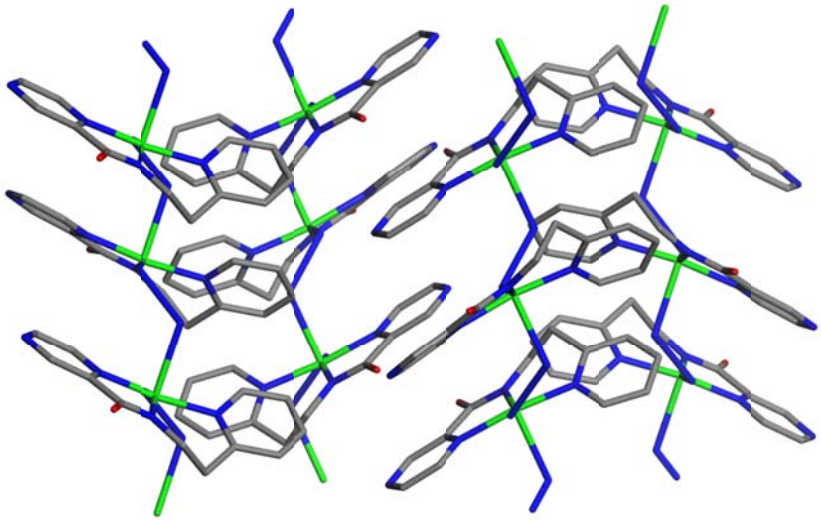

Figure 4-23. Packing structure of complex $[Cu(L^{Pz'})(N_3)]_n$ **(13)**.

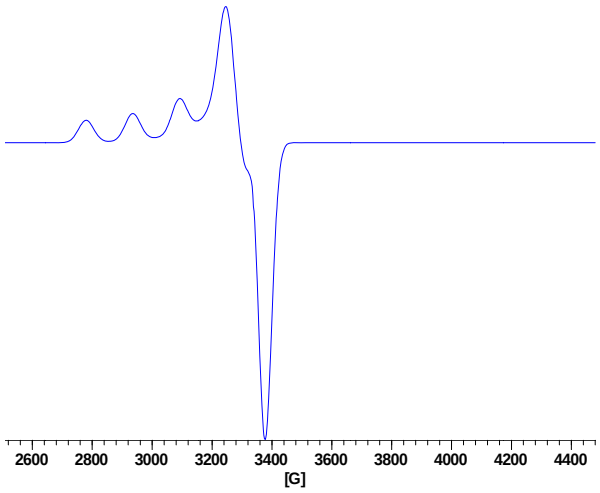

Figure 4-24. EPR spectrum of complex **13** in CH_3OH at 77K.

Table 4-5. Selected bond distances (Å) and bond angles (deg) for complex **13.**

Cu1-N9	1.942(3)	Cu1-N18	1.983(4)
Cu1-N17	1.993(3)	Cu1-N1	1.997(4)
Cu1-N20	2.470(4)		
N9-Cu1-N18	160.98(15)	N9-Cu1-N17	93.86(15)
N18-Cu1-N17	94.63(14)	N9-Cu1-N1	82.09(15)
N18-Cu1-N1	91.62(14)	N17-Cu1-N1	171.08(15)
N9-Cu1-N20	101.90(14)	N18-Cu1-N20	95..33(15)
N17-Cu1-N20	88.32(15)	N18-Cu1-N20	84.77(13)

4.5. Conclusions

In this chapter, with the goal to synthesized Cu-S clusters by metathesis reaction, we carried out the reaction of HL^{Pz} ligand, copper triflate and Na_2S in different reaction conditions. The reaction of deprotonated L^{Pz-} and copper triflate produced a green solution in CH_2Cl_2, then addition of a suspension of Na_2S into the green solution led to dark mixture with black precipitate. The reaction in CH_3OH also led to the formation of black precipitate and light green filtrate. No crystals were obtained from the vapor diffusion of diethyl ether into the filtrate. Comparing with Tolman's neutral bidentate ligand, the HL^{Pz} ligand needs to be deprotonated with the base to form an anionic ligand. Maybe this is the reason why the black precipitate was formed in the reaction. The targeted Cu-S complexes were not

obtained from the metathesis reaction.

We also set the goal to synthesize coordination polymers with the pyrazine-containing ligand HL^{Pz} and $HL^{Pz'}$. One copper(I) and four copper(II) complexes were synthesized and characterized by X-ray crystallography. Complex **9** is a one dimension coordination polymer in which Cu_2Cl_2 cores are bridged by two HL^{Pz} ligands. The pyridyl N and 4-positon pyrazine N coordinate with the copper center. The reactions of both deprotonated ligand L^{Pz-} and $L^{Pz'-}$ with $Cu(OTf)_2$ produced dark blue clear solution, the crystallization of both filtrate to obtain the mononuclear copper complexes is not successful. Then the reactions of above solution with different organic linkers were carried. No coordination polymer was obtained when 4,4′-bipyridine used as a linker. Instead unexpected monomeric copper complex **10** and dicopper **11** were synthesized. In complex **10**, 4,4′-bipyridine was replaced by pyridine solvent to coordinate to the copper ion. The 4-position payazine N does not coordinate with the copper ion in both **10** and **11**. When azide was used as a linker, two 1D coordination polymers, **12** and **13**, were synthesized and characterized by X-ray analysis. The bridging mode of azide is different (EO in **12** and EE in **13**) due to the difference of the terminal ligand HL^{Pz} and $HL^{Pz'}$.

Comparing with some reported tetranuclear copper complexes from the Brooker group, the HL^{Pz} and HL^{Pz} ' ligands have different coordination modes than her ligands. There is only one pyrazine N atom involved in the coordination with copper ions (out-sphere N in complex 9 and in-sphere N from complex 10-12). Her ligand has two more N donors to coordinate with copper ions and prefers to form [2 x 2] grid framework with coordination of four copper ions. So, one ligand has six N

donor atoms to coordinate with two copper ions. The [2 x 2] grid tetranuclear copper complex is very stable and easy isolated from the crystallization. The HL^{Pz} and $HL^{Pz'}$ ligand can act as terminal ligands to coordinate with one copper ion. The differences of the two ligand systems lead to different copper chemistry.

4.6. Experimental

General Procedures. All reagents were purchased from commercial suppliers and used as received without further purification, unless otherwise stated. The ligand HL^{Pz} (N-(pyridine-2-yl)methyl)pyrazine-2-carboxamide) and $HL^{Pz'}$ (N-(pyridine-2-yl)ethyl)pyrazine-2-carboxamide) were synthesized according to previously reported procedures.[12-13] The solvents used were doubly purified using alumina columns in a MBraun solvent purification system (MB-SPS). Infrared spectra were measured from 4000 to 400 cm^{-1} as KBr pellets on a NEXUS 470 FTIR spectrometer using the KBr pellet technique. Elemental analyses were carried out by Atlantic Microlabs, Norcross, GA. ^1H NMR spectra were measured using a Varian 300 MHz instrument. ESI (positive) spectra were measured in Q-TOF quadrupole time-of flight mass spectrometer (Micromass, Manchester, U. K.) containing a Z-spray electrospray ionization source (ESI). UV-visible spectra were measured on a Shimadzu UV2401PC spectrophotometer in the range of 250 to 1000 nm. X-Band EPR spectra of the complexes were recorded using Bruker EMX spectrometer in CH_3OH at 77K in frozen solutions.

Pyrazine-2-carboxylic acid (pyridin-2-ylmethyl)-amide (HL^{Pz}): The ligand HL^{Pz}

was prepared by the reported method. Pyrazine-2-carboxylic acid methyl ester (1.627 g, 0.0118 mol) dissolved in 15 mL methanol and 2-aminomethylpyridine (1.52 g, 0.0142 mol) solution of methanol was added dropwise. The solution was refluxed overnight and then dried down to an off-white powder. Excess 2-aminomethylpyridine was removed by vacuum while heating in water bath. The resulting product was dissolved in a minimal amount of warmed methanol solvent and then cooled to produce colorless crystals. Yield: 1.97 g, 79%. FTIR (KBr disk): 3249, 1669,1570, 1517, 1422, 1388, 1286, 1167, 1021, 753, 610. $C_{11}H_{10}N_4O$ (214.23). Calcd. C, 61.67; H, 4.71; N, 26.15. Found: C, 61.88; H, 4.47; N, 26.39. ^{1}H NMR (300 MHz, $CDCl_3$) δ = 9.40 (s, 1H), 8.78 (s, 1H), 8.67 (d, 1H), 8.52 (m, 2H), 7.63 (m, 1H), 7.30 (d, 2H), 7.18 (m, 2H), 4.80 (d, 2H) ppm. ESI-MS: *m/z* = 215.1 $[HL^{Pz} + H]^+$.

Pyrazine-2-carboxylic acid (pyridin-2-ylethyl)-amide ($HL^{Pz'}$): The synthesis of **$HL^{Pz'}$** was similar to HL^{Pz} with 2-aminoethylpyridine to replace 2-aminomethylpyridine as the starting material. Yield: 67%. FTIR (KBr disk): 3341, 2937, 1662, 1529, 1437, 1152, 1021, 774, 611, 509. ^{1}H NMR (300 MHz, $CDCl_3$) δ = 9.40 (s, 1H), 8.72 (s, 1H), 8.60 (d, 1H), 8.51 (m, 2H), 7.65 (m, 1H), 7.26 (d, 2H), 7.16 (m, 2H), 3.88 (d, 2H), 3.15 (d, 2H) ppm. ESI-MS: *m/z* = 229 $[HL^{Pz'} + H]^+$.

$[Cu(HL^{Pz})Cl]_n$ (9): A solution of CuCl (0.0123 g, 0.125 mmol) in CH_3CN was added drop wise into a stirred solution of HL^{Pz} (0.0267g, 0.125 mmol) in CH_3CN, whereupon the color changed from light yellow to yellow. After the reaction was

stirred for 1h, the solution was filtered, and vapor diffusion of diethyl ether into the yellow filtrate resulted in the formation of the red block-shaped crystals of **9** suitable for crystallographic characterization. Yield: 0.0266 g, 68%. Anal. Calcd for $C_{11}H_{10}ClCuN_4O$: C, 42.18; H, 3.22; N, 17.89. Found: C, 41.95; H, 3.13; N, 17.74. FTIR (KBr): 3339, 1680, 1520, 1397, 1168, 1025, 871, 767, 658, 615 cm^{-1}.

$[Cu(L^{Pz})(py)_2][OTf]\cdot H_2O$ (10): A solution of $Cu(OTf)_2$ (0.090 g, 0.25 mmol) in methanol was added into a solution of HL^{Pz} (0.0535 g, 0.25 mmol) and triethylamine (0.025 g, 0.25 mmol) in methanol. To the resulting dark blue solution was added a solution of 4,4′-bipyridine (0.039 g, 0.25 mmol), resulting in the formation of a purple precipitate. The precipitate was collected by the filtration, dried and dissolved in pyridine to form a dark blue solution. Vapor diffusion of diethyl ether into this solution for one week afforded green needle-shaped crystals of **10** suitable for X-ray analysis. Yield: 0.0903 g, 60%. Anal. Calcd for $C_{22}H_{21}CuF_3N_6O_5S$: C, 43.89; H, 3.52; N, 13.96. Found: C, 43.62; H,3.47; N, 13.80. FTIR (KBr): 3436, 1636, 1486, 1389, 1280, 1160, 1030, 763, 708, 637, 517 cm^{-1}. ESI-MS (MeOH): *m/z* = 276 $[Cu(L^{Pz})]^+$. $)]^+$, *m/z* = 355 $[Cu(L^{Pz})(Py)]^+$. UV-Vis [CH_3OH, λmax, nm (ε, M^{-1} cm^{-1})]: 305(3369), 624(104).

$[Cu_2(L^{Pz})_2$(4,4′-bipy)$(OTf)_2]$ (11): A solution of $Cu(OTf)_2$ (0.09 g, 0.25 mmol) in methanol was added to a solution of HL^{Pz} (0.0535 g, 0.25 mmol) and triethylamine (0.025 g, 0.25mmol) in methanol, affording a dark green solution. A solution of 4,4′-bipyridine (0.039 g, 0.25 mmol) was layered on the above solution, from which

purple crystals of **3** suitable for X-ray analysis were obtained. Yield: 0.176 g, 70%. Anal. Calcd for $C_{34}H_{26}Cu_2F_6N_{10}O_8S_2$: C, 40.52; H, 2.60; N, 13.90 Found: C, 40.27; H, 2.53; N, 13.63. FTIR (KBr): 3447, 1647, 1416, 1380, 1291, 1245, 1224, 1158, 1033, 816, 772, 638, 518 cm^{-1}. ESI-MS (MeOH): *m/z* = 276 $[Cu(L^{Pz})]^+$. $)]^+$, *m/z* = 432 $[Cu(L^{Pz})(4,4'\text{-bipy})]^+$, *m/z* = 490 $[Cu(L^{Pz})_2+ H^+]^+$.

$[Cu(L^{Pz})(N_3)]_n$ (12): A solution of $Cu(OTf)_2$ (0.09 g, 0.25 mmol) in methanol was added to a solution of HL^{Pz} (0.0535 g, 0.25 mmol) and triethylamine (0.025 g, 0.25mmol) in methanol, affording dark green solution. A solution of NaN_3 (0.0163 g, 0.25 mmol) was then layered on the above solution from which blue crystals of **4** suitable for X-ray analysis were obtained (0.0558 g, 70% yield). Anal. Calcd for $C_{11}H_9CuN_7O$: C, 41.44; H, 2.85; N, 30.76. Found: C, 40.56 ; H, 2.77; N, 30.18. FTIR (KBr): 3430, 2055, 1640, 1376, 1164, 1050, 866, 769, 660 cm^{-1}. EPR (9.450 GHz, Mod. Amp. 5.0 G , CH_3OH, 77K) : $g_{\|}$ = 2.248, $g_{\perp}$ = 2.037, and $A_{\|}$ = 165 G. ESI-MS (MeOH): *m/z* = 341 $[Cu(L^{Pz})N_3 + Na]^+$, *m/z* = 659 $\{[Cu(L^{Pz})N_3]_2 + Na\}^+$, *m/z* = 977 $\{[Cu(L^{Pz})N_3]_3 + Na\}^+$. UV-Vis [$CH_3OH$, λmax, nm (ε, M^{-1} cm^{-1})]: 354(5000), 646(288).

$[Cu(L^{Pz'})(N_3)]_n$ (13): A solution of $Cu(OTf)_2$ (0.09 g, 0.25 mmol) in methanol was added to a solution of $HL^{Pz'}$ (0.0535 g, 0.25 mmol) and triethylamine (0.025 g, 0.25 mmol) in methanol, affording a dark blue solution. A solution of NaN_3 (0.0163 g, 0.25 mmol) was then layered on the above solution from which blue crystals suitable for X-ray analysis were obtained (0.054 g, 65% yield). Anal. Calcd for

$C_{12}H_{11}CuN_7O$: C, 43.31; H, 3.33; N, 29.46. Found: C, 43.68; H, 3.35; N, 29.59. FTIR (KBr): 2855, 2054, 1624, 1366, 1168, 1043, 773 cm^{-1}. EPR (9.447 GHz, Mod. Amp. 5.0 G, CH_3OH, 77K): $g_{\|}$ = 2.249, $g_{\perp}$ = 2.037, and $A_{\|}$ = 170 G. ESI-MS (MeOH): *m/z* = 355 $[Cu(L^{Pz'})N_3 + Na]^+$, *m/z* = 687 $\{[Cu(L^{Pz'})N_3]_2 + Na\}^+$, *m/z* = 1019 $\{[Cu(L^{Pz'})N_3]_3 + Na\}^+$. UV-Vis [$CH_3OH$, λmax, nm (ε, M^{-1} cm^{-1})]: 346(5000), 637(241).

X-ray Crystal Structure Determination. Single crystals of **9** and **10** were obtained by vapor diffusion of Et_2O into solutions of the respective complex. Single crystals of **11-13** were obtained by layering the bridging ligand onto the solution of $Cu(OTf)_2$ and deprotonated ligand. Data for **9-13** were collected on a Bruker Apex CCD area detector[26] diffractometer with graphite-monochromated Mo Kα (λ = 0.71073 Å) radiation at 100(2) K. The cell parameters for all complexes were determined from a non-linear least squares fit of the data. The data of these complexes were corrected for absorption by the semi-empirical method.[27] The structures were solved by direct methods by use of the SHELXTL program, and refined by full-matrix least-squares on F^2 by use of all reflections.[28] Hydrogen atom positions were initially determined by geometry and refined by a riding model. Non-hydrogen atoms were refined with anisotropic displacement parameters. All crystal data for these complexes are summarized in following tables.

For complex **10**, the water site, O1S, was disordered and was modeled in **12** orientations with occupancies refined to 0.439(4), 0.168(9), 0.191(9), and 0.203(9) for the unprimed, primed, double-primed, and "#" labeled atoms. Hydrogens bonded

to the waters could not be located on a difference map. The displacement parameters of the water oxygen were restrained. For complex **13**, the molecule forms an infinite array parallel with the *b* axis.

Table 4-6. Summary of crystal data and refinement parameters for complexes **9-13**

	9	**10**	**11**	**12**	**13**
formula	$C_{11}H_{10}ClCuN_4O$	$C_{22}H_{21}CuF_3N_6O_5S$	$C_{34}H_{26}Cu_2F_6N_{10}O_8S_2$	$C_{11}H_9CuN_7O$	$C_{12}H_{11}CuN_7O$
fw	313.22	602.05	1007.85	318.79	332.82
space group	*C*2/c	$P\bar{1}$	$P\bar{1}$	$P2_1/c$	*Pbca*
a (Å)	16.791(6)	8.127(3)	8.6449(16)	12.604(6)	14.0009(12)
b (Å)	7.705(3)	10.907(4)	14.617(2)	14.927(14)	7.9424(6)
c (Å)	18.714(6)	15.445(5)	16.855(3)	6.426(3)	22.6840(18)
α (deg)	90	69.447(8)	64.577(5)	90	90
β (deg)	106.060(9)	75.164(8)	84.332(8)	93.660(7)	90
γ (deg)	90	83.099(9)	75.766(9)	90	90
Z	8	2	2	4	8
V (Å^3)	2326.6(14)	1238.5(8)	1864.5(5)	1270.3(14)	2522.5(4)
ρ_{calcd} (g/cm^3)	1.788	1.614	1.795	1.754	1.753
μ(mm^{-1})	2.098	1.036	1.351	1.816	2.560
*R*1[I>2σ(*I*)]	0.0300	0.0729	0.0377	0.0328	0.0473
*wR*2[I>2σ(*I*)]	0.0725	0.1662	0.1039	0.0823	0.1067
GOF on F^2	1.018	1.009	1.001	1.002	1.001

4.7. References

1. (a) Lin, X.; Blake, A. J.; Wilson, C.; Sun, X. Z.; Champness, N. R.; George, M. W.; Hubberstey, P.; Mokaya, R.; Schröder, M., A Porous Framework Polymer Based on a Zinc(II) 4,4‘-Bipyridine-2,6,2‘,6‘-tetracarboxylate: Synthesis, Structure, and “Zeolite-Like” Behaviors. *J Am Chem Soc* **2006,** *128* (33), 10745-10753; (b) Lin, X.; Telepeni, I.; Blake, A. J.; Dailly, A.; Brown, C. M.; Simmons, J. M.; Zoppi, M.; Walker, G. S.; Thomas, K. M.; Mays, T. J.; Hubberstey, P.; Champness, N. R.; Schröder, M., High Capacity Hydrogen Adsorption in Cu(II) Tetracarboxylate Framework Materials: The Role of Pore Size, Ligand Functionalization, and Exposed Metal Sites. *J Am Chem Soc* **2009,** *131* (6), 2159-2171.

2. (a) Shultz, A. M.; Farha, O. K.; Hupp, J. T.; Nguyen, S. T., A Catalytically Active, Permanently Microporous MOF with Metalloporphyrin Struts. *J Am Chem Soc* **2009,** *131* (12), 4204-4205; (b) Hwang, Y. K.; Hong, D.-Y.; Chang, J.-S.; Jhung, S. H.; Seo, Y.-K.; Kim, J.; Vimont, A.; Daturi, M.; Serre, C.; Férey, G., Amine Grafting on Coordinatively Unsaturated Metal Centers of MOFs: Consequences for Catalysis and Metal Encapsulation. *Angewandte Chemie International Edition* **2008,** *47* (22), 4144-4148.

3. (a) Ouellette, W.; Prosvirin, A. V.; Whitenack, K.; Dunbar, K. R.; Zubieta, J., A Thermally and Hydrolytically Stable Microporous Framework Exhibiting Single-Chain Magnetism: Structure and Properties of $[Co_2(H_{0.67}bdt)_3]\cdot 20\,H_2O$. *Angewandte Chemie International Edition* **2009,** *48* (12), 2140-2143; (b) Zhang, X.-M.; Hao, Z.-M.; Zhang, W.-X.; Chen, X.-M., Dehydration-Induced Conversion from a Single-Chain Magnet into a Metamagnet in a Homometallic Nanoporous Metal–Organic

Framework. *Angewandte Chemie International Edition* **2007,** *46* (19), 3456-3459.

4. Blake, A. J.; Champness, N. R.; Easun, T. L.; Allan, D. R.; Nowell, H.; George, M. W.; Jia, J.; Sun, X.-Z., Photoreactivity examined through incorporation in metal−organic frameworks. *Nat Chem* **2010,** *2* (8), 688-694.

5. Kitagawa, S.; Kitaura, R.; Noro, S.-i., Functional Porous Coordination Polymers. *Angewandte Chemie International Edition* **2004,** *43* (18), 2334-2375.

6. (a) Batten, S. R.; Robson, R., Interpenetrating nets: Ordered, periodic entanglement. *Angew Chem Int Edit* **1998,** *37* (11), 1460-1494; (b) Khlobystov, A. N.; Blake, A. J.; Champness, N. R.; Lemenovskii, D. A.; Majouga, A. G.; Zyk, N. V.; Schroder, M., Supramolecular design of one-dimensional coordination polymers based on silver(I) complexes of aromatic nitrogen-donor ligands. *Coordin Chem Rev* **2001,** *222*, 155-192; (c) Moulton, B.; Zaworotko, M. J., From molecules to crystal engineering: Supramolecular isomerism and polymorphism in network solids. *Chem Rev* **2001,** *101* (6), 1629-1658.

7. Hausmann, J.; Jameson, G. B.; Brooker, S., Control of molecular architecture by the degree of deprotonation: self-assembled di- and tetranuclear copper(II) complexes of N,N'-bis(2-pyridylmethyl)pyrazine-2,3-dicarboxamide. *Chem Commun* **2003,** (24), 2992-2993.

8. Klingele, J.; Boas, J. F.; Pilbrow, J. R.; Moubaraki, B.; Murray, K. S.; Berry, K. J.; Hunter, K. A.; Jameson, G. B.; Boyd, P. D. W.; Brooker, S., A [2 x 2] nickel(II) grid and a copper(II) square result from differing binding modes of a pyrazine-based diamide ligand. *Dalton T* **2007,** (6), 633-645.

9. Cati, D. S.; Ribas, J.; Ribas-Arino, J.; Stoeckli-Evans, H., Self-assembly of

Cu-II and Ni-II [2x2] grid complexes and a binuclear Cu-II complex with a new semiflexible substituted pyrazine ligand: Multiple anion encapsulation and magnetic properties. *Inorg Chem* **2004,** *43* (3), 1021-1030.

10. Hausmann, J.; Brooker, S., Control of molecular architecture by use of the appropriate ligand isomer: a mononuclear "corner-type" versus a tetranuclear [2 x 2] grid-type cobalt(iii) complex. *Chem Commun* **2004,** (13), 1530-1531.

11. Klingele, J.; Moubaraki, B.; Murray, K. S.; Boas, J. F.; Brooker, S., Dinuclear copper(II) complexes of two homologous pyrazine-based bis(terdentate) diamide ligands. *Eur J Inorg Chem* **2005,** (8), 1530-1541.

12. Cockriel, D. L.; McClain, J. M.; Patel, K. C.; Ullom, R.; Hasley, T. R.; Archibald, S. J.; Hubin, T. J., The design and synthesis of pyrazine amide ligands suitable for the "tiles" approach to molecular weaving with octahedral metal ions. *Inorg Chem Commun* **2008,** *11* (1), 1-4.

13. Hellyer, R. M.; Larsen, D. S.; Brooker, S., Cobalt and Silver Complexes of Terdentate Pyrazine-Based Amide Ligands and Assembly of Monocobalt Building Blocks through a Silver Connector. *Eur J Inorg Chem* **2009,** (9), 1162-1171.

14. Yang, L.; Houser, R. P., Copper(I) coordination chemistry of (pyridylmethyl)amide ligands. *Inorg Chem* **2006,** *45* (23), 9416-9422.

15. (a) Healy, P. C.; Kildea, J. D.; Skelton, B. W.; Waters, A. F.; White, A. H., Lewis-Base Adducts of Group 11 Metal(I) Compounds .60. Binuclear Adducts of Copper(I) Halides with 2-Hindered Pyridine Bases. *Acta Crystallogr C* **1991,** *47*, 1721-1723; (b) Gustafsson, B.; Hakansson, M.; Jagner, S., Complexes between copper(I) chloride and polydentate aromatic amines. *Inorg Chim Acta* **2003,** *350*,

209-214; (c) Lu, J.; Crisci, G.; Niu, T. Y.; Jacobson, A. J., A polymeric structure containing Cu2Cl2 units bridged by 4,4'-bipyridine: $(PPh_3)_2Cu_2(\mu\text{-}Cl)_2(\mu\text{-}4,4'\text{-}$ bipyridine). *Inorg Chem* **1997,** *36* (22), 5140-5141.

16. Yang, L.; Powell, D. R.; Houser, R. P., Structural variation in copper(I) complexes with pyridylmethylamide ligands: structural analysis with a new four-coordinate geometry index, τ4. *Dalton T* **2007,** (9), 955-964.

17. Addison, A. W.; Rao, T. N.; Reedijk, J.; Vanrijn, J.; Verschoor, G. C., Synthesis, Structure, and Spectroscopic Properties of Copper(II) Compounds Containing Nitrogen Sulfur Donor Ligands - the Crystal and Molecular-Structure of Aqua[1,7-Bis(N-Methylbenzimidazol-2'-Yl)-2,6-Dithiaheptane]Copper(Ii) Perchlorate. *J Chem Soc Dalton* **1984,** (7), 1349-1356.

18. (a) Escuer, A.; Vicente, R.; Mautner, F. A.; Goher, M. A. S.; Abu-Youssef, M. A. M., $[M(N_3)_2(L)](n)$: building 3-D M-II-azido networks with new topologies. *Chem Commun* **2002,** (1), 64-65; (b) Blanchet-Boiteux, C.; Mouesca, J. M., End-on azido-bridged copper dimers: Spin population analysis and spin polarization effect as exhibited by valence-bond/broken symmetry, density functional methods. *J Am Chem Soc* **2000,** *122* (5), 861-869.

19. Yang, C. I.; Wernsdorfer, W.; Lee, G. H.; Tsai, H. L., A pentanuclear manganese single-molecule magnet with a large anisotropy. *J Am Chem Soc* **2007,** *129* (3), 456-457.

20. Zhang, Y.-Z.; Wernsdorfer, W.; Pan, F.; Wang, Z.-M.; Gao, S., An azido-bridged disc-like heptanuclear cobalt(ii) cluster: towards a single-molecule magnet. *Chem Commun* **2006,** (31), 3302-330421.

21. (a) Data Collection: SMART Software Reference Manual (1998). Bruker-AXS, 5465 E. Cheryl Parkway, Madison, WI 53711-5373 USA. (b) Data Reduction: SAINT Software Reference Manual (1998). Bruker-AXS, 5465 E. Cheryl Parkway, Madison, WI 53711-5373, USA.

22. G. M. Sheldrick (2002). SADABS. Program for Empirical Absorption Correction of Area Detector Data. University of Göttingen, Germany.

23. (a) G. M. Sheldrick (2000). SHELXTL Version 6.10 Reference Manual. Bruker-AXS, 5465 E. Cheryl Parkway, Madison, WI 53711-5373 USA. (b) *International Tables for Crystallography, Vol C,* Tables 6.1.1.4, 4.2.6.8, and 4.2.4.2, Kluwer: Boston (1995).

CHAPTER 5

SYNTHESIS AND CHARACTERIZATION OF COPPER COMPLEXES WITH THIOETHER-CONTAINING PYRIDYLALKYLAMIDE LIGANDS

5.1. Introduction

Copper chemistry of sulfur-containing ligands has been widely explored due to its relevance with many metalloproteins or metalloenzymes in bioinorganic chemistry.[1] Copper thiolate and thioether complexes attract much interest related to their important roles in some unique metalloproteins such as the blue copper (type 1) and the binuclear Cu_A electron transfer sites as shown in Figure 5-1.

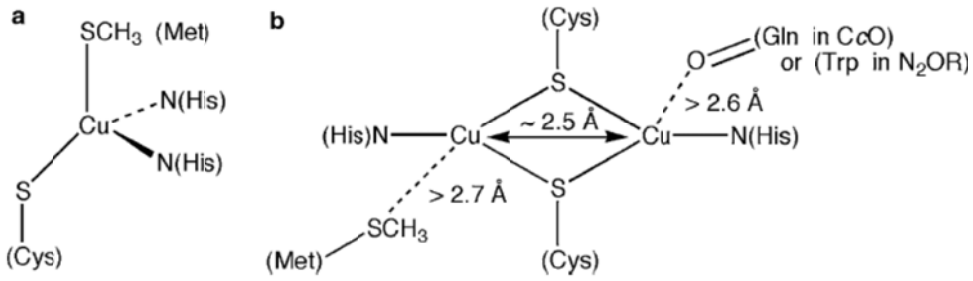

Figure 5-1. Schematic drawing of (a) the mononuclear copper site in plastocyanin and (b) binuclear Cu_A centers in cytochrome *c* oxidase and in nitrous oxide reductase. The figure is adapted from the reference [1].

Blue copper proteins, also named as type 1 copper proteins, are a family of electron transferases from many sources. They display spectroscopic features different than normal (type 2) copper centers. In type 1 copper centers, the copper ion is coordinated by a distorted tetrahedral arrangement of $His_2CysMet$ side-chain donors, as seen in plastocynin,[2] or a distorted trigonal planar of His_2Cys side-chain donors, as seen in azurin mutants. In both cases, the cysteine residue donates a

thiolate sulfur atom to coordinate with the copper center.

Compared to type 2 copper centers, the type 1 blue copper proteins exhibit a strong absorption at about 600 nm assigned as a ligand-to-metal charge transfer (LMCT) transition. In addition, they have smaller $A_{\|}$ copper hyperfine coupling constants in the EPR spectra compared to type 2 copper sites (typically 40-60 G, where as type 2 copper have $A_{\|} > 140$ G). This difference can be assigned to the highly covalent thiolate S-Cu bond that delocalizes the electron spin of the metal center and reduces its interaction with the nuclear spin of the copper.[3]

Since the elucidation of the crystal structure of the blue copper proteins, much work has been done to synthesize model complexes to mimic the geometry and spectroscopic features of the enzyme. The main challenge to synthesize the models comes from the reactivity of the copper(II)-thiolate bond, which is sensitive to a redox process leading to the formation of copper(I) and disulfide. The most interesting and successful models have been developed by Holland and Tolman.[4]A three-coordinate trigonal planar Cu(II) complex was isolated with thiolate coordination to mimic the fungal laccase site by using a sterically bulky ß-diketiminate ligand as shown in Figure 5-2. In addition, the first model complex with a N_2S(thioether)S(thiolate) donor set copper(II) complex has been synthesized by the same ligand. These models help us to understand the insight into the effects of the number and nature of the sulfur donor in both synthetic and biological systems.[5]

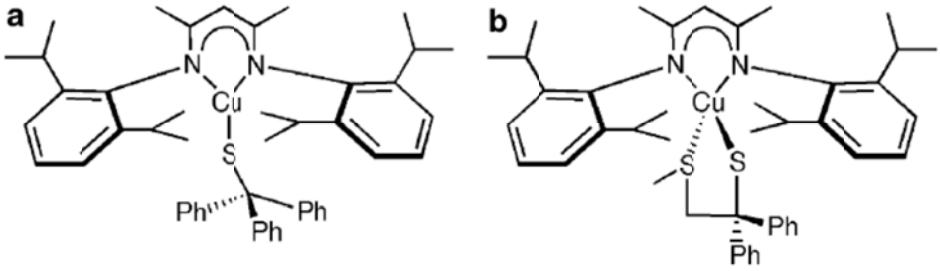

Figure 5-2. Schematic picture of Type 1 model complexes. (a) Three-coordinate Cu(II) thiolate complex modeling the fungal laccase site, (b) Four-coordinate thiolate and thioether complex modeling the coordination site in plastocanin. Figure is adapted from reference [1].

Cu_A electron transfer centers are found in both cytochrome c oxidease (CcO)[6] and nitrous oxide reductase (N_2OR).[2] It shares some common spectroscopic features with the blue copper proteins, such as strong electronic absorptions in the visible region and a small copper hyperfine coupling constant in the EPR spectrum. The X-ray crystallographic data support a novel dithiolate-bridged symmetrical site with two bridging cysteine ligands, two terminal histidine ligands, a terminal methionine ligand, and a glutamic acid residue as shown in Figure 5-1. The average $Cu^{1.5}\cdots Cu^{1.5}$ distance is 2.47 Å consistent with a metal-metal bonding interaction.[1]

The most well-designed model complex of the Cu_A site was described by Tolman's group, which is a mixed-valence dicopper complex bridged by two thiolate groups as shown in Figure 5-3. This complex replicates the Cu_A site with the geometry, oxidation level and high degree of electron delocalization, as reflected from the seven-line hyperfine features in the EPR spectrum.[7]

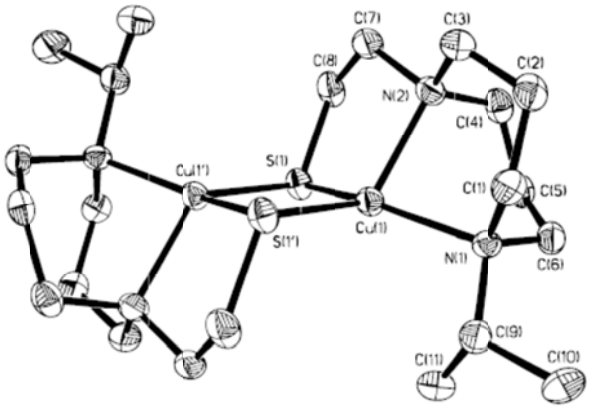

Figure 5-3. X-ray crystal structure showing mixed-valence dicopper complex $[Cu_2L_2]^+$, which mimics the Cu_A electron transfer site. Figure is adapted from reference [7].

In addition to type 1 blue copper and Cu_A, sulfur is also found in the catalytic Cu_Z center in N_2OR. Cu_Z is the catalytic site of N_2OR where N_2O is reduced to N_2 in the terminal step of the denitrification process. The site consists of four copper ions arranged in a 'butterfly' cluster and bridged by an inorganic sulfide as shown in Figure 5-4.[8] A more detailed description of Cu_Z and its model chemistry was covered in Chaper 1.

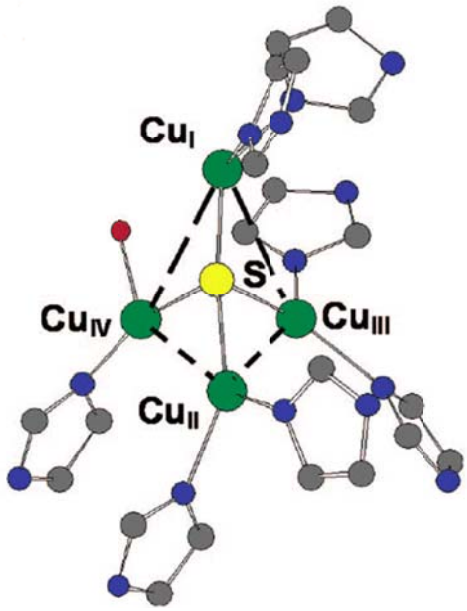

Figure 5-4. Active site from the crystal structure of PnN_2OR. Figure is adapted from reference [8].

So, the diversity of copper-sulfur systems in biology has attracted the attention of synthetic chemists to investigate the copper chemistry with sulfur-containing ligand systems. Much work has been focused on the model chemistry of mixed-valence Cu_A center. In our group, Lei Yang reported a mixed-valence dicopper complex $[Cu_2L_2]OTf$ (HL = *N*-(2-pyridylmethyl)acetamide). The EPR spectrum of this complex displays the distinct seven-line hyperfine feature from the coupling between the unpaired electron and two $I = 3/2$ copper centers in CH_2Cl_2 at both 296K and 77K, which supports a delocalized mixed-valence dicopper center to be the same as the Cu_A center.[9] But this complex does not have any thiolate or thioether sulfur to model the cysteine sulfur in the Cu_A site. We therefore wanted to introduce a thioether into our ligand system to model the cysteine and methionine in Cu_A

center.

In our previous work, , two mononuclear copper(II) complexes were reported from the ligand 2-HL^{N2S} .[10] Both complexes were synthesized from copper(II) chloride and the 2-HL^{N2S} ligand. So, we aimed to change the copper salt in order to obtain dicopper complexes. The chloride ion is a strong coordinating anion to coordinate with copper ions. With the change to a weak coordinating anion could lead to different copper complexes. In addition, we also sought to synthesize similar 2-$HL^{N2S'}$ ligand (2-$HL^{N2S'}$ = 2-methylthio-*N*-(2-pyridylethyl)acetamide) and investigate the copper chemistry. We expected to obtain different copper complexes by the change from the ligand 2-HL^{N2S} to the ligand 2-$HL^{N2S'}$.

5.2. Synthesis of the Ligands

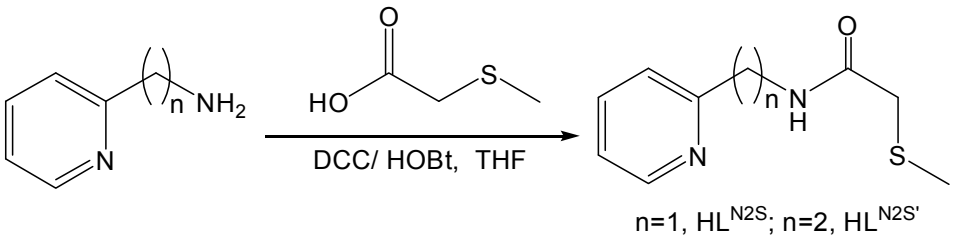

Figure 5-5. Synthesis of the ligands 2-HL^{N2S} and 2-$HL^{N2S'}$.

The ligands 2-methylthio-*N*-(2-pyridylmethyl)acetamide (2-HL^{N2S}, previously reported by Klein, et. al[10]) and 2-methylthio-*N*-(2-pyridylethyl)acetamide (2-$HL^{N2S'}$), were synthesized by DCC-mediated coupling reaction of methylthioacetic acid 2-pyridylethyl amine as shown in Figure 5-5. In both ligands, they consist of pyridyl and thioether functional groups connected by an amide group. Both ligands

have four potential coordination donors, N(Py), N(amide), O(amide) and S(thioether). Both ligands were fully characterized by ^{1}H NMR, IR, ESI-MS and elemental analysis.

5.3. Copper(II) Chemistry of Ligands

5.3.1. [Cu(2-L^{N2S})(CH$_3$OH)]$_n$(OTf) ***(14)***

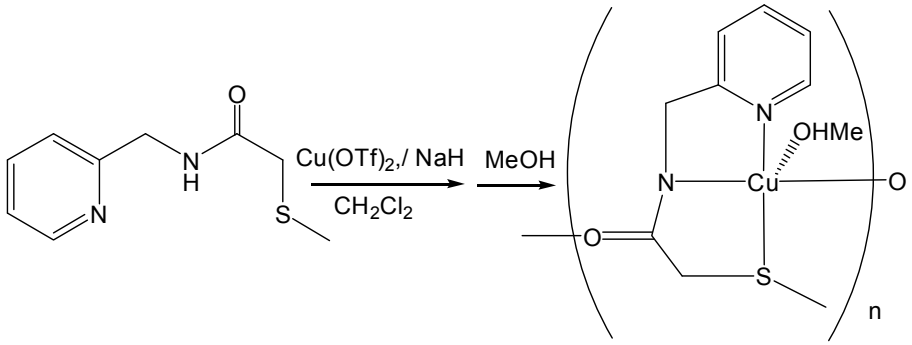

Figure 5-6. Synthesis of [Cu(2-L^{N2S})(CH$_3$OH)]$_n$(OTf) **(14)**

Complex **14** was synthesized by the reaction of Cu(OTf)$_2$ and 2-HL^{N2S} ligand in the presence of the base NaH in CH_2Cl_2. Initially a green precipitate was obtained, which was then dissolved in methanol, resulting in the formation of a blue solution. Crystals of [Cu(2-L^{N2S})(CH$_3$OH)]$_n$(OTf) **(14)** were obtained by vapor diffusion of diethyl ether into the blue filtrate. X-ray analysis reveals that **14** is a one dimensional coordination polymer. The copper is five coordinate with two N atoms and one S atom from the ligand, and one carbonyl O atom from a second ligand. The fifth coordination site is occupied by the O atom from a methanol solvent molecule, forming a distorted square pyramidal geometry ($\tau_5 = 0.28$). The carbonyl

O atom acts as a bridging atom to connect the units together and forms a one dimensional coordination polymer as shown in Figure 5-8. Each layer is packed together in the same configuration.

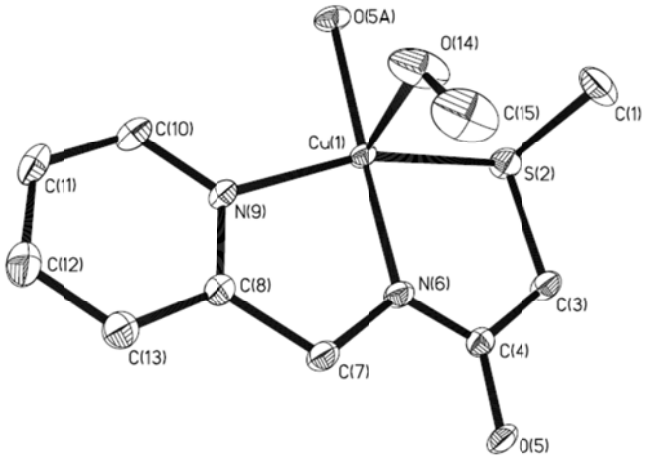

Figure 5-7. X-ray crystal structure of the subunit for complex [Cu(2-L^{N2S})(CH_3OH)]$_n$(OTf) **(14)** with thermal ellipsoids at the 50% Probability level.

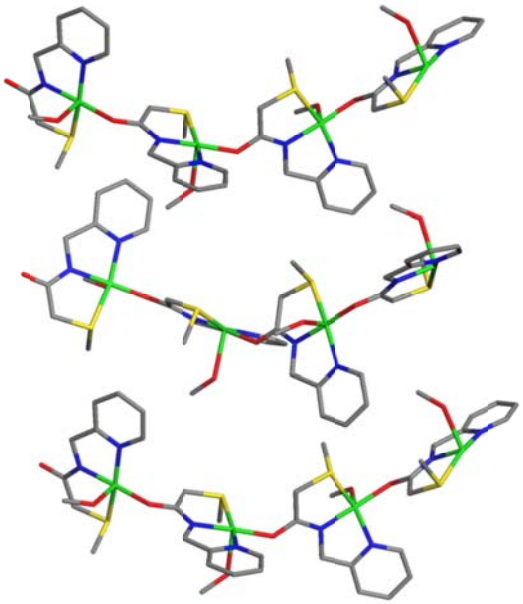

Figure 5-8. Packing structure of complex **14.**

Selected bond lengths and bond angles are listed in Table 5-1. The average Cu-N bond distance (1.9597 Å) is in the normal range of five-coordinate copper complex Cu-N distances (1.900-2.000 Å). The apical Cu(1)-O(14) distance (2.2615) is much longer than the basal Cu-O distance. The bond angles of N(6)-Cu(1)-O(5A) and N(9)-Cu(1)-S(2) are 177.45^{o} and 160.80^{o}, respectively.

Table 5-1. Selected bond distances (Å) and angles (deg) for complex **14**.

Bond Lengths (Å)		Bond Angles (deg)	
Cu(1)-N(6)	1.9135(17)	N(6)-Cu(1)-O(5A)	177.45(8)
Cu(1)-O(5A)	1.9241(14)	N(6)-Cu(1)-N(9)	82.57(7)
Cu(1)-N(9)	2.0059(19)	O(5A)-Cu(1)-N(9)	98.19(7)
Cu(1)-O(14)	2.2615(19)	N(6)-Cu(1)-O(14)	96.48(7)
Cu(1)-S(2)	2.3539(6)	O(5A)-Cu(1)-O(14)	81.09(7)
		N(9)-Cu(1)-O(14)	91.65(8)
		N(6)-Cu(1)-S(2)	85.35(6)
		O(5A)-Cu(1)-S(2)	94.53(5)
		N(9)-Cu(1)-S(2)	160.80(5)
		O(14)-Cu(1)-S(2)	104.54(6)

5.3.2. [Cu(2-$L^{N2S'}$)(OTf)]$_n$ ***(15)***

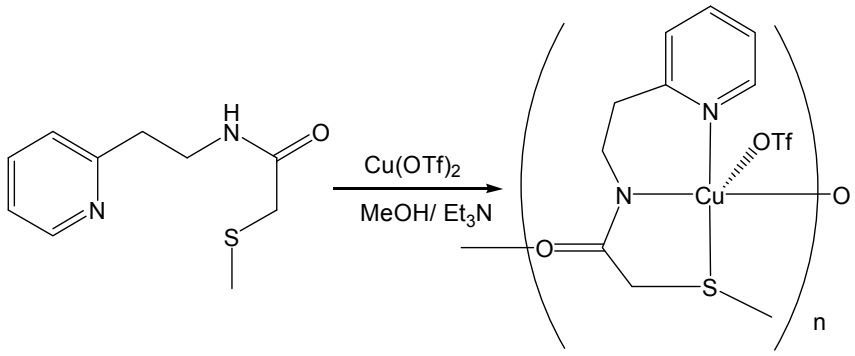

Figure 5-9. Synthesis of [Cu(2-$L^{N2S'}$)(OTf)]$_n$ **(15).**

Complex **15** was synthesized by the reaction of $Cu(OTf)_2$ and 2-$HL^{N2S'}$ ligand in the presence of the base Et_3N in methanol, forming a deep blue solution. Vapor diffusion of diethyl ether into the filtrate results in the formation of dark green crystals suitable for X-ray analysis. Complex **15** is also a one dimensional coordination polymer as shown in Figure 5-11. In the packing structure, the layer with the same configuration repeats alternately. The coordination mode of the copper center is similar to complex **14**. In **15**, the fifth position is occupied by the anionic triflate instead of a methanol solvent, forming a square pyramidal geometry (τ_5 = 0.005). Both Cu-N bond distances are very close to the value seen in complex **14**. The apical Cu(1)-O(11A) bond distance is longer than the basal Cu-N and Cu-O bond distances. The bond angles of N(9)-Cu(1)-O(11A) and N(1)-Cu(1)-S(13) are 172.5^o and 172.80^o, respectively. The bridging mode of the carbonyl O is the same as complex **14**.

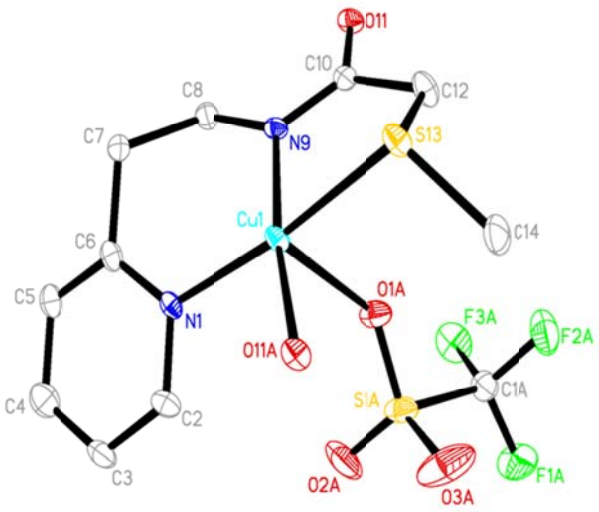

Figure 5-10. X-ray crystal structure of the subunit for complex $[Cu(2\text{-}L^{N2S'})(OTf)]_n$ **(15)** with thermal ellipsoids at the 50% probability level.

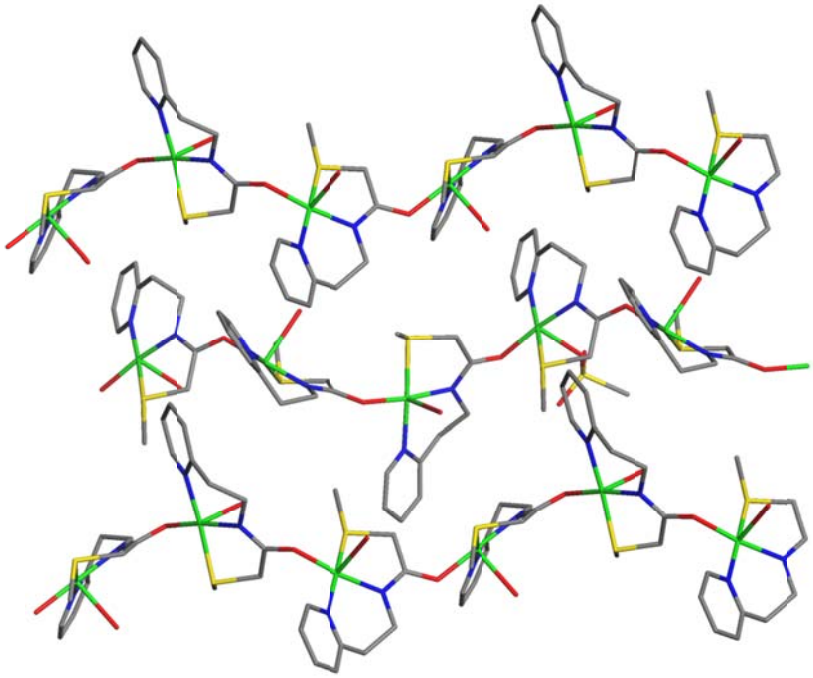

Figure 5-11. One dimensional coordination polymer structure of complex **15.**

Table 5-2. Selected bond distances (Å) and angles (deg) for complex **15**.

Bond Lengths (Å)		Bond Angles (deg)	
Cu(1)-O(11A)	1.943(3)	O(11A)-Cu(1)-N(9)	172.52(13)
Cu(1)-N(9)	1.948(3)	O(11A)-Cu(1)-N(1)	92.63(13)
Cu(1)-N(1)	2.020(3)	N(9)-Cu(1)-N(1)	94.66(13)
Cu(1)-S(13)	2.3399(11)	N(9)-Cu(1)-S(13)	83.85(10)
Cu(1)-O(1A)	2.358(3)	N(1)-Cu(1)-S(13)	172.82(10)
		O(11A)-Cu(1)-O(1A)	90.07(12)
		N(9)-Cu(1)-O(1A)	87.79(13)
		N(1)-Cu(1)-O(1A)	94.00(12)
		S(13)-Cu(1)-O(1A)	92.96(9)

5.3.3. [Cu(2-HL$^{N2S'}$)(CH$_3$OH)Cl] ***(16)***

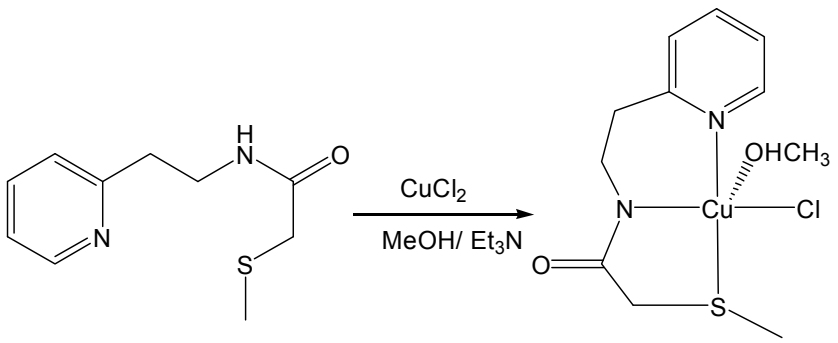

Figure 5-12. Synthesis of [Cu(2-HL$^{N2S'}$)(CH$_3$OH)Cl] **(16).**

Complex **16** was synthesized by the reaction of $CuCl_2$ and 2-HL$^{N2S'}$ ligand in the

presence of the base Et_3N in methanol, forming a deep blue solution. Vapor diffusion of diethyl ether into the filtrate results in the formation of blue crystals suitable for X-ray analysis. **16** is a mononuclear copper complex as shown in Figure 5-13. The copper is five coordinate with two N atoms and one S atom from the ligand, one chloride anion and one O from the methanol molecule, forming a distorted square pyramidal geometry (τ_5 = 0.27). There is intermolecular hydrogen bonding between the O atom from the methanol molecule and the carbonyl O atom [O···H···O = 2.6306(18) Å] as shown in Figure 5-13. Both Cu-N and Cu-S bond distances are close to the previous complexes **14** and **15**. The bond angles of N(9)-Cu(1)-Cl(1) and N(1)-Cu(1)-S(13) are 160.9^o and 177.10^o, respectively. In this complex, the fifth position is occupied by the chloride anion instead of carbonyl O atoms for complex **14** and **15**. Copper(II) prefers to be five-coordinate and so it is unacceptable to bind the carbonyl O to form a one dimensional coordination polymer in **16**.

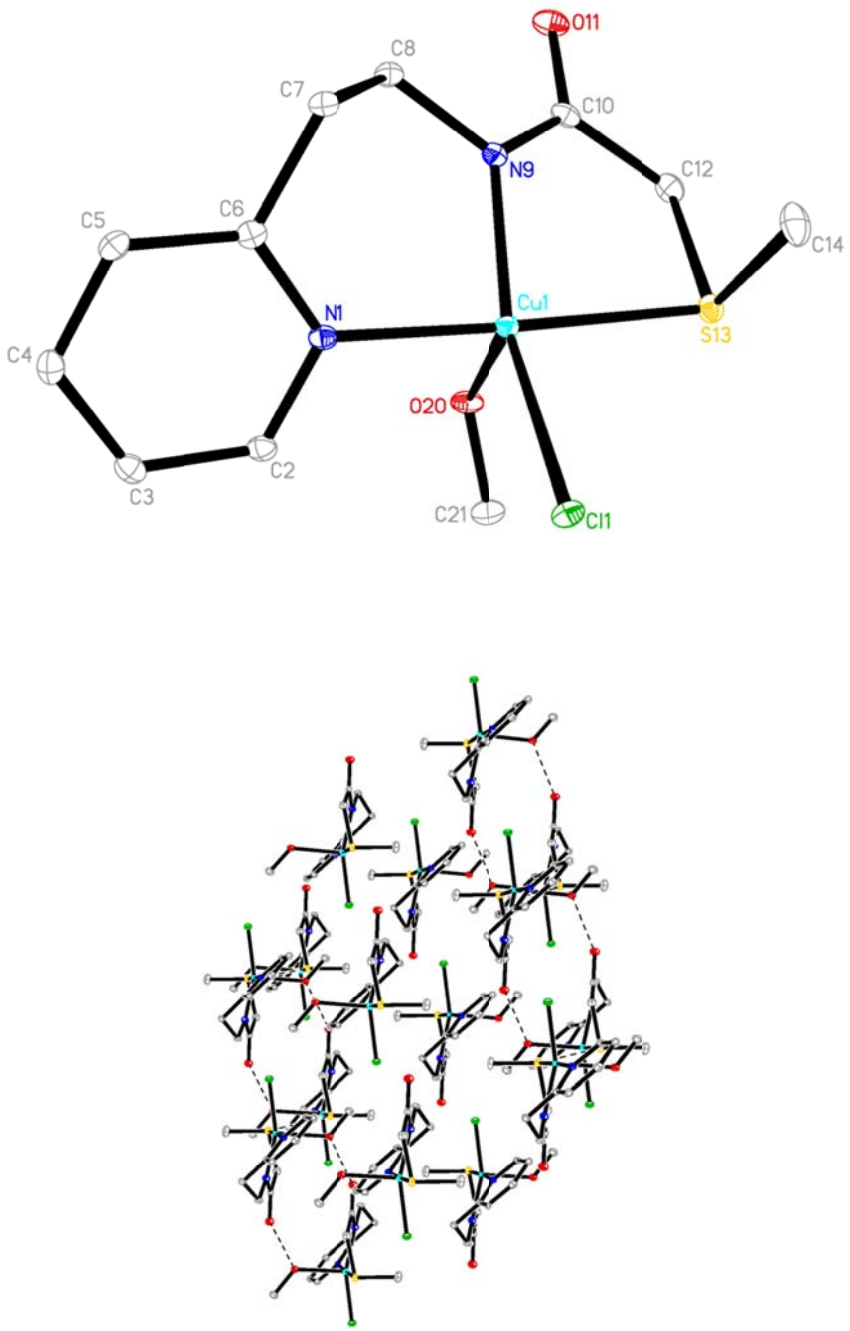

Figure 5-13. X-ray crystal structure of the subunit for complex [Cu(2-$HL^{N2S'}$)(CH_3OH)Cl] **(16)** with thermal ellipsoids at the 50% probability level (top). Packing structure of complex **16** (bottom).

Table 5-3. Selected bond distances (Å) and angles (deg) for complex **16**.

Bond Lengths (Å)		Bond Angles (deg)	
Cu(1)-N(9)	1.9563(14)	N(9)-Cu(1)-N(1)	93.37(6)
Cu(1)-N(1)	2.0125(15)	N(9)-Cu(1)-Cl(1)	160.89(5)
Cu(1)-Cl(1)	2.2605(5)	N(1)-Cu(1)-Cl(1)	93.73(4)
Cu(1)-O(20)	2.2755(13)	N(9)-Cu(1)-O(20)	96.77(5)
Cu(1)-S(13)	2.3587(5)	N(1)-Cu(1)-O(20)	91.77(5)
		Cl(1)-Cu(1)-O(20)	100.72(4)
		N(9)-Cu(1)-S(13)	84.18(4)
		N(1)-Cu(1)-S(13)	177.11(4)
		Cl(1)-Cu(1)-S(13)	89.071(18)
		O(20)-Cu(1)-S(13)	87.02(4)

5.4. Conclusions

In this chapter, we aim to synthesize mixed-valence dicopper complex based on the 2-HL^{N2S} and 2-$HL^{N2S'}$ ligands. The reaction of copper(II) trifilate and 2-HL^{N2S} with the presence of NaH to deprotonate the amide H in CH_2Cl_2 produced a one dimensional coordination polymer $[Cu(2\text{-}L^{N2S})(CH_3OH)]_n(OTf)$ **(14)**. The reaction condition is similar to the synthesis of the mixed-valence dicopper complex $[Cu_2L_2]OTf$. In complex **14**, the copper is five coordinate with two N atoms and one S atom from the ligand, and one carbonyl O atom from a second ligand. The fifth coordination position is occupied by the O atom from CH_3OH, forming a distorted square pyramidal geometry ($\tau_5 = 0.28$). The carbonyl O atom acts as a bridging atom to connect the units together and forms a one dimensional coordination polymer.

Two mononuclear copper(II) complexes were synthesized and characterized by Klein in our group with the ligand 2-HL^{N2S} as shown in Figure 5-14.[10] Both complexes were synthesized by the treatment of $CuCl_2 \cdot 2H_2O$ with the neutral or deprotonated ligand. In complex **a**, there is tautomerization of the ligand amide bond to its corresponding imidic acid form upon coordination to copper, which prevents the bond formation between the carbonyl O and copper. The fourth basal position and axial position are both occupied by chloride. In complex **b**, the fourth basal position is occupied by chloride and the axial position is occupied by oxygen from the methanol solvent. The copper center is saturated with five coordination number and failed to form a coordination polymer. The change of the salt from copper(II) chloride to copper(II) triflate leads to different copper complexes, which

have total different coordination modes of the copper center. But both reactions fail to obtain a dicopper complex to model the structure of the Cu_A center. One reason is that the carbonyl oxygen has priority to coordinate to copper center over the thioether. The coordination of CH_3OH to the copper ion makes it impossible to coordinate with the second thioether to form a dicopper complex.

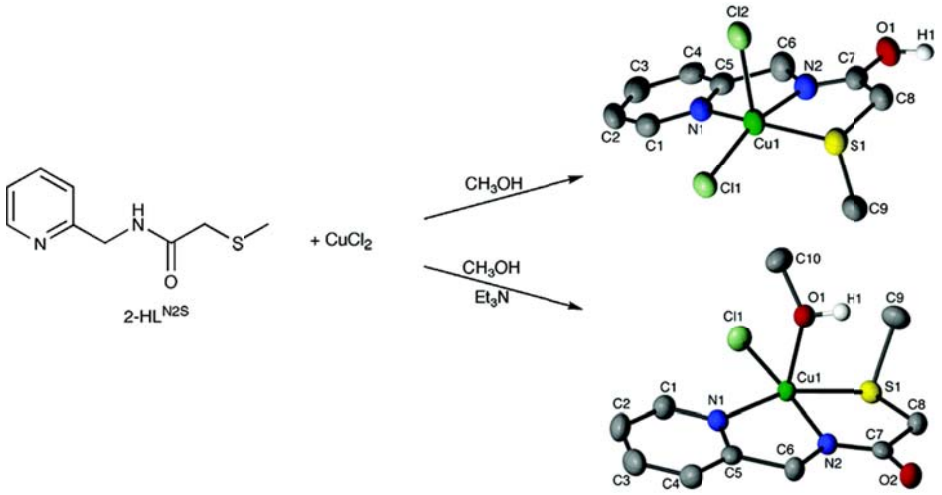

Figure 5-14. Synthesis and structures of complexes **a** (top) and **b** (bottom). Figure is adapted from reference [10].

We also investigated the copper chemistry of a new ligand 2-methylthio-*N*-(2-pyridylethyl)acetamide (2-$HL^{N2S'}$). The reaction of the ligand 2-$HL^{N2S'}$and copper(II) triflate or copper(II) chloride in the presence of Et_3N in CH_3OH leads to the formation of $[Cu(2\text{-}L^{N2S'})(OTf)]_n$ **(15)** and $[Cu(2\text{-}HL^{N2S'})(CH_3OH)Cl]$ **(16)** respectively. Complex **15** is also a one dimensional coordination polymer similar to complex **14**. The only difference for the coordination modes of the copper center is the fifth axial donor, which is a methanol solvent in **14** and a triflate anion in **15**.

Complex **16** is a mononuclear with a distorted square pyramidal geometry. The fifth position is occupied by the chloride anion instead of carbony oxygen. In sum, both the change of the copper salts and the ligand failed to obtain our targeted dicopper complexes. The reason can be assigned as the difficulty of the thioether sulfur to bridge two copper centers.

5.5. Experimental

General. All chemical reagents were purchased from commercial suppliers and used without further purification, unless otherwise stated. The solvents used were doubly purified using alumina columns in a MBraun solvent purification system (MB-SPS). ^{1}H NMR spectra were recorded on a Varian 300 MHz spectrometer with deuterated solvent as an internal standard. Elemental analysis were conducted by Atlantic Microlabs, Norcross, GA. FTIR spectra were collected on NEXUS 470 FTIR spectrometer with the KBr pellet technique. Mass spectra were recorded on a Q-TOF quadrupole time-of-flight mass spectrometer with an electrospray ionization (ESI) source.

2-(methylsulfanyl)-N-[2-(pyridine-2-yl)methyl]acetamide (2-HL^{N2S}): The synthesis of 2-HL^{N2S} followed the published method.[12] Yield: 1.31 g, 72%. Anal. Calcd for $C_9H_{12}N_2OS$: C. 55.08; H, 6.16; N, 14.27. Found: C. 54.88; H, 6.34; N, 13.68. FTIR (KBr): 3248, 3080, 2918, 2852, 1642, 1566, 1312, 1261, 1152, 1029, 761, 730, 583, 483 cm^{-1}.

2-(methylsulfanyl)-N-[2-(pyridine-2-yl)ethyl]acetamide (2-HL$^{N2S'}$): The ligand 2-HL$^{N2S'}$ was synthesized by the same procedure used for 2-HL^{N2S}, with 2-(aminoethyl)-pyridine as the starting material. Yield: 1.58 g, 80%. Anal. Calcd for $C_{10}H_{14}N_2OS$: C. 57.11; H, 6.71; N, 13.32. Found: C. 56.78; H, 6.64; N, 13.12. FTIR (KBr): 3233, 3072, 2930, 2845, 1634, 1554, 1302, 1268, 1142, 1032, 768, 720, 588, 486 cm^{-1}.

[[Cu(2-L^{N2S})(CH$_3$OH)]$_n$(OTf) (14): A CH_2Cl_2 slurry of $Cu(OTf)_2$ (0.036 g, 0.10 mmol) was added to a solution of 2-HL^{N2S} (0.0420 g, 0.20 mmol) and NaH (0.0048 g, 0.20 mmol) in CH_2Cl_2. A green precipitate was formed. After the filtration, a blue precipitate was separated and dried under vacuum. The precipitate was then dissolved in methanol, leading to a blue solution. Vapor diffusion of diethyl ether into the blue filtrate led to blue needle-shaped crystals suitable for X-ray analysis. Yield: 0.029 g, 65%. Anal. Calcd for $C_{10}H_{11}CuF_3N_2O_4S_2$: C. 29.45; H, 2.72; N, 6.87. Found: C. 28.33; H, 2.94; N, 6.58. FTIR (KBr): 2931, 1593, 1564, 1276, 1261, 1164, 1032, 640 cm^{-1}. ESI-MS (CH_3OH): *m/z* = 258 [Cu + 2-L^{N2S}]$^+$, *m/z* = 454 [Cu + 2-L^{N2S} + H]$^+$.

[Cu(2-L^{N2S})(OTf)]$_n$ (15): A solution of $Cu(OTf)_2$ (0.036 g, 0.10 mmol) in methanol was added to a solution of 2-HL$^{N2S'}$ (0.0420 g, 0.20 mmol) and triethylamine (0.0300 mL, 0.20 mmol) in methanol, forming a deep blue solution. After filtration, a blue filtrate was obtained. Vapor diffusion of diethyl ether into this filtrate resulted

in the formation of dark green crystals suitable for X-ray analysis. Yield: 0.032 g, 70%. Anal. Calcd for $C_{11}H_{13}CuF_3N_2O_4S_2$: C. 38.79; H, 4.99; N, 8.23. Found: C. 39.05; H, 4.88; N, 8.42. FTIR (KBr): 3204, 3046, 2938, 1626, 1539, 1312, 1255, 1122, 1024, 758, 722, 469 cm^{-1}. ESI-MS (CH_3OH): *m/z* = 272 $[Cu + 2\text{-}L^{N2S'}]^+$.

[Cu(2-HL$^{N2S'}$)(CH_3OH)Cl] (16): A solution of $CuCl_2$ (0.027 g, 0.20 mmol) in methanol was added to a solution of 2-$HL^{N2S'}$ (0.0420 g, 0.20 mmol) and triethylamine (0.0300 mL, 0.20 mmol) in methanol, forming a blue solution, which was stirred for 2 h. After filtration, a blue clear filtrate was isolated, and vapor diffusion of diethyl ether into the filtrate resulted in the formation of blue crystals. Yield: 0.022 g, 65%. Anal. Calcd for $C_{11}H_{17}ClCuN_2O_2S$: C. 31.28; H, 3.08; N, 6.63. Found: C. 30.86; H, 3.37; N, 6.09. FTIR (KBr): 3198, 3052, 2837, 1612, 1545, 1312, 1238, 1130, 748, 598, 472 cm^{-1}. ESI-MS (CH_3OH): *m/z* = 272 $[Cu + 2\text{-}L^{N2S'}]^+$.

X-ray Crystallography. All single crystals of **14-16** were grown by vapor diffusion of diethyl ether into solutions of the complex. Intensity data for complexes **14-16** were collected at 100(2) K using a diffractometer with a Bruker APEX ccd area detector[11] and graphite-monochromated Mo Kα radiation (λ= 0.71073 Å). The cell parameters for all complexes were determined from a non-linear least squares fit of the data. The data of these complexes were corrected for absorption by the semi-empirical method.[12] The structures were solved by direct methods by use of the SHELXTL program, and refined by full-matrix least-squares on F^2 by use of all reflections.[13] Hydrogen atom positions were initially determined by geometry and

refined by a riding model. Non-hydrogen atoms were refined with anisotropic displacement parameters. All crystal data for these complexes are summarized in Table 5-4.

For complex **15**, the molecule forms infinite chains spiraling around the *c* axis. The methanol solvent molecule was severely disordered and hence was modeled using the squeeze program.[14] For complex **16**, the molecules were found to form dimers by hydrogen bonding.

Table 5-4. Crystallographic data for complexes **14, 15** and **16.**

	14	**15**	**16**
formula	$C_{11}H_{15}CuF_3N_2O_5S_2$	$C_{12}H_{17}CuF_3N_2O_5S_2$	$C_{11}H_{17}ClCuN_2O_2S$
fw	439.91	453.94	340.32
Crystal system	Tetragonal	Hexagonal	Triclinic
Space group	$I4_1cd$	$P6_1$	$P\bar{1}$
a (Å)	17.8599(8)	13.8752(10)	7.9189(8)
b (Å)	17.8599(8)	13.8752(10)	8.7630(8)
c (Å)	21.0991 (19)	15.320(2)	10.9615(10)
α (deg)	90	90	77. 208(5)
β (deg)	90	90	83.738(5)
γ (deg)	90	120	68.440(4)
V ($Å^3$)	6730.1(7)	2554.3(4)	689.02(11)
Z	16	6	2
ρ_{calcd} mg/m^3	1.737	1.771	1.640
μ (mm^{-1})	1.601	0.71073	0.71073
θ (deg)	2.28 to 28.31	2.94 to 25.99	1.91 to 26.00
R1, wR2[I >2δ(I)]	0.0241, 0.0609	0.0388, 0.0964	0.0218, 0.0568
GOF on F^2	1.030	1.013	1.009

5.6. References

1. Belle, C.; Rammal, W.; Pierre, J. L., Sulfur ligation in copper enzymes and models. *J Inorg Biochem* **2005,** *99* (10), 1929-1936.

2. Brown, K.; Tegoni, M.; Prudencio, M.; Pereira, A. S.; Besson, S.; Moura, J. J.; Moura, I.; Cambillau, C., A novel type of catalytic copper cluster in nitrous oxide reductase. *Nat Struct Biol* **2000,** *7* (3), 191-195.

3. Solomon, E. I.; Penfield, K. W.; Gewirth, A. A.; Lowery, M. D.; Shadle, S. E.; Guckert, J. A.; LaCroix, L. B., Electronic structure of the oxidized and reduced blue copper sites: Contributions to the electron transfer pathway, reduction potential, and geometry. *Inorg Chim Acta* **1996,** *243* (1-2), 67-78.

4. (a) Holland, P. L.; Tolman, W. B., Three-coordinate Cu(II) complexes: structural models of trigonal-planar type 1 copper protein active sites. *J Am Chem Soc* **1999,** *121* (31), 7270-7271; (b) Holland, P. L.; Tolman, W. B., A structural model of the type 1 copper protein active site: N2S(thiolate)S(thioether) ligation in a Cu(II) complex. *J Am Chem Soc* **2000,** *122* (26), 6331-6332.

5. Randall, D. W.; George, S. D.; Holland, P. L.; Hedman, B.; Hodgson, K. O.; Tolman, W. B.; Solomon, E. I., Spectroscopic and electronic structural studies of blue copper model complexes. 2. Comparison of three- and four-coordinate Cu(II)-thiolate complexes and fungal laccase. *J Am Chem Soc* **2000,** *122* (47), 11632-11648.

6. Tsukihara, T.; Aoyama, H.; Yamashita, E.; Tomizaki, T.; Yamaguchi, H.; Shinzawaitoh, K.; Nakashima, R.; Yaono, R.; Yoshikawa, S., Structures of Metal

Sites of Oxidized Bovine Heart Cytochrome-C-Oxidase at 2.8 Angstrom. *Science* **1995,** *269* (5227), 1069-1074.

7. Houser, R. P.; Young, V. G.; Tolman, W. B., Thiolate-bridged, fully delocalized mixed-valence dicopper(I,II) complex that models the Cu-A biological electron-transfer site. *J Am Chem Soc* **1996,** *118* (8), 2101-2102.

8. Solomon, E. I.; Sarangi, R.; Woertink, J. S.; Augustine, A. J.; Yoon, J.; Ghosh, S., O-2 and N2O activation by bi-, tri-, and tetranuclear Cu clusters in biology. *Accounts Chem Res* **2007,** *40* (7), 581-591.

9. Yang, L.; Powell, D. R.; Klein, E. L.; Grohmann, A.; Houser, R. P., Delocalized mixed-valence Bi- and trinuclear complexes with short Cu-Cu bonds. *Inorg Chem* **2007,** *46* (17), 6831-6833.

10. Klein, E. L.; Khan, M. A.; Houser, R. P., Synthesis, characterization, and reactivity of new copper(II) complexes of 2-methylthio-N-(2-pyridylmethyl)acetamide. *Inorg Chem* **2004,** *43* (23), 7272-7274.

11. (a) Data Collection: SMART Software Reference Manual (1998). Bruker-AXS, 5465 E. Cheryl Parkway, Madison, WI 53711-5373 USA. (b) Data Reduction: SAINT Software Reference Manual (1998). Bruker-AXS, 5465 E. Cheryl Parkway, Madison, WI 53711-5373, USA.

12. G. M. Sheldrick (2002). SADABS. Program for Empirical Absorption Correction of Area Detector Data. University of Göttingen, Germany.

13. (a) G. M. Sheldrick (2000). SHELXTL Version 6.10 Reference Manual. Bruker-AXS, 5465 E. Cheryl Parkway, Madison, WI 53711-5373 USA. (b) *International*

Tables for Crystallography, Vol C, Tables 6.1.1.4, 4.2.6.8, and 4.2.4.2, Kluwer: Boston (1995).

CHAPTER 6

PROSPECTUS

6.1. Summary

As the last part of my dissertation, I want to summarize the work that has been done and the benefits for future work related to this project. My main project has been focused on the synthetic model chemistry of the Cu_Z active site in nitrous oxide reductase (N_2OR), which catalyzes the two electron reduction of N_2O to N_2 in the terminal step of the denitrification process in some anaerobic bacteria.[1] The approach used in this work involved the design and synthesis of 2-pyridylalkylbenzamide ligands, followed by the synthesis and characterization of the Cu-S model complexes to resemble the novel μ_4-sulfide bridged tetranuclear copper cluster in the Cu_Z active site.[2] The two most important strategies used for obtaining Cu-S complexes involved the reaction between copper(I) precursors and elemental sulfur, or polynuclear copper(II) complexes combined with sulfide reagents.

We have been working on the copper chemistry of (pyridylmethyl)amide ligand systems in the past several years in our group. A series of (pyridylmethyl)amide ligands (HL^R: R = H, Me_3, Ph and Ph_3) with different substituent groups on the amide were synthesized,[3] these ligands have been used to synthesize polynuclear copper clusters. A highly symmetrical copper(II) hydroxide "tennis ball" cluster, $[Cu_8L_8(OH)_4]^{4+}$, was characterized by X-ray analysis, EPR, and magnetism.[4] Two delocalized mixed-valence bi- and trinuclear copper complexes were synthesized with pyridylamide ligands *N*-(2-pyridylmethyl)acetamide and *N,N'*-(2-methyl-2-pyridyl-propan-1,3-diyl)bis(acetamide).[5] As an extension to these works, two new pyridylakylamide ligands containing phenol groups appended to the amide, 2-

hydroxy-*N*-(2-pyridylmethyl)benzamide (HL^{PhOH}) and 2-hydroxy-*N*-(2-pyridylethyl)benzamide ($HL^{PhOH'}$) were synthesized. Copper(II) complexes of these ligands were synthesized and characterized by X-ray crystallography, ESI-MS, FTIR, UV/Vis, and EPR spectroscopy.[6] When base was not used, mononuclear $[Cu(HL^{PhOH})_2Cl_2]$ (**3**) resulted. When basic Et_3N was used to deprotonate the ligand, tetracopper(II) $[Cu_4(L^{PhO})_4]$ (**4**) or dicopper(II) $[Cu_2(L^{PhO'})_2(CH_3OH)_2]$ (**5**) were obtained. In complex **3**, copper are six-coordinate with pyridyl N atoms and chloride ligands in equatorial plane positions, and long interactions with the amide carbonyl O atoms in the axial positions, forming a distorted octahedron geometry. Complex **4** has a distorted cubane-like structure, with the ligands bridging via the phenoxo oxygen atoms, and the copper atoms possessing a distorted square planar geometry. The ligands in complex **5** also bridge two copper(II) atoms via the phenoxo oxygen atoms, forming a square pyramidal geometry.

We were more interested in the tetracopper(II) complex **4** as a potential precursor to react with sulfide reagents, which is motivated by the novel μ_4-sulfide bridged tetranuclear copper cluster in the Cu_Z active site. The reactions of complex **4** with either Na_2S or Li_2S led to the formation of a green precipitate with poor solubility. However, when complex **4** reacted with (nBu$_4$N)SH, it led to the formation of a naked $[Cu_{16}S_{10}]^{4-}$ cluster with μ_3- and μ_4-sulfido ligands.[7] The same cluster was also synthesized by the treatment of three equivalents of (nBu$_4$N)SH in CH_3CN with the mixed-valence copper complex $[Cu_2(L1)_2]$OTf (HL1 = 2-phenyl-N-(2-pyridylmethyl)acetamide; OTf = trifluoromethanesulfonate).[5] The structure of (nBu$_4$N)$_4$[$Cu_{16}S_{10}$] was determined by X-ray analysis to contain four

tetrabutylammonium cations and an unprecedented tetra-anionic $[Cu_{16}S_{10}]^{4-}$ cluster. When NaSH was used with DMF solvent, the previously reported[8] twelve-copper cluster $[Cu_{12}S_8]^{4-}$ was isolated from the same copper precursor. The differences in reactivity between (nBu$_4$N)SH and NaSH are most likely related to steric and packing effects in the products.[7] Apparently, the solvent also plays a role in the synthesis of the cluster, since the synthesis in other solvents failed to obtain the cluster.

The bridging mode of sulfide is different in both clusters. All S^{2-} ligands are μ_3- in $[Cu_{12}S_8]^{4-}$. $[Cu_{16}S_{10}]^{4-}$ contain both μ_3- and μ_4-sulfido ligands. Eight μ_3-sulfido atoms decorate the eight triangular faces with an average Cu-S bond distance of 2.16(2) Å and an average Cu-S-Cu angle of 79.2(9)^o. Two μ_4-sulfido atoms cap the top and bottom position of the cluster with Cu-S bond distances from 2.146(13) to 2.182(11) Å and an average Cu-S-Cu angle of 77.7(6)^o.

Attempts to synthesize the cluster with simple copper(I) or copper(II) salts with NaSH or (nBu$_4$N)SH in the appropriate stoichiometric ratio are not successful due to the formation of insoluble copper sulfide precipitates. So, it is very necessary to rationalize the process for the synthesis. The ratio for the reaction is about 1 to 6 equivalent (nBu$_4$N)SH in order to reduce copper(II) to copper(I) with excess SH^- as shown in the following equation.

$$4[Cu_4L^{PhO}{}_4] + 26TBASH \xrightarrow{CH_3CN} TBA_4[Cu_{16}S_{10}] + 16L^{PhO2-} + 8HSSH + 22TBA^+ + 10H^+$$

The yield for the synthesis of the cluster is low. It is hard to obtain enough high quality crystal for N_2O reactivity studies. Some N_2O reactivity tests have been done with $[Cu_{12}S_8]^{4-}$ cluster by Lei Yang and Mike McClain in our group. Till now, there was no convincing data available to confirm the reduction of N_2O to N_2 with the small cluster. To sum up, the cluster can partially model the structure of the μ_4-sulfide bridged tetranuclear copper cluster in the Cu_Z active site. The goal to obtain accurate models of the $[(his)_7Cu_4(\mu\text{-}S)]^{n+}$ core was not achieved. But it developed a new synthetic strategy for the synthesis of high nuclearity naked Cu-S clusters.

The substituted pyridylbis(phenol) ligand system does not allow us to produce polynuclear copper(II) complexes for further reactivity studies with sulfide reagents presented in Chapter **3**. But interesting cyclic voltammetry of the copper complexes with different substituents has been observed and analyzed with the Hammett method.

Both pyrazine- and thioether-containing ligand systems lead us to the synthesis and characterization of a series of 1D coordination polymers presented in Chapter **4** and Chapter **5**. All of the results enrich the copper chemistry of the coordination polymers.

Although, we did not achieve the exact goal of this project to synthesize accurate structural and functional models of the Cu_Z center in N_2OR, We did investigate the copper chemistry of pyridylalkylbenzamide ligands. Sixteen copper complexes were synthesized and characterized by X-ray crystallography. One naked $[Cu_{16}S_{10}]^{4-}$ cluster was synthesized, which could partially model the Cu_4S center in the Cu_Z center of N_2OR. It also hints at the possibility to obtain similar Cu-S clusters based

on the precursors with similar ligand systems, which will be a very helpful guideline for further research on this project.

6.2. References

1. Soohoo, C. K.; Hollocher, T. C., Purification and Characterization of Nitrous-Oxide Reductase from Pseudomonas-Aeruginosa Strain-P2. *J Biol Chem* **1991,** *266* (4), 2203-2209.

2. Chen, P.; Cabrito, I.; Moura, J. J. G.; Moura, I.; Solomon, E. I., Spectroscopic and Electronic Structure Studies of the μ_4-Sulfide Bridged Tetranuclear Cu_Z Cluster in N_2O Reductase: Molecular Insight into the Catalytic Mechanism. *J Am Chem Soc* **2002,** *124* (35), 10497-10507.

3. Chaudhuri, U. P.; Whiteaker, L. R.; Yang, L.; Houser, R. P., Multinuclear copper complexes of pyridylmethylamide ligands. *Dalton T* **2006,** (15), 1902-1908.

4. Mondal, A.; Li, Y.; Khan, M. A.; Ross, J. H.; Houser, R. P., Supramolecular copper hydroxide tennis balls: Self-assembly, structures, and magnetic properties of octanuclear $[Cu_8L_8(OH)_4]^{4+}$ clusters (HL = N-(2-pyridylmethyl)acetamide). *Inorg Chem* **2004,** *43* (22), 7075-7082.

5. Yang, L.; Powell, D. R.; Klein, E. L.; Grohmann, A.; Houser, R. P., Delocalized mixed-valence Bi- and trinuclear complexes with short Cu-Cu bonds. *Inorg Chem* **2007,** *46* (17), 6831-6833.

6. Wang, Z. D.; Powell, D. R.; Houser, R. P., Syntheses and structures of a phenoxo-bridged copper(II) distorted cubane and related complexes with 2-hydroxy-N-(2-pyridylalkyl)benzamide ligands. *Inorg Chem Commun* **2009,** *12* (6), 511-514.

7. Yang, L.; Wang, Z. D.; Powell, D. R.; Houser, R. P., A $[Cu_{16}S_{10}]^{4-}$ cluster containing μ_3- and μ_4-sulfido ligands. *Dalton T* **2009,** (23), 4439-4441.

8. Betz, P.; Krebs, B.; Henkel, G., $[Cu_{12}S_8]^{4-}$ - a Closed Binary Copper(I) Sulfide Cage with Cuboctahedral Metal and Cubic Sulfur Arrangements. *Angewandte Chemie-International Edition in English* **1984,** *23* (4), 311-312.